APPLICATIONS OF MEMBRANE-BASED OPERATIONS IN SEPARATION OF NATURAL PHENOLIC COMPOUNDS

Thesis Submitted
In Partial Fulfillment of the Requirements
for the Degree of

DOCTOR OF PHILOSOPHY

in

Chemical Engineering

by

Ashwani Kumar Tiwari
(2K20/PHDCH/01)

Under the Supervision of
Dr. Manish Jain
Assistant Professor
Department of Applied Chemistry
Delhi Technological University

To the
Department of Applied Chemistry
DELHI TECHNOLOGICAL UNIVERSITY
(Formerly Delhi College of Engineering)
Shahbad Daulatpur, Main Bawana Road, Delhi-110042, India

January, 2026

ACKNOWLEDGMENTS

As I reach the culmination of my doctoral journey, I express my profound gratitude to those who have been instrumental in my academic success and personal growth. I have been extraordinarily fortunate to be guided by an exceptional mentor, **Dr. Manish Jain**. His brilliant mind and extensive experience have shaped my academic development in ways that words cannot adequately capture. He stands among the most remarkable intellectuals I have had the privilege to learn from throughout my educational journey. His mentorship shaped the trajectory of this work and profoundly influenced my overall growth as a good human being.

I am deeply grateful to **Prof. Prateek Sharma**, Vice Chancellor of Delhi Technological University, for allowing me to pursue my research at this esteemed institution. I also thank **Prof. Devendra Kumar,** Head of the Department of Applied Chemistry, for providing me with all the necessary facilities and support to carry out this research. I sincerely appreciate the distinguished faculty members of the Department of Applied Chemistry at Delhi Technological University. Their guidance and support have been invaluable to my research endeavours.

My heartfelt appreciation goes to my lab colleagues, **Dr. Kudzai Hamish Ruzvidzo, Dr. Ketan Mahawer, Mr. Mukesh Kumar Mishra, Mr. Ravi Shankar Gupta, and Mrs. Manisha Yadav**, whose mentorship has significantly enhanced my research capabilities. I am also indebted to **Dr. Ritu Sharma, Ms. Versha Joshi, Dr. Jigyasa Pathak, Ms. Priyanka, Ms. Tanvi, and Ms. Nishtha** for their steadfast support and invaluable counsel.

Words cannot adequately express my gratitude to my beloved parents for your unwavering support, unconditional love, and constant encouragement. I express my heartfelt gratitude to my mother, **Shrimati Ram Dulari Tiwari,** and my father, **Shri Ram Surat Tiwari,** whose life lessons and encouragement have been a candle at night. Their endless love and firm belief in me motivate me throughout this journey - special thanks to my **sisters and cousins** for their infectious enthusiasm. My family has been the cornerstone of my academic journey, and this achievement would not have been possible without your blessings.

Lastly, I sincerely thank **Almighty God** for providing me with strength, guidance, and every opportunity needed to embark on this journey. I am humbled by the blessings and provisions bestowed upon me throughout this endeavour.

I extend my deepest gratitude to all who have played a part in this journey, whether through encouragement, assistance, or companionship. This thesis is a testament to the collective efforts and contributions of all who have touched my life along this transformative path. I thank my laboratory colleagues and fellow researchers in the department for creating an environment conducive to academic excellence and scientific inquiry.

(Ashwani Kumar Tiwari)

DELHI TECHNOLOGICAL UNIVERSITY
(Formerly Delhi College of Engineering)
Shahbad Daulatpur, Main Bawana Road, Delhi-110042, India

CANDIDATE'S DECLARATION

I, **Ashwani Kumar Tiwari,** hereby certify that the work being presented in the thesis entitled **"Applications of membrane-based operations in separation of natural phenolic compounds"** in partial fulfillment for the award of the Degree of Doctor of Philosophy, submitted in the Department of **Applied Chemistry**, Delhi Technological University is an authentic record of my work carried out during the period from 26/8/2020 to 11/06/2025 under the supervision of **Dr. Manish Jain.**

I have not submitted the matter presented in the thesis for the award of any other degree from this or any other institute.

Ashwani Kumar Tiwari

DELHI TECHNOLOGICAL UNIVERSITY
(Formerly Delhi College of Engineering)
Shahbad Daulatpur, Main Bawana Road, Delhi-110042, India

CERTIFICATE BY THE SUPERVISOR(S)

Certified that **Ashwani Kumar Tiwari (2K20/PHDCH/01)** has carried out their research work presented in this thesis entitled **"Applications of membrane-based operations in separation of natural phenolic compounds"** for the award of **Doctor of Philosophy** from the Department of Applied Chemistry, Delhi Technological University, Delhi, under my supervision. The thesis presents the results of the student's original work. The contents of the thesis do not form the basis for the award of any other degree to the candidate or anybody else from this or any other University.

Dr. Manish Jain	**Prof. Devendra Kumar**
Supervisor	**Head of the Department**
Department of Applied Chemistry	**Department of Applied Chemistry**
Delhi Technological University	**Delhi Technological University**

Date:

ABSTRACT

With the growing global population, there is an increasing need to develop sustainable and green separation processes for high-value bioactive compounds. Naturally occurring phenolic compounds such as betanin and rutin have gained considerable importance in the food and pharmaceutical industries; however, existing separation methods often rely on solvent-intensive, energy-demanding, or non-scalable techniques that compromise product purity and biological activity. Although membrane-based processes have been explored for polyphenol recovery, there remains a lack of systematic, model-integrated, and scale-up-oriented studies that bridge laboratory experimentation with industrial feasibility, particularly for real feed streams.

In this context, the present thesis makes a distinct contribution by establishing nanofiltration (NF) as a quantitatively optimised and industrially translatable platform for the selective concentration of two structurally different phenolic compounds, namely betanin and rutin. A self-assembled NF setup using HFT-NF 150 membranes is employed to generate a comprehensive experimental dataset, wherein the individual and interactive effects of pressure, feed concentration, and feed flow rate on permeate flux and solute rejection are rigorously evaluated. Unlike prior studies that report only empirical trends, this work integrates a three-parameter Spiegler-Kedem transport model to extract membrane reflection coefficients, solute permeability, and hydraulic permeability, thereby providing mechanistic insight into solute-membrane interactions and enabling predictive validation of experimental performance.

A further aspect of this research is the application of variance-based global sensitivity analysis to membrane separations, allowing the quantitative ranking of operating and transport parameters by their influence on flux and rejection for phenolic solutes. This approach moves beyond conventional one-factor-at-a-time analyses and establishes a robust framework for rational process optimisation. Crucially, the thesis extends beyond model solute systems to address the separation of betanin from its natural matrix, beetroot juice, an area scarcely examined in existing literature. Comprehensive fouling studies using multiple theoretical fouling models are performed to elucidate

dominant fouling mechanisms, quantify flux decline behaviour, and assess long-term operational stability under realistic feed conditions. These results provide actionable design insights to mitigate fouling and extend membrane longevity.

Finally, scale-up simulations grounded in experimentally derived transport and sensitivity parameters demonstrate the technical feasibility of translating laboratory findings into an industrial-scale NF unit. Collectively, this thesis offers a unified experimental-modelling-scaling framework for phenolic compound recovery, delivering original contributions in mechanistic understanding, optimisation strategy, real-feed validation, and process design that advance the state of the art in sustainable membrane-based separations.

Dedicated with profound gratitude:

To the unwavering support of ***Shrimati Ram Dulari Tiwari and Shri Ram Surat Tiwari****,*
my cherished parents;

To my beloved sisters;

You all are the cornerstones of my world and the driving force behind this achievement

LIST OF PUBLICATIONS

1. **Ashwani Kumar Tiwari** and Manish Jain, “A novel process for rutin recovery from model solutions using nanofiltration: Experimental study, mathematical modeling, and scale-up design”, *J. Food Process. Eng.*, vol. 47(3), art. no. e14592, 2024, doi: 10.1111/jfpe.14592

2. **Ashwani Kumar Tiwari** and Manish Jain, “Concentration of betanin from model beetroot extracts using nanofiltration: Parameter estimation and sensitivity analysis*”, J. Chem. Technol. and Biotechnol.*, vol. 99, pp. 1976-1983, 2024, doi: 10.1002/jctb.7698

3. **Ashwani Kumar Tiwari,** Kudzai Hamish Ruzvidzo, Prafull Kumar Meena, and Manish Jain, “Extraction of Betanin From Beetroot Juice Using a Hybrid System: System Performance and Fouling Analysis of the Membrane”, *J. Food Process. Eng.*, vol. 48(11), art. no. e70272, 2025, doi: 10.1111/jfpe.70272

LIST OF CONFERENCES

1. **Ashwani Kumar Tiwari,** Manish Jain, oral presentation on the title: "Application of membrane-based operation in the separation of natural phenolic compounds," International Conference on Emerging Techno-Economic Development for Sustainable Environment, organized by IPS Academy, Institute of Engineering & Science, Indore, India, January 12-13, 2024.
2. **Ashwani Kumar Tiwari,** Manish Jain, "Mathematical modeling of membrane-based operations for the separation of phenolic compounds," Conference on Desalination, Brine Management, and Water Recycling (DeSaltM 23), organized by Indian Institute of Technology, Bombay, India, July 21-22, 2023.
3. **Ashwani Kumar Tiwari,** Manish Jain, "Parameter estimation and sensitivity analysis of nanofiltration for phenolic compound separation," International Workshop and Conference on Membrane-Assisted Water Purification Processes (ICMW-2023), organized by Mahatma Gandhi University, Kottayam, Kerala, India, March 9-12, 2023.
4. **Ashwani Kumar Tiwari,** Manish Jain, "Concentration of betanin using nanofiltration," 2nd International Conference on Chemical & Allied Science and their Applications, organized by Delhi Technological University, New Delhi, India, January 20, 2023.
5. **Ashwani Kumar Tiwari,** Manish Jain, "Concentration of phenolic compounds using membrane-based operations," 2nd International Conference on Green & Sustainable Energy Conference, organized by Manav Rachna University, Faridabad, Haryana, India, November 17-19, 2022. (**Best presentation award**)

LIST OF WORKSHOPS AND SEMINARS

1. Participated in an Industry-Academia Seminar on 'Petrochemicals in Today's World' organized by the Department of Applied Chemistry at Delhi Technological University, Delhi, held on 21st November 2023.

2. Participated in INUP-i2i 6th User Awareness Workshop on 'Fabrication & Characterization Facility for Nanotechnology' held at IIT Delhi – 4th - 5th March, 2023.

3. Attended a one-day national Seminar on 'Recent Advancements in Semiconductor Devices and Materials' organized by the Department of Applied Physics at Delhi Technological University, Delhi, held on 30th January 2023.

4. Attended the 'IP Awareness/Training Program Under National Intellectual Property Awareness Mission' organized by the IPR cell at Delhi Technological University, Delhi, held on 30th November 2022.

5. Participated in an online Workshop on 'Accelerators/Incubation-Opportunities for Students & Faculties Early-Stage Entrepreneurs' organized by the Department of Applied Chemistry, Delhi Technological University, Delhi - 19th June 2021.

CONTENT

LIST OF TABLES

LIST OF FIGURES

LIST OF SYMBOLS, ABBREVIATIONS & NOMENCLATURE

Abbreviations

a	Coefficient in mass transfer correlation
b	Exponent of Reynolds number in the mass transfer equation
B_m	Membrane solute permeability
c	Solute concentration
CA	Cellulose acetate
CTA	Cellulose triacetate
F	Flow parameter
FO	Forward osmosis
I-T	Irreversible thermodynamic
J	Flux
k	Mass transfer coefficient
k'	Fouling rate constant
K-K	Kedem-Katchalsky
L_p	Hydraulic permeability
LLE	Liquid-liquid extraction
mAPE	Maximum absolute percentage error
MAPE	Mean absolute percentage error
MATLAB	Matrix laboratory
MD	Membrane distillation
MF	Microfiltration
MSP	Membrane separation process
M_w	Molecular weight of solute
MWCO	Molecular weight cut-off

NF	Nanofiltration
OD	Osmotic distillation
P	Pressure
PA	Polyamide
PAN	Polyacrylonitrile
PE	Polyethylene
PEEK	Polyether ether ketone
PES	Polyethersulfone
P-F	Pore-Flow
PP	Polypropylene
PSU	Polysulfone
PTFE	Polytetrafluoroethylene
PVDF	Polyvinylidene fluoride
PVP	Polyvinylpyrrolidone
Q	Flow rate
R	Universal Gas Constant
R^2	Coefficient of goodness
R_e	Reynolds number
R_j	Rejection
RO	Reverse osmosis
S	First-order sensitivity
S_c	Schmidt number
S_h	Sherwood number
S_T	Total sensitivity
SEM	Scanning electron microscopy
S-D	Solution-Diffusion

S-K	Spiegler-Kedem
T	Temperature
TFC	Thin film composite
UF	Ultrafiltration
UV-Vis	Ultraviolet-Visible

Symbols

ϕ	Concentration polarization
υ	Vant Hoff factor
α	Proportionality constant for osmotic pressure
π	Osmotic pressure
σ	Reflection coefficient
ρ	Density

Subscript

p	Permeate side
b	Bulk side
m	Membrane–feed interface

Chapter – 1
Introduction and Literature Review

CHAPTER – 1

INTRODUCTION AND LITERATURE REVIEW

1.1 Introduction

Mother Earth, our generous provider, blesses us with the gifts of life through her abundant resources that nourish and sustain all living things. Plants, one of Mother Earth's gifts, perfectly illustrate her abundance and wisdom through three interconnected biochemical systems: hormones vegetal, primary metabolites, and secondary metabolites (Figure 1.1). Plants' secondary metabolites are compounds that not only provide defence to plants but are also very beneficial to human health due to their physiological activities.

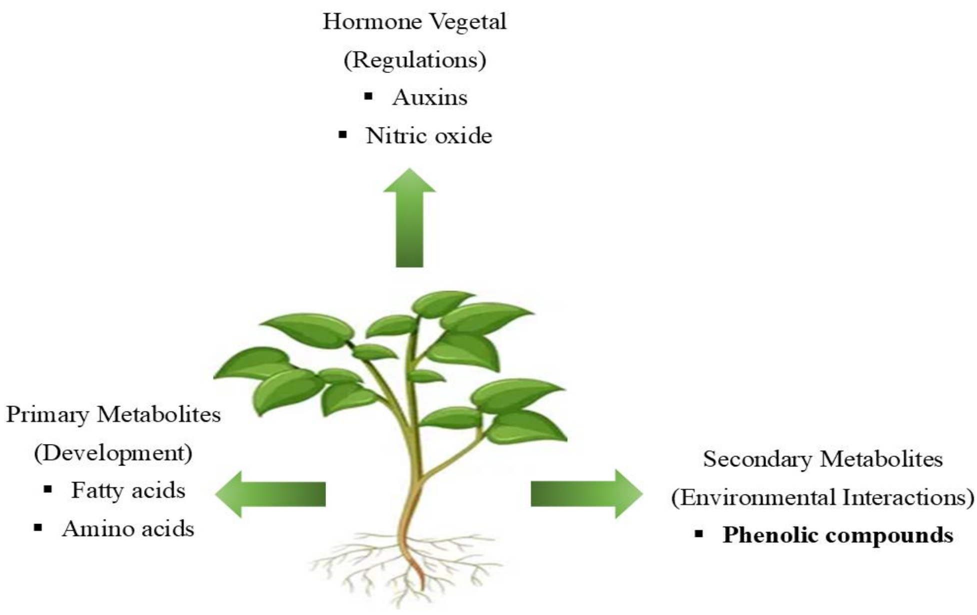

Figure 1.1 Plant metabolites

Over the past few years, the recovery of bioactive compounds from natural sources has attracted considerable attention across the pharmaceutical, nutraceutical, cosmetic, and food industries. Among all these naturally occurring bioactive compounds, polyphenols are the most searched [1]. Polyphenols are compounds with one or more aromatic rings and single or multiple hydroxyl groups and exhibit significant biological activities, including antioxidant, anti-inflammatory, antimicrobial, and anticancer properties. They are the most abundant secondary metabolites in plants, and over 8,000 species are known [2]. Polyphenols' structural variation ranges from simple structures such as phenolic acids to complex structures such as tannins (Figure 1.2). These phenolic compounds in plants make them a vital ingredient in the human diet [2], [3].

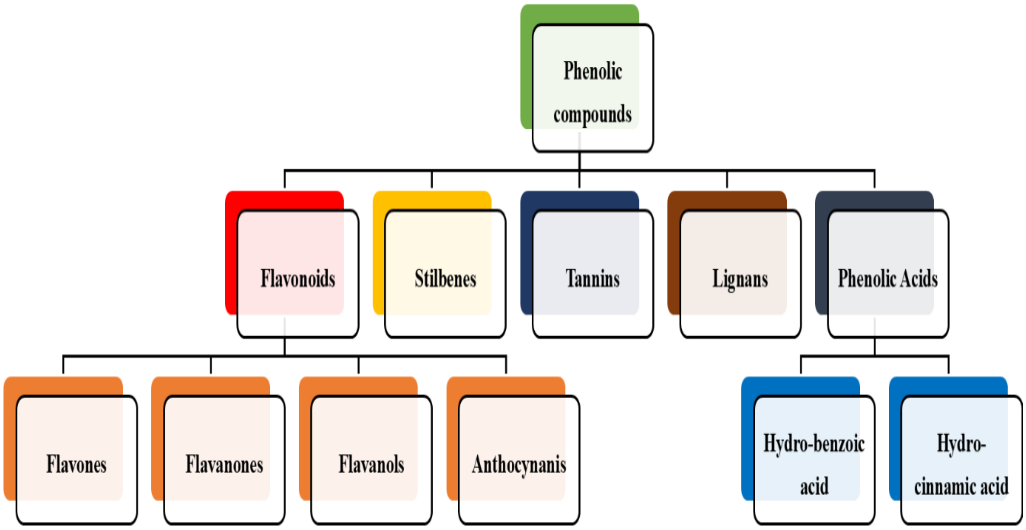

Figure 1.2 Classes of polyphenols

Polyphenols are mainly found in fruits, vegetables, tea, and coffee, and contribute to the organoleptic characteristics of plant food. Polyphenols impart color and flavor to many fruits and vegetables and defend against ultraviolet (UV) radiation, pathogens, and other predators. Not only this, but these compounds also help prevent various human diseases, such as cardiovascular disease, osteoporosis, and diabetes. Intrinsically, these health-protective activities of polyphenols are attributed to the presence of the phenolic hydroxyl group that donates hydrogen atoms to the reactive oxygen species and, hence, scavenges them by breaking the cycle of new radical generation. With this effect, the phenolic compounds prevent the oxidation of lipids, DNA, and proteins [4]-[6]. Therefore, there is a growing demand to separate and concentrate polyphenols from natural sources to meet human and industrial requirements. Also, there is notable interest in identifying tangible methods for extracting these compounds from their sources, which are limited by their instability at higher temperatures and the long extraction times required.

1.2 Polyphenols from natural sources

1.2.1 Flavonoids

Flavonoids represent the primary class of phenolic compounds in the human diet. These compounds have diphenylpropane as their essential skeleton, with two aromatic rings connected by a 3-carbon bridge, and more than 4,000 flavonoids have been identified to date [7]. These are the most varied polyphenols involved in color formation in flowery plants and play an essential role in protecting plants against UV damage and in resisting disease. Based on the pattern and degree of hydroxylation, glycosylation, methoxylation, or prenylation, flavonoids are subcategorized into six classes: flavones, flavanones, flavanols, flavonols, anthocyanins, and isoflavones. Various flavonoids are tested in a range of dietary plants, including fruits and vegetables, spices, and medicinal herbs. Some examples include quercetin, catechin, and cyanidin glycoside [8]-[10].

1.2.2 Phenolic acids

Phenolic acids are plants' primary class of polyphenols [11]. They are found in either free or bound forms and are usually present as esters or amides. These are subcategorized into mainly two groups: hydroxybenzoic acids (gallic acid, p-hydroxybenzoic acid, vanillic acid, syringic acid, and protocatechuic acid) and hydroxycinnamic acids (ferulic acid, caffeic acid, chlorogenic acid, p-coumaric acid, and sinapic acid) [12]. Gallic acid is broadly distributed in medicinal herbs and dietary plants [13]-[17]. Fruits (blueberry, blackberry, strawberry, red raspberry, black currant, and red currant) are generally rich in hydroxycinnamic acids (caffeic, ferulic, and p-coumaric acids), which contribute to their antioxidant activity.

1.2.3 Tannins

Tannins are polyphenols with molecular weights ranging from 500 to 20,000 Da. They are classified into hydrolyzable tannins (tannic acid) and condensed tannins (proanthocyanidins). They can be degraded into sugars and phenolic acids through pH change or hydrolysis (enzymatic or non-enzymatic). They are widely distributed in cereals, fruits, and vegetables and possess various activities, including antimicrobial, antiparasitic, antiviral, and immunomodulatory [18].

1.2.4 Stilbenes

These polyphenols have two aromatic rings linked by an ethane bridge (a core chemical structure is 1,2-diphenylethylene). They are distributed in higher plants and found in monomeric and oligomeric forms. Grapes, berries, red wine, and peanut products are rich in stilbenes. Recently, stilbenes have attracted the attention of researchers due to their wide range of health-related benefits, including anticarcinogenic, anti-inflammatory, and antidiabetic activities [19]. The primary representative of stilbenes is resveratrol, which has anti-oxidant effects on the heart and blood vessel systems [20]. Other examples of stilbenes include pterostilbene, oxyresveratrol, and 3'-hydroxypterostilbene.

1.2.5 Lignans

These are biologically active natural polyphenols derived from the oxidative dimerization of two phenyl-propane units. Their primary sources include linseed, fruits, nuts, garlic, olive oil, wine, tea, beer, and coffee. In recent years, they have been used in conventional and ethnic medicines due to their antioxidant, antitumor, antiviral, and anti-inflammatory properties [21].

1.3 Conventional methods for the separation and purification of polyphenols

Natural sources of polyphenols contain various components, such as monosaccharides, disaccharides, and other compounds. Therefore, efficient extraction and concentration of phenolic compounds from step present considerable challenges due to their chemical diversity, varying polarities, and susceptibility to degradation [22]. Traditional methods to purify polyphenols include adsorption [23]-[30], column chromatography [31]-[36], and solvent extraction [37]-[40].

Adsorption-based methodologies use solid adsorbents, such as activated carbon, silica, polyamide, and synthetic resins, to concentrate phenolic compounds from dilute solutions. The process involves passing the solution through a column packed with the adsorbent, allowing species to bind via weak chemical or polar interactions, followed by elution of the adsorbed phenolics with appropriate solvents (typically ethanol or methanol). Column chromatography is used to purify phenolic compounds based on their polarity and hydrophobicity. This method separates solute particles using adsorbents, molecular sieves, or ion-exchange materials. The compounds move at different rates through columns, allowing them to get separated in other columns. Liquid-liquid extraction (LLE) has historically been employed as a primary technique for isolating phenolics from their natural sources by partitioning them between two immiscible phases. This method employs organic solvents, including ethyl acetate, methanol, and acetone. Phenolic compounds preferentially migrate to the organic layer due to their polarity, separating and evaporating to concentrate them. Similarly, solid-liquid extraction techniques, including maceration and soxhlet extraction, have been widely used to extract phenolics from solid plant materials. While these traditional methodologies continue to serve as fundamental techniques, they still have certain limitations, including extensive solvent use, dependence on phase change phenomena, potential thermal degradation, extended processing times, and variable selectivity.

In recent years, membrane-based separation technologies have emerged as promising alternatives to traditional processes. Understanding these classical approaches provides crucial context for developing and evaluating emerging technologies for concentrating phenolic compounds from natural sources. Considering all factors, membrane-based separation technologies are growing across various industrial sectors due to multiple benefits, such as an athermal process, no phase change or chemical or solvent use, high efficiency, low energy requirements, and continuous operation, which enables easy scalability. Additionally, these processes can be coupled in an integrated system to separate large molecules (proteins, polypeptides) and small molecules (salts, sugars) using different membrane types [41], [42].

1.4 Principles and general aspects of membrane processes

A membrane is a selective barrier that allows some species to pass through and prevents others based on their sizes or molecular weights. These entities may be ions, molecules, or tiny particles. The separation occurs through mechanisms such as diffusion, sieving, or sorption. There are mainly four types of driving force for transporting species across the membrane: pressure difference (micro-filtration (MF), ultra-filtration (UF), nano-filtration (NF), and reverse osmosis (RO), pizodialysis), concentration gradient (dialysis, gas separation, pervaporation, diffusion dialysis), electric potential gradient (electrodialysis, electro-osmosis), or temperature difference (thermos-osmosis, membrane distillation) [43]. Two types of flow direction are possible for the feed stream: stream direction is perpendicular to the membrane (dead-end filtration), and stream direction is tangential or parallel to the surface of the membrane (cross-flow filtration). In the dead-end filtration process, particulate matter accumulates on the membrane surface, forming a barrier that reduces the filtration rate and flux over time. In cross-flow filtration, the parallel flow of the feed stream creates a sweeping action that minimizes the buildup of the accumulation layer. As shown in Figure 2, these processes can separate a feed solution into two streams: permeate and retentate. The permeate stream contains all components with molecular weights below the membrane's nominal molecular weight cut-off (MWCO). MWCO is a membrane characterization parameter that refers to the molecular mass of a solute that will effectively diffuse across the membrane. The retentate stream contains particles and dissolved compounds rejected by the membrane with some solvents [44], [45]. The separation efficiency of these membrane processes depends on various factors like the physicochemical composition of the feed solution (type, polarity, weight, concentration); the operating parameters (feed flow rate, pressure, temperature); and membrane characteristics (membrane material, module configuration, pore size) [46]. In addition to various factors, phenomena such as concentration polarization and membrane fouling can also affect separation efficiency [47], [48]. The efficiency of pressure-driven membrane processes is primarily evaluated by measuring the permeate flux (equation 1) and the rejection percentage (equation 2).

$$J_p = \frac{V}{A \times t} \quad \ldots (1.1)$$

V is the volume of permeate collected (m^3) at a particular time interval in t (sec), and A is the active membrane area (m^2).

$$R = \left(1 - \frac{C_p}{C_f}\right) \times 100 \quad \ldots (1.2)$$

Here, C_p is the solute concentration in the permeate (mg/L), and C_f is the solute concentration in the feed (mg/L). Rejection values are between 0% (for solutes having the highest probability of passing through the membrane) and 100% (when the membrane completely retains solutes).

Several polymeric membranes are widely utilized in industrial applications due to their cost-effectiveness, ease of fabrication, and versatility in pore size distribution. Common polymeric materials include polypropylene (PP), polyethylene (PE), polysulfone (PS), polyethersulfone (PES), polytetrafluoroethylene (PTFE), cellulose acetate (CA), polyvinylidene fluoride (PVDF), polyacrylonitrile (PAN), and polyamide (PA). For continuous operations, membranes are assembled into specialized modules, which vary in design, operational efficiency, and energy consumption. Hollow fiber, spiral wound, tubular, plate-and-frame, and capillary are the primary configurations used in large-scale industrial applications.

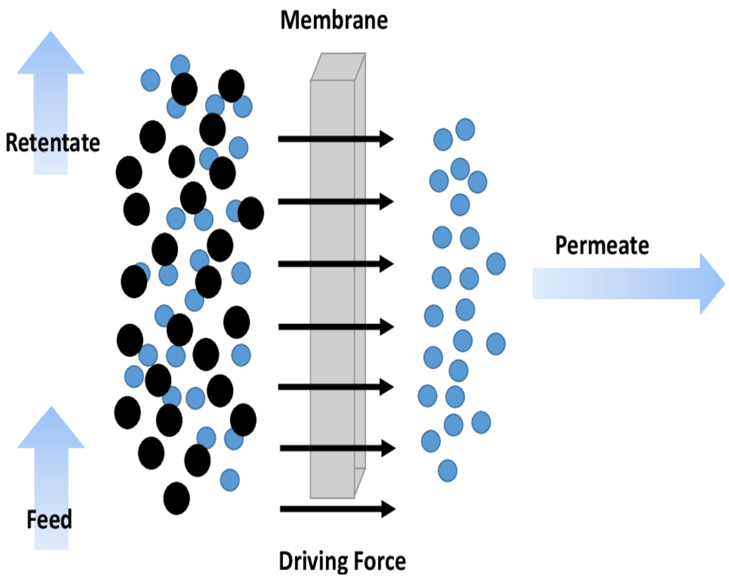

Figure 1.3 Membrane filtration process (cross-flow)

1.4.1 Membrane processes: An approach to concentrate or recover natural bioactives and phenolic compounds

In recent years, growing economic interest has been in recovering and purifying bioactive compounds, particularly soluble polyphenols, from food processing streams and by-products. Membrane processes have emerged as practical techniques for selectively fractionating or concentrating phenolic compounds from various natural sources, extracts, and by-product streams. These methods offer distinct advantages over conventional separation techniques, including high efficiency, scalability, and lower energy consumption. Table 1.1 summarizes the previous literature on the recovery or concentration of phenolic compounds.

Table 1.1 Summary of membrane-based operations in concentrating or recovering phenolic compounds

Natural Source	**Process; material; MWCO**	**Recovered component**	**Findings**	**Ref.**
Pomegranate juice	FO; TFC	Anthocyanin	4.2-fold concentration of anthocyanins	[49]
Apple juice	NF; TFC; 200-300 Da	TPC	83.7 % recovery	[50]
Beetroot juice	FO; CTA	TPC	10-fold concentration of anthocyanins	[51]
Jambolan fruit extract	UF & NF; 140 – 4000 Da	Gallic acid; Catechin	1.1-fold and 5-fold concentration of gallic acid for UF and NF, respectively; 1.8-fold and 4.9-fold concentration of gallic acid for UF and NF, respectively.	[52]
Carob pulp juice	FO; CTA	TPC	2.24-fold concentration of TPC	[53]
Broccoli juice	UF; PES;	TPC	94% recovery	[54]
Cactus pear juice	OMD; PTFE	TPC	2.6-fold concentration of TPC	[55]
Cactus pear juice	UF; PSU; 10000 Da	Betacyanins; Betaxanthins	The rejection rates for betaxanthins and betacyanins were 6.5% and 36%, respectively.	[56]

Cactus pear juice	MF; PVDF; 0.20 µm; & UF; PVDF; 200000 Da	Flavonoids	The rejection of flavonoids for MF and UF was 37 % and 42%, respectively.	[57]
Clementine mandarin juice	UF; Modified PEEK and PSU	Total polyphenols	The rejection towards total phenolics was 16.4% and 8.2% for modified PEEK & PSU membranes, respectively.	[58]
Pomegranate juice	UF; Modified PEEK; 10% rejection dextran 68800 MW	Polyphenols; Anthocyanins	Rejections towards polyphenols and anthocyanins were 16.5% and 11.7%, respectively.	[59]
Kiwifruit juice	UF; Cellulose; 30000 Da	Total polyphenols	The rejection of total phenolics was 13.5%.	[60]
Bergamot juice	UF; PSU, and Fluoropolymer; 1000 and 100000 Da; & NF; TiO_2 450 and 700 Da	Narirutin, Hesperidin, Neohesperidin,	The UF showed very low rejections in the range of 0-22% for different flavonoids, whereas NF showed rejection percentages in the range of 48-63% for 750 Da and 92-99% for 450 Da membranes.	[61]
Roselle extract	MF; Ceramic; 0.20 µm	Anthocyanins	98.4 % recovery rate of anthocyanin in the permeate.	[62]
Roselle extract	UF; PA, PES, and thin film; 1000 -	Anthocyanins	The anthocyanins' recovery rate in retentate	[63]

	150000 Da; & NF; PA, PES; 200 - 400 Da		varied from 60-100% and 90-100% for different UF and NF membranes, respectively.	
Lemon juice	UF; PVDF;	Hesperidin	65.8% recovery rate of hesperidin in the permeate.	[64]
Castanea sativa leaves aqueous extract	UF; Modified PES; 5000 and 10000 Da	Total phenolics	Recovery rate of 92% and 82.5% of total phenolics in the retentate for 5000 and 10000 Da, respectively.	[65]
Sideritis extract	NF; Modified polyimide; 300 - 500 Da	Flavonoids	All membranes showed high rejection of flavonoids, i.e., from 97% up to 99%.	[66]
Raspberry juice	MF; Ceramic, 0.20 µm; & UF; PSU; 30000 Da;	Anthocyanins	Recovery rate of 83% and 56% of anthocyanins in the permeate for MF and UF, respectively.	[67]
Clove basil	UF; PES; 10000 Da	Rosmarinic, Chlorogenic, and other phenolic acids	76.80 ± 0.59 % and 52.52 ± 0.04 % of polyphenols and rosmarinic acid were retained, respectively	[68]

Pressure-driven membrane systems play a crucial role in recovering phenolic compounds from their natural sources, spanning operations from pre-filtration to concentration. By integrating these processes sequentially or combining them with other separation technologies, researchers and engineers can enhance recovery efficiency while preserving the bioactivity of phenolic compounds. This approach provides a cost-effective solution with reduced energy, capital, and labor expenditures.

Current applications include the extraction of valuable components from the agro-food and dairy industries and their by-products [69]-[72], as well as from natural sources such as fruits, juices, and botanical extracts [56], [73]-[78]. Historically, membrane technology in natural product processing primarily targeted turbidity reduction in juices [76], [79]. While this "clarification" process removes suspended solids and various components, contemporary membrane operations provide additional benefits beyond removing high-molecular-weight compounds; they enable selective recovery of specific constituents in either the permeate or retentate streams, depending on the membrane selected.

1.4.1.1 MF in concentrating/recovering polyphenols or natural bioactives

MF uses membranes with large pore sizes (0.1–10 μm) and is ideal for removing emulsions, colloids, suspended particles, spoilage microorganisms, and high-molecular-weight compounds [80]. This filtration process can positively impact the physical properties of natural products, such as improving colorimetric analysis by removing suspended solids [81]. Moreover, the high efficiency of MF membranes in removing these components facilitates the production of clarified permeates enriched in low-molecular-weight solutes. For instance, several valuable solutes have been recovered in permeate streams, including vitamin C [62], malic acid, sugars [82], and polyphenols [83], [84]. While the molecular weight of these compounds, such as polyphenols, ranges from 150 to 600 Da [85], [86], suggesting potential recovery rates of nearly 100%, the actual recovery rates range from 45% to 100%. Membrane fouling plays a significant role in solute retention, attributed to partial pore blocking, complete pore blocking, cake formation, and internal pore blocking. [47], [87].

Dos Santos *et al.* [88] investigated membrane separation processes (MSP) to clarify extracts rich in betalains from red beet stalks, which are typically treated as agro-industrial waste despite their potential as natural food colorants. The researchers employed a two-stage process combining MF with a 0.05 μm nominal-pore-size ceramic membrane, followed by UF with a 20 kDa membrane. The results showed that the MF membrane retained approximately 20% of betanin, while the UF membrane retained about 35%. During processing, MF showed approximately 75% reduction in permeate flux after 4 hours, while UF showed about 60% reduction after 45 minutes, indicating significant fouling and concentration polarization.

1.4.1.2 UF in concentrating/recovering polyphenols or natural bioactives

UF membranes have smaller pore sizes (0.01–0.1 μm) and represent the predominant membrane-based separation methodology for isolating valuable components from natural products, demonstrating superior efficiency compared to MF processes. UF technology exhibits separation efficiencies ranging from 56% to 100%. The permeate streams typically contain recovered bioactive compounds, including antioxidant components [89], betacyanins, betaxanthins, and glutamic acid [56], [90], polyphenols [58], [91], flavonoids [57], and anthocyanins [92]. While MWCO represents a primary consideration in membrane selection, it is not an absolute barrier to solute recovery. The asymmetric structure of membrane pores often exhibits variable MWCOs, facilitating the separation of lower-molecular-weight components [93], [94]. This structural characteristic enables UF membranes with narrow pore sizes (1-5 kDa) to achieve high recovery rates of low molecular weight compounds, including various anthocyanins (cyanidin 3,5-O-diglucoside, delphinidin 3-O-glucoside, pelargonidin 3,5-O-diglucoside) [62] and polyphenols [91]. Indeed, these narrow-pore-size membranes operate at the technological boundary between UF and NF.

Cassano *et al.* [59] investigated an integrated membrane process combining UF and OD to produce concentrated pomegranate juice while preserving its nutritional value and bioactive compounds. The hollow-fiber UF process showed low rejection rates for polyphenols (16.5%) and anthocyanins (11.7%) and complete removal of suspended solids. The clarified juice was then concentrated using OD at ambient temperature, increasing the TSS content from 162 g/kg to 520 g/kg. Another study by Wei *et al.* [95] investigated the separation characteristics of binary mixtures of rutin and glucose using Pellicon-2 regenerated cellulose UF membrane with a MWCO of 1000 Da. For the separation of rutin (in the retentate) and glucose (in the permeate), the best results were obtained at rutin enrichment of 2.9 and recovery of 72.5%, respectively. Also, diafiltration further improved the performance of this system, with only approximately 11% of glucose in the retentate. Díaz-Reinoso *et al.* [65] also investigated UF to concentrate antioxidant compounds from aqueous extracts of *Castanea sativa* (chestnut) leaves. The authors scaled up an aqueous extraction process of chestnut leaves and employed a sequential UF system using two membranes (5 kDa and 10 kDa) to concentrate the active phenolic compounds. Two configurations were evaluated: Configuration I involved direct sequential filtration, while Configuration II incorporated batch dilution of the retentate between filtration steps. Membrane fouling was analyzed using four models: total pore blocking, standard pore blocking, intermediate pore blocking, and cake layer formation. For the 5 kDa membrane, the cake layer formation model provided the best fit, while the standard pore-blocking model best described the 10 kDa membrane behavior in Configuration II. The study found that both membranes exhibited similar rejection patterns for phenolic compounds and soluble proteins, with no preferential separation between them. The final retentate product contained 40% phenolic compounds and demonstrated radical-scavenging capacity comparable to that of Trolox and BHA (synthetic antioxidants). Analysis revealed the selective concentration of certain flavonoids (rutin, quercetin, apigenin) in the retentate, while some simple phenolics were found in the permeate.

Acosta *et al.* [96] also investigated the feasibility of using UF membranes to selectively separate ellagitannins from blackberry (*Rubus adenotrichus Schltdl.*) juice. The researchers tested six organic tight UF membranes with nominal MWCOs ranging from 1 to 150 kDa. Experiments were conducted at a constant temperature of 30°C, cross-flow velocity of 0.3 m/s, and varying pressures (0.5-3 MPa). The results showed that complete retention (100%) of ellagitannins was achieved by all membranes except for the membrane with a nominal MWCO of 150 kDa when pressure exceeded 1 MPa.

Anthocyanin retention increased with pressure for all membranes, reaching over 90% at 3 MPa. The membrane with a nominal MWCO of 2 kDa showed the highest anthocyanin flux at 2 MPa, making it the most promising for fractionating blackberry polyphenolic compounds.

1.4.1.3 NF in concentrating/recovering polyphenols or natural bioactives

Unlike MF and UF, which typically recover solutes in the permeate stream, NF proves more effective by concentrating target compounds in the retentate. NF membranes feature even smaller pores (1–10 nm) that can filter out divalent and larger monovalent ions, making them suitable for water softening, desalination, and the removal of organic compounds such as pesticides. Recovery rates with NF processes are notably high, ranging from over 85% to nearly 100%. This efficiency largely depends on the membrane material and the specific interactions between solutes and the membrane surface [65]. NF is particularly effective in recovering high-value bioactives such as phenolic compounds, anthocyanins, and flavonoids. Accordingly, NF has been recognized as an emerging technology for producing nutraceuticals from agri-food sources and by-products [93], [97]. For phenolic compounds specifically, processing natural sources appears to be a more economically viable approach for industrial applications [98]-[100].

Cai *et al.* [101] investigated the rejection mechanisms of six typical phenolic compounds in fruit juice during NF using model solutions with two commercial NF membranes (VNF1 and VNF2). For the VNF1 membrane, rejection rates demonstrated clear stratification based on molecular structure complexity: higher molecular weight compounds showed superior retention (rutin: 99.14%, chlorogenic acid: 96.80%), while simpler phenolic structures exhibited moderate to low rejection (caffeic acid: 55.04%, ferulic acid: 45.82%, protocatechuate: 26.20%, gallic acid: 18.91%). The VNF2 membrane displayed generally higher rejection rates but with notable differences in compound-specific behavior: both rutin and chlorogenic acid achieved near-complete rejection (99.75% and 98.23%, respectively), while gallic acid and protocatechuate showed substantial retention (86.34% and 79.97%), and caffeic acid and ferulic acid demonstrated identical moderate rejection (39.69%). Operational parameters significantly influenced separation efficiency, with gallic acid rejection in VNF1 increasing from 8% to 22% as pressure increased from 2 to 8 bar. VNF2 showed greater pressure sensitivity, with rejection rising from 58% to 83% over the same pressure range. Uyttebroek *et al.* [102] investigated the extraction and concentration of phenolic compounds from apple pomace using NF technology at laboratory and pilot scales, coupled with a techno-economic assessment. In the membrane screening phase, various commercial NF membranes were evaluated, with NFX ultimately selected for its high retention of phenolic compounds (95-99%) and suitable permeate flux. Laboratory-scale concentration tests achieved a volume concentration factor (VCF) of 32.4, resulting in an 18.6-fold increase in phenolic compound concentration. At the pilot scale, the process was scaled up using a spiral-wound membrane module, eventually achieving a total VCF of 28.5 and concentrating the ten selected phenolic compounds and quinic acid by a factor of 21.1 (from 59.5 mg/L to 1256.1 mg/L). Tundis *et al.* [103] investigated the use of three commercial NF membranes (NP010, ETNA 01PP (both 1000 Da), and NP030 (400 Da)) to concentrate bioactive compounds from elderberry (*Sambucus nigra L.*) juice. HPLC analysis revealed that the main constituents of the untreated elderberry juice were cyanidin-3-O-sambubioside (300.7 mg/L), cyanidin-3-O-glucoside (147.1 mg/L), and quercetin (142.9 mg/L). All selected membranes showed high rejection rates (>75%) for anthocyanins, quercetin-3-O-rutinoside, and astragalin, with lower rejections (25-42%) for protocatechuic acid and catechin. The NP030 membrane, with the lowest MWCO, exhibited the highest rejection for all bioactive compounds, completely rejecting anthocyanins and quercetin-3-O-rutinoside. Mejia *et al.* [104] employed NF membranes to extract and purify phenolic compounds from grape pomace. The results of the study showed that the CA400-22 membrane had the highest permeate flux and the best separation performance between sugars and phenolic compounds, with rejection coefficients of 19% and 12% for glucose and fructose, respectively, and 73% and 92% for TPC and proanthocyanidins, respectively.

1.5 Research Gaps

The following gaps were considered for this research work based on the literature survey.

I. Limited studies were found on the concentration of model solutions of natural phenolic compounds using NF, especially betanin and rutin.

II. The reported studies lack detailed analyses of the membrane transport phenomenon, and only a few scale-up studies have been conducted to assess NF process viability at larger scales.

III. Limited studies were found on the concentration of phenolic compounds from real sources using NF.

1.6 Research Objectives

The research aimed to apply the membrane-based operation to concentrate different phenolic compounds. The detailed objectives of the present study are as follows.

I. To examine the performance of the HFT-NF 150 membrane in concentrating different molecular weight phenolic compounds.

II. Mathematical modeling, determination of the transport parameters, and optimization of the operating parameters.

III. Scale-up of the process using a mathematical model to analyze its viability in a commercial operation.

IV. Concentrate a phenolic compound from a natural resource using an NF membrane.

1.7 Overview of the Thesis

The work embodied in the thesis entitled **"Applications of membrane-based operations in separation of natural phenolic compounds"** has been divided into SEVEN chapters to fulfill the above objectives.

Chapter 1 provides the foundation for understanding the research context by introducing the background of phenolic compounds, their sources, and their importance. It also outlines traditional separation methods and their inherent limitations for the separation and concentration of phenolic compounds, providing an overview, identifying research gaps, and establishing the significance of the proposed work. It also presents a comprehensive literature review of membrane technology fundamentals, progress in the separation/concentration of phenolic compounds, and the associated challenges. It also highlights critical research gaps and a roadmap to position membrane filtration as a viable, efficient, and sustainable approach for concentration.

Chapter 2 focuses on the theoretical foundations and mathematical modeling essential to understanding membrane transport phenomena. This chapter explains the mass transfer mechanisms in membrane processes by introducing the basics of several models, including the Solution-Diffusion (S-D) and Pore Flow (P-F) models, with particular emphasis on the Spiegler-Kedem (S-K) model. The chapter provides an overview of the mathematical equation of the S-K model used to determine membrane transport parameters. The theoretical underpinnings of the S-K model approach are presented in detail, along with the governing equations and computational frameworks utilized. A variance-based sensitivity analysis is also given to understand the impact and interdependence of various input variables on membrane performance. This chapter also includes the detailed theory and simulation equations used for the scale-up studies, emphasizing increasing the filtration area to process larger volumes within the specified timeframes. Chapter 2 lays the groundwork for the successful implementation and analysis within the broader context of the thesis.

Chapter 3 details the key instrumentation and experimental procedure employed in the concentration/separation of different phenolic compounds. The chapter discusses the extensive characterization techniques used to analyze the membrane and its output characteristics, including measurements of permeate flow rates and concentrations. Furthermore, the self-assembled experimental setup, including the NF membrane test cell and other key components, is comprehensively covered. It then describes the step-by-step experimental procedures for NF and the optimization technique used. Emphasis is placed on the design considerations, operational parameters, and control mechanisms to ensure data reliability.

Chapter 4 investigates the potential of NF for the recovery of rutin from different model solutions. The aim was to optimize the separation process and validate a mathematical model for mass transport. The chapter systematically evaluates the performance of the HFT-NF 150 membrane across 5 binary systems of rutin + water with concentrations ranging from 20 mg/L to 100 mg/L. Each binary system was analyzed for 25 points by varying pressure (2×10^6 Pa - 6×10^6 Pa) and feed flow rates (6 L/h – 36 L/h). The chapter also discusses the results of the mathematical modeling performed using the three-parameter S-K model. The key parameters, such as hydraulic permeability, solute permeability, and reflection coefficient, were optimized as 5.52×10^{-11} m^3/m^2sPa, 2.15×10^{-7} m/s, and 0.98, respectively. The experimental values were then compared with the theoretical values to validate the results using the S-K model. The validation of 125 data points showed low mean absolute percentage errors (MAPEs) for permeate flow rate (16.6%), concentration (14.85%), and rejection percentage (0.46%). The chapter also presents the findings of a global sensitivity analysis, examining the sensitivities of various operating conditions and membrane parameters. The chapter then discusses the performance of the scale-up simulations for rutin to check the overall system's efficiency.

Chapter 5 explores the use of NF to concentrate betanin from model beetroot solutions, including the experimental outcomes for 5 binary systems of betanin and water using the polyamide HFT-NF 150 membrane, with concentrations ranging from 0.1 g/L to 0.5 g/L. Each binary system was analyzed at 25 points, varying pressure (0.2 MPa – 0.6 MPa) and feed flow rate (200 mL/min – 600 mL/min). The chapter presents two optimization methods and their MAPE values. The best-fit optimization method involved optimizing all parameters, such as hydraulic permeability, solute permeability, and reflection coefficient, mass transfer coefficients a and b as 5.046×10^{-11} m^3/m^2sPa, 4.35×10^{-7} m/s, 0.967, 1.285×10^{-2}, 1.355×10^{-1}, respectively. The chapter also uses global sensitivity analysis to discuss the sensitivities of various operating conditions and membrane parameters. The chapter then discusses the performance of the scale-up simulations for betanin to check the overall system's efficiency.

Chapter 6 presents the significant findings from experiments conducted to determine betanin concentration in beetroot juice. The chapter integrates the description of a self-assembled hybrid system (UF+NF) for the experimental procedure. The chapter also includes the experimental outcomes from 125 filtration data sets through a hybrid system, varying time (5 min - 25 min), pressure (2 bar - 6 bar), and feed flow rate (200 mL/min - 600 mL/min). This chapter also discusses the effects of various operating conditions on permeate flux and rejection, provides a detailed account of membrane fouling behavior, and compares different fouling mechanisms.

Chapter 7 discusses the significant findings that will help conclude the thesis. It also presents the social impact of the research on the concentration of different phenolic compounds. The chapter outlines the research outcomes and provides a view of the open path for future work. Key suggestions include developing hybrid processes, adopting a data-driven modeling approach for process optimization, and advancing membrane technology.

The thesis employs a chapter-wise reference system to ensure clear organization and easy access to source materials.

References

[1] M. Daglia, "Polyphenols as antimicrobial agents," *Curr. Opin. Biotechnol.*, vol. 23, no. 2, pp. 174–181, 2012, doi: 10.1016/j.copbio.2011.08.007

[2] N. Balasundram, K. Sundram, and S. Samman, "Phenolic compounds in plants and agri-industrial by-products: Antioxidant activity, occurrence, and potential uses," *Food Chem.*, vol. 99, no. 1, pp. 191–203, 2006, doi: 10.1016/j.foodchem.2005.07.042

[3] S. R. Shah, C. I. Ukaegbu, H. A. Hamid, and O. R. Alara, "Evaluation of antioxidant and antibacterial activities of the stems of *Flammulina velutipes* and *Hypsizygus tessellatus* (white and brown var.) extracted with different solvents," *J. Food Meas. Charact.*, vol. 12, pp. 1947-1961, 2018, doi: 10.1007/s11694-018-9810-8

[4] H. Tapiero, K. D., and G., "Polyphenols: do they play a role in the prevention of human pathologies?" *Biomed Pharmacother*, vol. 56, no. 4, pp. 200–207, 2002, doi: 10.1016/S0753-3322(02)00178-6

[5] C. Manach, G. Williamson, C. Morand, A. Scalbert, and C. Rémésy, "Bioavailability and bioefficacy of polyphenols in humans. I. Review of 97 bioavailability studies," *Am. J. Clin. Nutr.*, vol. 81, no. 1, pp. 230–242, 2005, doi: 10.1093/ajcn/81.1.230s

[6] S. Petti and C. Scully, "Polyphenols, oral health and disease: A review," *J. Dent.*, vol. 37, no. 6, pp. 413–423, 2009, doi: 10.1016/j.jdent.2009.02.003

[7] R. Tsao, "Chemistry and biochemistry of dietary polyphenols," *Nutrients*, vol. 2, no. 12, pp. 1231–1246, 2010, doi: 10.3390/nu2121231

[8] J. Shi, H. Nawaz, J. Pohorly, G. Mittal, Y. Kakuda, and Y. Jiang, "Extraction of polyphenolics from plant material for functional foods - Engineering and technology," *Food Rev. Int.*, vol. 21, no. 1, pp. 139–166, 2005, doi: 10.1081/FRI-200040606

[9] M. Naczk and F. Shahidi, "Phenolics in cereals, fruits and vegetables: Occurrence, extraction and analysis," *J. Pharm. Biomed. Anal.*, vol. 41, no. 5,

pp. 1523–1542, 2006, doi: 10.1016/j.jpba.2006.04.002

[10] O. R. Alara, N. H. Abdurahman, and C. I. Ukaegbu, "Extraction of phenolic compounds: A review," *Curr. Res. Food Sci.*, vol. 4, pp. 200–214, 2021, doi: 10.1016/j.crfs.2021.03.011

[11] Y. Cai, Q. Luo, M. Sun, and H. Corke, "Antioxidant activity and phenolic compounds of 112 traditional Chinese medicinal plants associated with anticancer," *Life Sci.*, vol. 74, no. 17, pp. 2157–2184, 2004, doi: 10.1016/j.lfs.2003.09.047

[12] Y. Z. Cai, Mei Sun, Jie Xing, Q. Luo, and H. Corke, "Structure-radical scavenging activity relationships of phenolic compounds from traditional Chinese medicinal plants," *Life Sci.*, vol. 78, no. 25, pp. 2872–2888, 2006, doi: 10.1016/j.lfs.2005.11.004

[13] A. Wojdyło, J. Oszmiański, and R. Czemerys, "Antioxidant activity and phenolic compounds in 32 selected herbs," *Food Chem.*, vol. 105, no. 3, pp. 940–949, 2007, doi: 10.1016/j.foodchem.2007.04.038

[14] F. Shahidi, P. K. Janitha, and P. D. Wanasundara, "Phenolic Antioxidants," Crit. Rev. Food Sci. Nutr., vol. 32, no. 1, pp. 67-103, 2009, doi: 10.1080/10408399209527581

[15] B. Shan, Y. Z. Cai, M. Sun, and H. Corke, "Antioxidant capacity of 26 spice extracts and characterization of their phenolic constituents," *J. Agric. Food Chem.*, vol. 53, no. 20, pp. 7749–7759, 2005, doi: 10.1021/jf051513y

[16] Y. Cai, M. Sun, and H. Corke, "Antioxidant activity of betalains from plants of the *Amaranthaceae*," *J. Agric. Food Chem.*, vol. 51, no. 8, pp. 2288–2294, 2003, doi: 10.1021/jf030045u

[17] C. A. Rice-Evans, N. J. Miller, and G. Paganga, "Antioxidant properties of phenolic compounds," *Trends Plant Sci.*, vol. 2, no. 4, pp. 152–159, 1997, doi: 10.1016/S1360-1385(97)01018-2

[18] A. Smeriglio, D. Barreca, E. Bellocco, and D. Trombetta, "Proanthocyanidins and hydrolysable tannins: occurrence, dietary intake and pharmacological

effects," *Br. J. Pharmacol.*, vol. 174, no. 11, pp. 1244–1262, 2017, doi: 10.1111/bph.13630

[19] C. G. Fraga, K. D. Croft, D. O. Kennedy, and F. A. Tomás-Barberán, "The effects of polyphenols and other bioactives on human health," *Food Funct.*, vol. 10, no. 2, pp. 514–528, 2019, doi: 10.1039/c8fo01997e

[20] N. Xia, A. Daiber, U. Förstermann, and H. Li, "Antioxidant effects of resveratrol in the cardiovascular system," *Br. J. Pharmacol.*, vol. 174, no. 12, pp. 1633–1646, 2017, doi: 10.1111/bph.13492

[21] R. A. Pietrofesa *et al.*, "Flaxseed lignans enriched in secoisolariciresinol diglucoside prevent acute asbestos-induced peritoneal inflammation in mice," *Carcinogenesis*, vol. 37, no. 2, pp. 177–187, 2015, doi: 10.1093/carcin/bgv174

[22] J. Dai and R. J. Mumper, "Plant phenolics: Extraction, analysis and their antioxidant and anticancer properties," *Molecules*, vol. 15, no. 10, pp. 7313–7352, 2010, doi: 10.3390/molecules15107313

[23] D. R. Kammerer, Z. S. Saleh, R. Carle, and R. A. Stanley, "Adsorptive recovery of phenolic compounds from apple juice," *Eur. Food Res. Technol.*, vol. 224, no. 5, pp. 605–613, 2007, doi: 10.1007/s00217-006-0346-5

[24] P. Tapia-Quirós *et al.*, "Recovery of polyphenols from agri-food by-products: The olive oil and winery industries cases," *Foods*, vol. 11, no. 3, pp. 1–26, 2022, doi: 10.3390/foods11030362

[25] I. Drevelegka and A. M. Goula, "Recovery of grape pomace phenolic compounds through optimized extraction and adsorption processes," *Chem. Eng. Process. - Process Intensif.*, vol. 149, pp. 107845, 2020, doi: 10.1016/j.cep.2020.107845

[26] A. K. Sandhu and L. Gu, "Adsorption/desorption characteristics and separation of anthocyanins from muscadine (*Vitis rotundifolia*) juice pomace using macroporous adsorbent resins," *J. Agric. Food Chem.*, vol. 61, no. 7, pp. 1441–1448, 2013, doi: 10.1021/jf3036148

[27] Y. Dong *et al.*, "Absorption and desorption behaviour of the flavonoids from

Glycyrrhiza glabra L. leaf on macroporous adsorption resins," *Food Chem.*, vol. 168, pp. 538–545, 2015, doi: 10.1016/j.foodchem.2014.07.109

[28] T. J. Buran, A. K. Sandhu, Z. Li, C. R. Rock, W. W. Yang, and L. Gu, "Adsorption/desorption characteristics and separation of anthocyanins and polyphenols from blueberries using macroporous adsorbent resins," *J. Food Eng.*, vol. 128, pp. 167–173, 2014, doi: 10.1016/j.jfoodeng.2013.12.029

[29] L. Campone, R. Celano, S. Rizzo, A. L. Piccinelli, L. Rastrelli, and M. Russo, "Development of an enriched polyphenol (natural antioxidant) extract from orange juice (*Citrus sinensis*) by adsorption on macroporous resins," *J. Food Qual.*, vol. 2020, no. 1, pp. 1-9, 2020, doi: 10.1155/2020/1251957

[30] M. L. Soto, A. Moure, H. Domínguez, and J. C. Parajó, "Recovery, concentration and purification of phenolic compounds by adsorption: A review," *J. Food Eng.*, vol. 105, no. 1, pp. 1–27, 2011, doi: 10.1016/j.jfoodeng.2011.02.010

[31] T. G. Gini and G. Jeya Jothi, " Column chromatography and HPLC analysis of phenolic compounds in the fractions of Salvinia molesta mitchell," *Egypt. J. Basic Appl. Sci.*, vol. 5, no. 3, pp. 197–203, 2018, doi: 10.1016/j.ejbas.2018.05.010

[32] F. Cacciola, P. Jandera, Z. Hajdú, P. Česla, and L. Mondello, "Comprehensive two-dimensional liquid chromatography with parallel gradients for separation of phenolic and flavone antioxidants," *J. Chromatogr. A*, vol. 1149, no. 1, pp. 73–87, 2007, doi: 10.1016/j.chroma.2007.01.119

[33] M. A. Rodríguez-Delgado, S. Malovaná, J. P. Pérez, T. Borges, and F. J. García Montelongo, "Separation of phenolic compounds by high-performance liquid chromatography with absorbance and fluorimetric detection," *J. Chromatogr. A*, vol. 912, no. 2, pp. 249–257, 2001, doi: 10.1016/S0021-9673(01)00598-2

[34] R. Amarowicz, P. P. Kolodziejczyk, and R. B. Pegg, "Chromatographic separation of phenolic compounds from rapeseed by a Sephadex LH-20 column with ethanol as the mobile phase," *J. Liq. Chromatogr. Relat. Technol.*, vol. 26, no. 13, pp. 2157–2165, 2003, doi: 10.1081/JLC-120022400

[35] C. D. Stalikas, "Extraction, separation, and detection methods for phenolic acids and flavonoids," *J. Sep. Sci.*, vol. 30, no. 18, pp. 3268–3295, 2007, doi: 10.1002/jssc.200700261

[36] I. Susanti, R. Pratiwi, Y. Rosandi, and A. N. Hasanah, "Separation methods of phenolic compounds from plant extract as antioxidant agents candidate," *Plants*, vol. 13, no. 7, pp. 1–38, 2024, doi: 10.3390/plants13070965

[37] X. Ni *et al.*, "Selective liquid-liquid extraction of natural phenolic compounds using amino acid ionic liquids: A case of α-tocopherol and methyl linoleate separation," *Ind. Eng. Chem. Res.*, vol. 51, no. 18, pp. 6480–6488, 2012, doi: 10.1021/ie201682h

[38] M. Pinelo, A. Ruiz-Rodríguez, J. Sineiro, F. J. Señoráns, G. Reglero, and M. J. Núñez, "Supercritical fluid and solid-liquid extraction of phenolic antioxidants from grape pomace: A comparative study," *Eur. Food Res. Technol.*, vol. 226, no. 1–2, pp. 199–205, 2007, doi: 10.1007/s00217-006-0526-3

[39] O. R. Alara, N. H. Abdurahman, and C. I. Ukaegbu, "Soxhlet extraction of phenolic compounds from Vernonia cinerea leaves and its antioxidant activity," *J. Appl. Res. Med. Aromat. Plants*, vol. 11, pp. 12–17, 2018, doi: 10.1016/j.jarmap.2018.07.003

[40] A. Bucić-Kojić, M. Planinić, S. Tomas, M. Bilić, and D. Velić, "Study of solid-liquid extraction kinetics of total polyphenols from grape seeds," *J. Food Eng.*, vol. 81, no. 1, pp. 236–242, 2007, doi: 10.1016/j.jfoodeng.2006.10.027

[41] P. Ghosh, R. C. Pradhan, S. Mishra, and P. K. Rout, "Quantification and concentration of anthocyanidin from Indian blackberry (*Jamun*) by combination of ultra- and nano-filtrations," *Food Bioprocess Technol.*, vol. 11, no. 12, pp. 2194–2203, 2018, doi: 10.1007/s11947-018-2176-4

[42] A. Cassano, C. Conidi, R. Ruby-Figueroa, and R. Castro-Muñoz, "Nanofiltration and tight ultrafiltration membranes for the recovery of polyphenols from agro-food by-products," *Int. J. Mol. Sci.*, vol. 19, no. 2, pp. 351, 2018, doi: 10.3390/ijms19020351

[43] K. Staszak, "Membrane processes," *Phys. Sci. Rev.*, vol. 2, no. 12, pp. 20170142, 2017, doi: 10.1515/psr-2017-0142

[44] B. Van Der Bruggen, L. Lejon, and C. Vandecasteele, "Reuse, treatment, and discharge of the concentrate of pressure-driven membrane processes," *Environ. Sci. Technol.*, vol. 37, no. 17, pp. 3733–3738, 2003, doi: 10.1021/es0201754

[45] B. Van Der Bruggen, C. Vandecasteele, T. Van Gestel, W. Doyen, and R. Leysen, "A review of pressure-driven membrane processes in wastewater treatment and drinking water production," *Environ. Prog.*, vol. 22, no. 1, pp. 46–56, 2003, doi: 10.1002/ep.670220116

[46] B. Van Der Bruggen, J. Schaep, D. Wilms, and C. Vandecasteele, "Influence of molecular size, polarity, and charge on the retention of organic molecules by nanofiltration," *J. Memb. Sci.*, vol. 156, no. 1, pp. 29–41, 1999, doi: 10.1016/S0376-7388(98)00326-3

[47] A. Cassano, M. Marchio, and E. Drioli, "Clarification of blood orange juice by ultrafiltration: Analyses of operating parameters, membrane fouling and juice quality," *Desalination*, vol. 212, no. 1–3, pp. 15–27, 2007, doi: 10.1016/j.desal.2006.08.013

[48] A. Cassano, L. Donato, and E. Drioli, "Ultrafiltration of kiwifruit juice: Operating parameters, juice quality and membrane fouling," *J. Food Eng.*, vol. 79, no. 2, pp. 613–621, 2007, doi: 10.1016/j.jfoodeng.2006.02.020

[49] D. Trishitman, P. S. Negi, and N. K. Rastogi, "Concentration of pomegranate juice by forward osmosis or thermal evaporation and its shelf-life kinetic studies," *Food Chem.*, vol. 399, pp. 133972, 2023, doi: 10.1016/j.foodchem.2022.133972

[50] M. Gaglianò, C. Conidi, G. De Luca, and A. Cassano, "Partial removal of sugar from apple juice by nanofiltration and discontinuous diafiltration," *Membranes (Basel)*, vol. 12, no. 7, pp. 712, 2022, doi: 10.3390/membranes12070712

[51] D. Trishitman, P. S. Negi, and N. K. Rastogi, "Concentration of beetroot juice colorant (betalains) by forward osmosis and its comparison with thermal

processing," *LWT*, vol. 145, pp. 111522, 2021, doi: https://doi.org/10.1016/j.lwt.2021.111522

[52] B. L. Koop *et al.*, "Bioactive compounds from jambolan (*Syzygium cumini L.*) extract concentrated by ultra- and nanofiltration: a potential natural antioxidant for food," *Plant Foods Hum. Nutr.*, vol. 76, no. 1, pp. 90–97, 2021, doi: 10.1007/s11130-021-00878-8

[53] J. Wang *et al.*, "Low-energy membrane-based processes to concentrate and encapsulate polyphenols from carob pulp," *J. Food Eng.*, vol. 281, pp. 109996, 2020, doi: 10.1016/j.jfoodeng.2020.109996

[54] E. Yilmaz and P. O. Bagci, "Production of phytotherapeutics from broccoli juice by integrated membrane processes," *Food Chem.*, vol. 242, pp. 264–271, 2018, doi: 10.1016/j.foodchem.2017.09.056

[55] L. Terki *et al.*, "Implementation of osmotic membrane distillation with various hydrophobic porous membranes for concentration of sugar solutions and preservation of the quality of cactus pear juice," *J. Food Eng.*, vol. 230, pp. 28–38, 2018, doi: https://doi.org/10.1016/j.jfoodeng.2018.02.023

[56] A. Cassano, C. Conidi, R. Timpone, M. D'Avella, and E. Drioli, "A membrane-based process for the clarification and the concentration of the cactus pear juice," *J. Food Eng.*, vol. 80, no. 3, pp. 914–921, 2007, doi: 10.1016/j.jfoodeng.2006.08.005

[57] A. Cassano, C. Conidi, and E. Drioli, "Physico-chemical parameters of cactus pear (*Opuntia ficus-indica*) juice clarified by microfiltration and ultrafiltration processes," *desal.*, vol. 250, pp. 1101–1104, 2010, doi: 10.1016/j.desal.2009.09.117

[58] A. Cassano, F. Tasselli, C. Conidi, and E. Drioli, "Ultrafiltration of Clementine mandarin juice by hollow fibre membranes," *Desalination*, vol. 241, no. 1–3, pp. 302–308, 2009, doi: 10.1016/j.desal.2007.10.102.

[59] A. Cassano, C. Conidi, and E. Drioli, "Clarification and concentration of pomegranate juice (*Punica granatum L.*) using membrane processes," *J. Food*

Eng., vol. 107, no. 3–4, pp. 366–373, 2011, doi: 10.1016/j.jfoodeng.2011.07.002

[60] A. Cassano, L. Donato, C. Conidi, and E. Drioli, “Recovery of bioactive compounds in kiwifruit juice by ultrafiltration,” *Innov. Food Sci. Emerg. Technol.*, vol. 9, no. 4, pp. 556–562, 2008, doi: 10.1016/j.ifset.2008.03.004

[61] C. Conidi, A. Cassano, and E. Drioli, “A membrane-based study for the recovery of polyphenols from bergamot juice,” *J. Memb. Sci.*, vol. 375, no. 1–2, pp. 182–190, 2011, doi: 10.1016/j.memsci.2011.03.035

[62] M. Cisse, F. Vaillant, D. Soro, M. Reynes, and M. Dornier, “Crossflow microfiltration for the cold stabilization of roselle (*Hibiscus sabdariffa L.*) extract,” *J. Food Eng.*, vol. 106, no. 1, pp. 20–27, 2011, doi: 10.1016/j.jfoodeng.2011.04.001

[63] M. Cissé, F. Vaillant, D. Pallet, and M. Dornier, “Selecting ultrafiltration and nanofiltration membranes to concentrate anthocyanins from roselle extract (*Hibiscus sabdariffa L.*),” *Food Res. Int.*, vol. 44, no. 9, pp. 2607–2614, 2011, doi: 10.1016/j.foodres.2011.04.046

[64] P. M. Chornomaz, C. Pagliero, J. Marchese, and N. A. Ochoa, “Impact of structural and textural membrane properties on lemon juice clarification,” *Food Bioprod. Process.*, vol. 91, no. 2, pp. 67–73, 2013, doi: 10.1016/j.fbp.2012.12.001

[65] B. Díaz-Reinoso, A. Moure, H. Domínguez, and J. C. Parajó, “Membrane concentration of antioxidants from Castanea sativa leaves aqueous extracts,” *Chem. Eng. J.*, vol. 175, no. 1, pp. 95–102, 2011, doi: 10.1016/j.cej.2011.09.059

[66] B. Tylkowski, I. Tsibranska, R. Kochanov, G. Peev, and M. Giamberini, “Concentration of biologically active compounds extracted from *Sideritis ssp. L.* by nanofiltration,” *Food Bioprod. Process.*, vol. 89, no. 4, pp. 307–314, 2011, doi: 10.1016/j.fbp.2010.11.003

[67] G. T. Vladisavljević, P. Vukosavljević, and M. S. Veljović, “Clarification of red raspberry juice using microfiltration with gas backwashing: A viable

strategy to maximize permeate flux and minimize a loss of anthocyanins," *Food Bioprod. Process.*, vol. 91, no. 4, pp. 473–480, 2013, doi: 10.1016/j.fbp.2013.05.004

[68] K. R. Dorneles, A. C. Da Rocha, V. L. Cardoso, & M. H. M. Reis, "Recovery of health-promoting phenolic compounds from clove basil (*Ocimum gratissimum L.*) by aqueous extraction and ultrafiltration," *Food Bioprod. Process.*, vol 149, pp. 392-400, 2024, doi: 10.1016/j.fbp.2024.12.005

[69] R. Castro-Muñoz, J. Yáñez-Fernández, and V. Fíla, "Phenolic compounds recovered from agro-food by-products using membrane technologies: An overview," *Food Chem.*, vol. 213, pp. 753–762, 2016, doi: 10.1016/j.foodchem.2016.07.030

[70] C. M. Galanakis, "Recovery of high added-value components from food wastes: Conventional, emerging technologies and commercialized applications," *Trends Food Sci. Technol.*, vol. 26, no. 2, pp. 68–87, 2012, doi: 10.1016/j.tifs.2012.03.003

[71] A. Cassano, C. Conidi, C. M. Galanakis, and R. Castro-Muñoz, "Recovery of polyphenols from olive mill wastewaters by membrane operations," *Membr. Technol. Biorefining*, pp. 163–187, 2016, doi: 10.1016/B978-0-08-100451-7.00007-4

[72] J. de Toledo Guimarães, E. K. Silva, M. Q. de Freitas, M. A. de Almeida Meireles, and A. G. da Cruz, "Non-thermal emerging technologies and their effects on the functional properties of dairy products," *Curr. Opin. Food Sci.*, vol. 22, pp. 62–66, 2018, doi: 10.1016/j.cofs.2018.01.015

[73] F. Destani, A. Cassano, A. Fazio, J. P. Vincken, and B. Gabriele, "Recovery and concentration of phenolic compounds in blood orange juice by membrane operations," *J. Food Eng.*, vol. 117, no. 3, pp. 263–271, 2013, doi: 10.1016/j.jfoodeng.2013.03.001

[74] A. N. Negrão Murakami *et al.*, "Concentration of phenolic compounds in aqueous mate (*Ilex paraguariensis A. St. Hil*) extract through nanofiltration," *Lwt – Food Sci. Tech.*, vol. 44, no. 10, pp. 2211–2216, 2011, doi:

10.1016/j.lwt.2011.06.002

[75] Z. Ma *et al.*, "A comprehensive review on the recent advances in membrane-based processes for fruit juice concentration," *Food Bioprod. Process.*, vol. 145, pp. 42–66, 2024, doi: 10.1016/j.fbp.2024.02.010

[76] Z. Zhu, J. Luo, L. Ding, O. Bals, M. Y. Jaffrin, and E. Vorobiev, "Chicory juice clarification by membrane filtration using rotating disk module," *J. Food Eng.*, vol. 115, no. 2, pp. 264–271, 2013, doi: 10.1016/j.jfoodeng.2012.10.028

[77] A. P. Echavarría, C. Torras, J. Pagán, and A. Ibarz, "Fruit juice processing and membrane technology application," *Food Eng. Rev.*, vol. 3, no. 3–4, pp. 136–158, 2011, doi: 10.1007/s12393-011-9042-8

[78] R. Castro-Muñoz and V. Fíla, "Membrane-based technologies as an emerging tool for separating high-added-value compounds from natural products," *Trends Food Sci. Technol.*, vol. 82, pp. 8–20, 2018, doi: 10.1016/j.tifs.2018.09.017

[79] H. Mirsaeedghazi, Z. Emam-Djomeh, S. M. Mousavi, A. Aroujalian, and M. Navidbakhsh, "Clarification of pomegranate juice by microfiltration with PVDF membranes," *Desalination*, vol. 264, no. 3, pp. 243–248, 2010, doi: 10.1016/j.desal.2010.03.031

[80] R. Castro-Muñoz, B. E. Barragán-Huerta, V. Fíla, P. C. Denis, and R. Ruby-Figueroa, "Current role of membrane technology: From the treatment of agro-industrial by-products up to the valorization of valuable compounds," *Waste Biomass Valori.*, vol. 9, no. 4, pp. 513–529, 2018, doi: 10.1007/s12649-017-0003-1

[81] A. Laorko, S. Tongchitpakdee, and W. Youravong, "Storage quality of pineapple juice non-thermally pasteurized and clarified by microfiltration," *J. Food Eng.*, vol. 116, no. 2, pp. 554–561, 2013, doi: 10.1016/j.jfoodeng.2012.12.033

[82] C. A. Fuenmayor, S. M. Lemma, S. Mannino, T. Mimmo, and M. Scampicchio, "Filtration of apple juice by nylon nanofibrous membranes," *J. Food Eng.*, vol. 122, no. 1, pp. 110–116, 2014, doi: 10.1016/j.jfoodeng.2013.08.038

[83] A. Laorko, Z. Li, S. Tongchitpakdee, S. Chantachum, and W. Youravong, "Effect of membrane property and operating conditions on phytochemical properties and permeate flux during clarification of pineapple juice," *J. Food Eng.*, vol. 100, no. 3, pp. 514–521, 2010, doi: 10.1016/j.jfoodeng.2010.04.039

[84] M. R. Moßhammer, F. C. Stintzing, and R. Carle, "Evaluation of different methods for the production of juice concentrates and fruit powders from cactus pear," *Innov. Food Sci. Emerg. Technol.*, vol. 7, no. 4, pp. 275–287, 2006, doi: 10.1016/j.ifset.2006.04.003

[85] A. Bendini *et al.*, "Phenolic molecules in virgin olive oils: A survey of their sensory properties, health effects, antioxidant activity and analytical methods. An Overview of the last decade," *Molecules*, vol. 12, no. 8, pp. 1679–1719, 2007, doi: 10.3390/12081679

[86] J. W. Drynan, M. N. Clifford, and N. Kuhnert, "The chemistry of low molecular weight black tea polyphenols," *Nat. Prod. Rep.*, vol. 27, pp. 417–462, 2010, doi: 10.1039/b912523j

[87] B. Razi, A. Aroujalian, and M. Fathizadeh, "Modeling of fouling layer deposition in cross-flow microfiltration during tomato juice clarification," *Food Bioprod. Process.*, vol. 90, no. 4, pp. 841–848, 2012, doi: 10.1016/j.fbp.2012.05.004

[88] C. D. Dos Santos, R. K. Scherer, A. S. Cassini, L. D. F. Marczak, and I. C. Tessaro, "Clarification of red beet stalks extract by microfiltration combined with ultrafiltration," *J. Food Eng.*, vol. 185, pp. 35–41, 2016, doi: 10.1016/j.jfoodeng.2016.03.031

[89] A. Cassano *et al.*, "Clarification and concentration of citrus and carrot juices by integrated membrane processes," *J. Food Eng.*, vol. 57, no. 2, pp. 153–163, 2003, doi: 10.1016/S0260-8774(02)00293-5

[90] B. E. Barrag, Y. Jorge, and R. Castro-Munoz, "Use of gelatin-maltodextrin composite as an encapsulation support for clarified juice from purple cactus pear (*Opuntia stricta*)," *LWT- Food Sci. Tech.*, vol. 62, no. 1, pp. 242–248, 2015, doi: 10.1016/j.lwt.2014.09.042

[91] C. Conidi, A. Cassano, F. Caiazzo, and E. Drioli, "Separation and purification of phenolic compounds from pomegranate juice by ultrafiltration and nanofiltration membranes," *J. Food Eng.*, vol. 195, pp. 1-13, 2017, doi: 10.1016/j.jfoodeng.2016.09.017

[92] M. Cissé, F. Vaillant, D. Pallet, and M. Dornier, "Selecting ultrafiltration and nanofiltration membranes to concentrate anthocyanins from roselle extract (*Hibiscus sabdariffa L.*)," *Food Res. Int.*, vol. 44, no. 9, pp. 2607–2614, 2011, doi: 10.1016/j.foodres.2011.04.046

[93] C. M. Galanakis, "Separation of functional macromolecules and micromolecules: From ultrafiltration to the border of nanofiltration," *Trends Food Sci. Technol.*, vol. 42, no. 1, pp. 44–63, 2015, doi: 10.1016/j.tifs.2014.11.005

[94] A. F. Ismail and A. R. Hassan, "Effect of additive contents on the performances and structural properties of asymmetric polyethersulfone (PES) nanofiltration membranes," vol. 55, no. 1, pp. 98–109, 2007, doi: 10.1016/j.seppur.2006.11.002

[95] S. Wei, M. M. Hossain, and Z. S. Saleh, "Concentration of rutin model solutions from their mixtures with glucose using ultrafiltration," *Int. J. Mol. Sci.*, vol. 11, no. 2, pp. 672–690, 2010, doi: 10.3390/ijms11020672

[96] O. Acosta, F. Vaillant, A. M. Pérez, and M. Dornier, "Potential of ultrafiltration for separation and purification of ellagitannins in blackberry (*Rubus adenotrichus Schltdl.*) juice," *Sep. Purif. Technol.*, vol. 125, pp. 120–125, 2014, doi: 10.1016/j.seppur.2014.01.037

[97] C. M. Galanakis, "Emerging technologies for the production of nutraceuticals from agricultural by-products: A viewpoint of opportunities and challenges," *Food Bioprod. Process.*, vol. 91, no. 4, pp. 575–579, 2013, doi: 10.1016/j.fbp.2013.01.004

[98] R. Castro-Muñoz, B. E. Barragán-Huerta, and J. Yáñez-Fernández, "The use of nixtamalization waste waters clarified by ultrafiltration for production of a fraction rich in phenolic compounds," *Waste Biomass Valori.*, vol. 7, no. 5, pp.

1167–1176, 2016, doi: 10.1007/s12649-016-9512-6

[99] R. Castro-muñoz, J. Yáñez-fernández, and V. Fíla, "Phenolic compounds recovered from agro-food by-products using membrane technologies: An overview," *Food Chem.*, vol. 213, pp. 753-762, 2016, doi: 10.1016/j.foodchem.2016.07.030

[100] C. M. Galanakis, R. Castro-Muñoz, A. Cassano, and C. Conidi, "Recovery of high-added-value compounds from food waste by membrane technology," *Membr. Technol. Biorefining*, no. 1, pp. 189–215, 2016, doi: 10.1016/B978-0-08-100451-7.00008-6

[101] M. Cai, W. Hou, Y. Lv, and P. Sun, "Behavior and rejection mechanisms of fruit juice phenolic compounds in model solution during nanofiltration," *J. Food Eng.*, vol. 195, pp. 97–104, 2017, doi: 10.1016/j.jfoodeng.2016.09.024

[102] M. Uyttebroek *et al.*, "Concentration of phenolic compounds from apple pomace extracts by nanofiltration at lab and pilot scale with a techno-economic assessment," *J. Food Process Eng.*, vol. 41, no. 1, pp. 1–10, 2018, doi: 10.1111/jfpe.12629

[103] R. Tundis *et al.*, "Concentration of bioactive compounds from elderberry (*Sambucus Nigra L.*) juice by nanofiltration membranes," *Plant Foods Hum. Nutr.*, vol. 73, no. 4, pp. 336–343, 2018, doi: 10.1007/s11130-018-0686-x

[104] J. A. Arboleda Mejia *et al.*, "Recovery of phenolic compounds from red grape pomace extract through nanofiltration membranes," *Foods*, vol. 9, no. 11, pp. 1649, 2020, doi: 10.3390/foods9111649

Chapter – 2
Theory and Mathematical Modeling

CHAPTER – 2

THEORY AND MATHEMATICAL MODELING

2.1 Introduction

Over the last few decades, membrane-based operations have indeed revolutionized the scientific communities by offering efficient, eco-friendly, sustainable, and cost-effective solutions in various industries, including water treatment [1]-[3], food and beverage processing [4]-[9], pharmaceuticals [10], [11], and biotechnology [12]. The selective permeability of membranes is based on factors such as pore size, charge, or affinity, which underlie the separation, concentration, or recovery of compounds. Due to its high selectivity, membrane-based operations enable precise control over product quality and process efficiency [13], [14]. With the ongoing worldwide increase in demand for cleaner, environmentally friendly methods for the recovery or concentration of natural bioactives, the advancement and optimization of membrane technologies have become critical for scaling up these processes.

Developing membrane processes to meet the specific separation objective for any application, including the recovery or concentration of phenolic compounds, basically requires designing, testing, optimizing, and scaling up membrane systems. The development process usually begins by selecting appropriate membrane materials and configurations, taking into account the molecular weight and nature of the target compounds. For instance, UF membranes (10-100 nm) often remove larger particles, while NF membranes (1-10 nm) effectively target dissolved ions and organic molecules. Membrane separation efficiency is governed by multiple factors, including operating conditions (pressure, feed flow rate, and feed composition) and membrane module parameters (hydraulic permeability, solute permeability, and reflection coefficient). Consequently, rigorous experimental investigation is imperative to optimize critical process variables and maximize permeate flux, separation selectivity, and compound recovery indices [15]-[18].

Process optimization is a critical dimension in membrane technology development, ensuring maximal system efficiency while preserving the structural integrity and bioactive functionality of phenolic constituents. The optimization protocol requires nuanced equilibration among competing operational parameters, simultaneously achieving elevated permeate flux and rejection percentages without exacerbating membrane fouling phenomena or diminishing separation selectivity. Contemporary methodological approaches, particularly computational mathematical modeling techniques, facilitate the identification of optimal operational conditions and membrane parameters, thereby enabling predictive assessment of separation performance metrics. Furthermore, implementing fouling mitigation strategies, establishing systematic cleaning regimens, and incorporating turbulence-promoting spacer elements constitute essential components for sustaining longitudinal performance stability and minimizing operational expenditures [19].

Optimizing the membrane process at the laboratory or pilot scale is followed by the next critical step: scale-up to industrial production. Scale-up poses many challenges, including fluid dynamics and integration with larger active membrane areas, which become progressively more complex as the process progresses. Deep and thorough knowledge of the basic principles of membrane science, along with considerations of aspects related to real-world industrial operations, is essential to facilitate successful scale-up. Rigorous experiments, iterative testing, modeling, and validation are critical requirements for the scale-up system to ensure robustness, reliability, and economic viability when deployed in real-world applications. Developing and expanding membrane techniques for concentrating natural phenolic compounds can significantly advance the quest for sustainable, effective separation methods. By addressing challenges such as concentration polarisation, selectivity, and process integration, researchers and engineers can fully utilise membrane systems, enabling the production of superior phenolic-rich extracts for various uses.

2.2 Transport Models for Membrane Processes

Nanofiltration (NF) is one of the pressure-driven membrane operations that exhibits very low rejection of monovalent ions and high rejection of larger solutes or multivalent ions. Transport models are essential for predicting key parameters and enhancing membrane performance, such as permeate fluxes and rejection percentages [20].

Various mathematical models have been developed to characterize the complex transport phenomena occurring during filtration. The evolution of transport models in membrane technology begins with the transition from the Kedem-Katchalsky (K-K) model of 1958 to the Spiegler-Kedem (S-K) model presented in 1966 [21]. The K-K model, which calculates solute rejection relative to the bulk-phase solute concentration, could not accurately predict membrane rejection rates. The S-K model rectified the K-K model's limitations by estimating the actual rejection percentage based on solute concentration at the membrane interface, thereby improving prediction accuracy. Due to the requirement of different mass transfer coefficients, the S-K model integrated with the film theory showed less accuracy in predictions [22]. However, combining the S-K model with the K-K model yielded the Spiegler-Kedem (S-K) model, which shows better accuracy and is widely used due to its "black box" assumption [23], [24].

2.2.1 Solution-Diffusion (S-D) Model

The S-D model is the fundamental theoretical model that describes the solute and solvent transport mechanism of the molecules across the non-porous membrane via three stages: adsorption of the solute molecules onto the membrane surface on the feed side, diffusion of the solutes through the membrane matrix, and desorption of the solutes on the permeate side (Figure 2.1) [25]. Because the absorption and desorption rates are higher and occur much more rapidly, solute diffusion becomes the rate-determining step among these stages [26].

This model assumes that the pressure across the membrane matrix equals the feed pressure, resulting in a zero pressure gradient across the membrane [27]. In the absence of a pressure gradient, the concentration gradient serves as the sole driving force for solute transport, making it particularly useful for RO, FO, and specific NF applications.

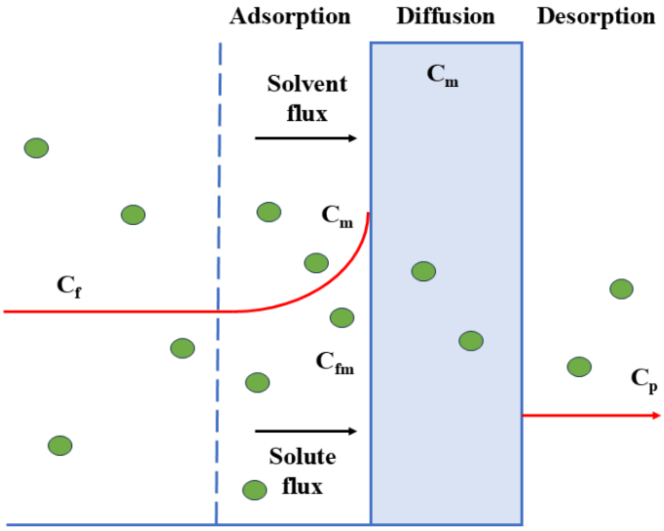

Figure 2.1 Solution-Diffusion model

2.2.2 Pore Flow (P-F) Model

Unlike the S-D model, the P-F model assumes the membranes are porous. The convective solute transport across the membrane occurs through these tiny pores and depends on the membrane's pressure gradient. According to this model, filtration selectivity arises from size exclusion, as depicted in Figure 2.2. The solute particles larger than the membrane's pore size are physically trapped or retained, while smaller ones pass through. This model generally applies to UF and MF processes where pores are more pronounced and convective transport dominates over diffusive transport.

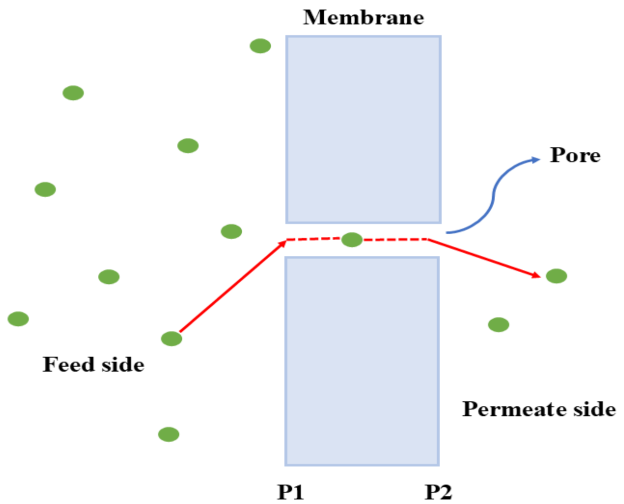

Figure 2.2 Pore-Flow model

2.2.3 Irreversible Thermodynamics (I-T) Models

The irreversible thermodynamic (I-T) models describe membrane transport from a different perspective. These I-T models are based on the principles of non-equilibrium thermodynamics and assume that the solute and solvent fluxes are linearly correlated to all the driving forces acting in the system (Figure 2.3) [28]-[30].

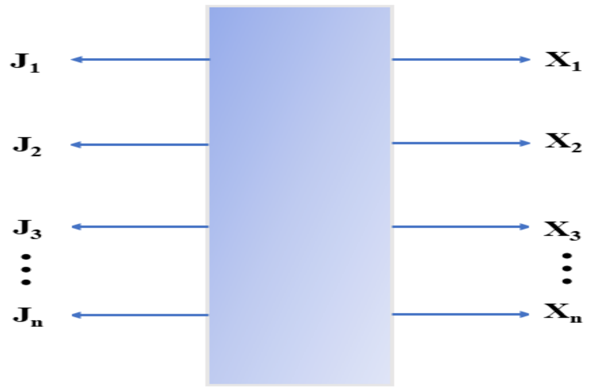

$$J_i = \sum_{k=1}^{n} L_{ik} X_i$$

Figure 2.3 Irreversible-Thermodynamic model

The most important feature of this model is the use of phenomenological coefficients that encapsulate the membrane's transport properties without specifying the underlying physical mechanism. This makes them versatile and applicable to porous and non-porous membranes, making them suitable for RO, FO, and NF operations.

2.2.3.1 Kedem-Katchalsky (K-K) Model

Based on irreversible thermodynamics principles, the K-K model quantifies solute and solvent transport across membrane interfaces using phenomenological equations. This model employs three critical parameters: the hydraulic permeability (L_p), reflection coefficient (σ), and solute permeability (B_m), which collectively characterize the membrane's selective permeation properties. Hydraulic permeability is a parameter that describes how readily a membrane allows solvent (typically water) to pass through under an applied pressure and reflects the membrane's intrinsic resistance to flow. The reflection coefficient is a dimensionless measure of membrane selectivity toward a specific solute, indicating the extent to which the membrane "reflects" the solute; a value close to one signifies near-complete rejection, whereas a value close to zero indicates that the solute passes freely with the solvent. Solute permeability is the inherent ability of a solute to diffuse across the membrane driven by a concentration gradient, independent of convective flow, and higher values indicate easier solute transport. The development of the Kedem-Katchalsky model incorporates several key simplifying assumptions to address the complex interactions inherent in membrane filtration processes [30], [31].

- The model assumes that the transport parameters (L_p, B_m, and σ) are constant for a given membrane type.
- The solute and solvent transport across the membrane is driven by pressure and concentration gradients.
- The model overlooks the effects of solute charge, solvent type, and membrane material on the transport of solutes.

For instance, it linearly relates the solvent fluxes to the osmotic and pressure gradients across the membrane (equation (2.1)) [18].

$$J_p = L_p\,(\Delta p - \sigma\Delta\pi) \ldots (2.1)$$

Where L_p is the hydraulic permeability, σ is the reflection coefficient, $\Delta\pi$ is the osmotic pressure difference, and ΔP is the pressure gradient across the membrane.

The solute flux combines diffusion and convection-driven fluxes, as expressed in equation (2.2). The term $B_m\Delta c$ indicates the diffusive flux driven by the concentration gradient, and the term $J_v(1-\sigma)c$ represents the convective flux driven by the pressure gradient.

$$J_s = B_m\Delta c + J_p(1-\sigma)c \ldots (2.2)$$

B_m is the solute permeability, and c is the mean solute concentration.

2.2.3.2 Spiegler-Kedem (S-K) model

The S-K model is widely used in membrane technology, particularly for RO and NF processes. Unlike purely mechanistic models, the S-K model accounts for non-ideal membrane behavior, including solute rejection and diffusion effects. It provides a mathematical framework for predicting solute and solvent fluxes, accounting for both convective and diffusive transport mechanisms. The S-K model's solute and solvent flux equations are based on the K-K model, differing only in the membrane rejection rate [31]. The model is useful for estimating membrane performance, optimizing operational parameters, and understanding membrane fouling. Recent studies have explored modifications and extensions of the S-K model, integrating film theory to account for concentration polarization effects. Additionally, its application in forward osmosis has revealed intriguing deviations from ideal semi-permeability, prompting further refinements. Comparative analyses suggest that the original S-K model remains effective for fundamental transport predictions, though hybrid approaches may enhance accuracy.

2.3 Mathematical Foundation for Transport Modeling

Because the membrane, HFT-NF 150, has both porous and non-porous surfaces, the three-parameter Spiegler-Kedem model was preferred over a solution-diffusion model for predicting its performance. The Spiegler-Kedem model has been widely used for reverse osmosis (RO) systems [32], and the same is applied in the present study of the NF system. According to this model, the permeate volumetric flux (J_P) through the membrane is given by equation (2.3)

$$J_P = \frac{L_P}{\rho}\left(\Delta p - \sigma\Delta\pi\right) \quad \dots (2.3)$$

Where L_p is the hydraulic permeability in kg/m^2sPa, σ is the reflection coefficient, ρ is the density in kg/m^3, $\Delta\pi$ is the osmotic pressure difference, and ΔP is the pressure across the membrane. The value of osmotic pressure is given by equation (2.4).

$$\pi = \frac{\upsilon RT}{M} c \quad \dots (2.4)$$

Here, M is the molecular weight in kg/mol, and R is the universal gas constant in $m^3.Pa/kg.mol$, υ is the van't Hoff factor, T is the temperature in Kelvin, and c is the concentration in kg/m^3

2.3.1 Concentration Polarization (ϕ)

The performance of the membrane-based process is restricted by a phenomenon known as concentration polarization, which establishes a concentration gradient between the feed solution and the solution present at the solution-membrane interface [33]-[37]. This is because a layer develops at the membrane surface due to the accumulation of impermeable solute particles known as the concentration polarization layer. This results in a reduction in the solvent permeation flux due to counter-diffusion. The boundary layer thickness decreases as the feed flow rate increases.

Concentration polarization must be accounted for in NF and RO models to determine the membrane's intrinsic rejection, which depends on the membrane surface concentration. In contrast, the observed rejection depends on the feed concentration. Figure 2.4 shows the concentration profile and boundary-layer formation during the filtration process.

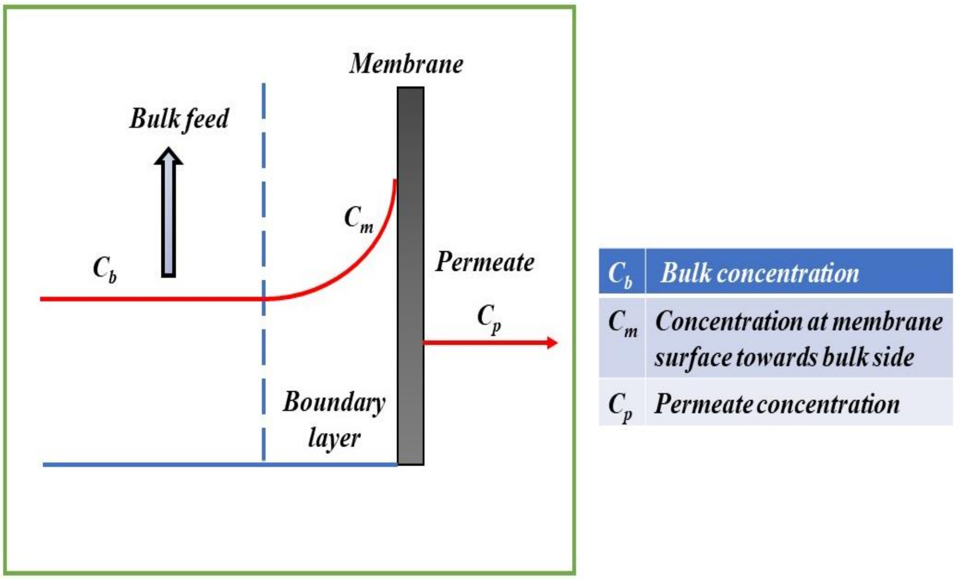

Figure 2.4 Concentration profile in the membrane process

The film theory is used to define the concentration polarization, and its mathematical expression is given in equation (2.5)

$$\phi = \frac{C_m - C_p}{C_f - C_p} = \exp\left(\frac{J_w}{k}\right) \quad \dots (2.5)$$

C_p is the permeate concentration, C_f is the feed concentration, and C_m is the concentration at the feed and membrane interface. The mass transfer coefficient (k) used in equation (2.5) is calculated by equation (2.6)

$$k = a \times Q_f^b \quad \dots (2.6)$$

Q_f is the volumetric feed flow rate; a and b are constant coefficients for a given system. Now, rewriting the equation for volumetric permeate flux in terms of bulk variable and permeate variable gives equation (2.7)

$$J_w = \frac{A}{\rho}\left(\Delta p - \sigma \frac{\upsilon RT}{M} \phi\left(C_f - C_p\right)\right) \quad \dots (2.7)$$

2.3.2 Equation for Rejection (R_j)

Intrinsic rejection is a measure of the membrane's separation efficiency. According to the Spiegler-Kedem model, the true rejection can be calculated by using equation (2.8)

$$R_j = \frac{(1-F)\sigma}{1-\sigma F} = 1 - \frac{C_p}{C_m} \quad \dots (2.8)$$

Where F is the flow parameter and is given by equation (2.9)

$$F = \exp\left(-J_w \frac{1-\sigma}{B_m}\right) \quad \dots (2.9)$$

Here, B_m represents the solute permeability in m/s.

2.3.3 Equations for Permeate Concentration (C_p)

The equation for permeate concentration can be derived in terms of concentration polarization and rejection by eliminating C_m from equations (2.5) and (2.8) and simplifying for C_p, and is given by equation (2.10)

$$C_p = \frac{\phi(1-R_j)C_f}{\phi + R_j(1-\phi)} \quad \dots (2.10)$$

The above equation (2.10) can be further simplified in terms of bulk parameters to obtain equation (2.11)

$$C_p = \frac{C_f}{1+\left(\frac{\sigma}{(1-\sigma)}\right)\left(\frac{(1-F)}{\phi}\right)} \quad \dots (2.11)$$

2.3.4 Equation for Permeate Flux (J_w)

Combining all the above equations, the equation for permeate volumetric flux can be written as equation (2.12)

$$J_w = \frac{A}{\rho}\left[\Delta p - \sigma\frac{\upsilon RT}{M_w}\phi C_f\left(\frac{\frac{(1-F)}{\phi}}{\frac{(1-F)}{\phi}+\frac{(1-\sigma)}{\sigma}}\right)\right] \quad \dots (2.12)$$

The three parameters of the Spiegler-Kedem model are hydraulic permeability (L_p), reflection coefficient (σ), and solute permeability (B_m).

2.3.5 Equation for recovery percentage (R)

Recovery percent is defined as the ratio of permeate flow rate (Q_p) to feed flow rate (Q_f) multiplied by 100. When all other factors, such as feed water total dissolved solids (TDS), operating pressure, and temperature, remain constant, percentage recovery and rejection are inversely related.

$$R = \frac{Q_p}{Q_f} \times 100 \quad \dots (2.13)$$

Here, Q_p and Q_f are in m^3/sec.

Equation (2.13) can be further simplified in terms of permeate flux as equation (2.14)

$$R = \frac{J_w A_m}{Q_f} \times 100 \quad \dots (2.14)$$

Here, A_m is the active membrane area in m^2.

2.4 Variance-based sensitivity

Variance-based sensitivity analysis is a powerful approach for understanding how different input parameters contribute to uncertainty in model outputs. This methodology is particularly valuable in research contexts where complex models with numerous parameters simulate real-world systems. It analyzes how the variance of model outputs can be apportioned to different input parameters and their interactions. The fundamental concept is to decompose the total output variance into components attributable to each input parameter or to parameter combinations. The most common method for this framework is the Sobol's method, which provides the following indices: First-order sensitivity indices (S_i), which measure the direct contribution of each parameter to output variance; total sensitivity indices (S_{Ti}): Measure the total contribution of a parameter, including all its interactions with other parameters; and higher-order sensitivity indices measuring interaction effects between specific combinations of parameters.

2.4.1 Mathematical Foundation for Sensitivity Analysis

Consider a mathematical equation ϖ as a function of input parameters A_1, A_2, A_3, ..., A_n. (equation (2.15))

$$\varpi = f(A_1, A_2, \dots A_n) \quad \dots (2.15)$$

Total unconditional variance V(ϖ) can be defined as in equation (2.16) and is obtained by the summation of first to highest-order partial variance for all parameters [38].

$$V(\varpi) = \sum_i^n V_i + \sum_i^n \sum_{j>i}^n V_{ij} + \cdots + \sum V_{ij\dots n} \quad \dots (2.16)$$

Here, V_i represents the partial variance component of the ith input parameter, V_{ij} represents the partial variance component due to the interaction between the i^{th} and j^{th} input parameters, and so on. Now, dividing equation (2.16) by V(ϖ) gives equation (2.17)

$$1 = \sum_i^n S_i + \sum_i^n \sum_{j>i}^n S_{ij} + \cdots + \sum S_{ij\dots n} \quad \dots (2.17)$$

Where S_i is the first-order sensitivity of the i^{th} input parameter, S_{ij} is the second-order sensitivity representing combined variation due to components A_i and A_j taken together, and so on. The total sensitivity of the i^{th} input parameter (S_{Ti}), including first and highest-order sensitivities, can be calculated using equation (2.18)

$$S_{Ti} = S_i + \sum_{i\neq j}^n S_{ij} + \cdots + \sum S_{ij\dots n} \quad \dots (2.18)$$

Here, (S_{Ti}-S_i) can be calculated to estimate the higher-order sensitivity of the i^{th} input parameter due to its interaction with other input parameters.

The first-order and total sensitivities were computed using equations (2.19) and (2.20).

$$S_i = \frac{\left[\left(\frac{1}{N}\sum_{n=1}^N (y_Q^n)(y_{Ri}^n) - y_P^n\right)\right]}{\left(\frac{1}{N}\sum_{n=1}^N \left((y_P^n)^2\right) - f_o^2\right)} \quad \dots (2.19)$$

$$S_{Ti} = \left[\frac{\left(\frac{1}{2N}\sum_{n=1}^N (y_P^n - y_{Ri}^n)^2\right)}{\left(\frac{1}{N}\sum_{n=1}^N \left((y_P^n)^2\right) - f_o^2\right)}\right] \quad \dots (2.20)$$

Where equation (2.21) represents the value of f_o^2

$$f_o^2 = \left(\frac{1}{N}\right)\sum_{n=1}^N (y_P^n)^2 \quad \dots (2.21)$$

P and Q are the independent matrices with each N row of input datasets. The matrix R_i contains all the input parameters of matrix P except the i^{th} column, which is taken from matrix Q. To evaluate the first order and total order sensitivity of n number of input parameters, total n+2 number of matrices are required, where P and Q are the independent matrices and other (R_1, R_2, … R_n) are constituted by the replacement of i^{th} column of matrix P and Q [38]-[40].

2.5 Scale-up Studies

The transition from laboratory-scale experiments to industrial applications is a complex, multi-stage process that encompasses technical, economic, and operational considerations. One critical phase of this transition is scale-up, which focuses on increasing the effective filtration area to enable the processing of substantially larger feed volumes within predefined production timeframes.

2.5.1 Mathematical Foundation for Scale-up Studies

The volume and concentration of the feed and permeate streams are functions of time. Hence, the mathematical model based on material and component balance predicts the variations in feed volume and feed concentration over time.

Assumptions for the scale-up mathematical model

1. The mass transfer properties of the membrane do not change during the entire process.
2. Input conditions like feed flow rate, temperature, and pressure remain invariable throughout the process.
3. The membrane test cell functions under a quasi-steady state (QSS).
4. During the membrane filtration, the compounds are neither generated nor consumed within the test cell, indicating the absence of any chemical reaction.

2.5.1.1 Unsteady State Mass Balance for Membrane Test Cell

The total mass balance and solute mass balance across the feed side can be expressed by equations (2.22) and (2.23), respectively [20].

$$Q_f - Q_r = J_p A_m \quad \dots (2.22)$$

$$Q_f C_f - Q_r C_r = J_s A_m \quad \ldots (2.23)$$

J_p and J_s represent the permeate and solute flux, and Q_f and Q_r are the feed and retentate stream flow rates, respectively. C_f and C_r are the feed concentration and retentate concentration, respectively. A_m is the active membrane area of the setup.

2.5.1.2 Tank Mass Balance Equations

The volume and solute concentration of the feed solution change during the process. A dynamic tank model was used to incorporate feed volume and concentration variations in the feed tank. The outward flow of the feed tank is connected to the inlet of the test cell, and the outward flow from the test cell is again recirculated as an inflow to the tank.

Let V_t be the feed tank's initial volume at time t. After time Δt, the volume of the feed tank becomes $V_{t+\Delta t}$. The change in volume and concentration of the feed solution tank can be expressed as equations (2.24) and (2.25).

$$\frac{dV}{dt} = Q_r - Q_f \quad \ldots(2.24)$$

$$\frac{dVC_f}{dt} = Q_f C_f - Q_r C_r \quad \ldots(2.25)$$

Combining all the equations,

$$\frac{dV}{dt} = -J_p A_m \quad \ldots (2.26)$$

$$\frac{dVC_f}{dt} = J_s A_m \quad \ldots (2.27)$$

On solving equation (2.27), we get

$$V\frac{dC_f}{dt} + C_f\frac{dV}{dt} = J_s A_m \quad \ldots (2.28)$$

Putting the value from equation (2.26) in equation (2.28), we get

$$V\frac{dC_f}{dt} - C_f J_p A_m = J_s A_m \quad \ldots (2.29)$$

$$\frac{dC_f}{dt} = \frac{C_f J_p A_m}{V}\left(\frac{J_s A_m}{C_f J_w A_m} + 1\right) \quad \ldots (2.30)$$

Equations (2.29) and (2.30) can be used to predict the performance of the scale-up setup.

References

[1] E. O. Ezugbe and S. Rathilal, “Membrane technologies in wastewater treatment: A review,” *Membranes*, vol. 10, no. 5, 2020, doi: 10.3390/membranes10050089

[2] B. Girard and L. R. Fukumoto, “Membrane processing of fruit juices and beverages: A review,” *Crit. Rev. Biotechnol.,* vol. 20, no. 2, pp. 109-75, 2000, doi: 10.1080/07388550008984168

[3] C. Bhattacharjee, V. K. Saxena, and S. Dutta, “Fruit juice processing using membrane technology: A review,” *Innov. Food Sci. Emerg. Technol.*, vol. 43, pp. 136–153, 2017, doi: 10.1016/j.ifset.2017.08.002

[4] Z. Ma *et al.*, “A comprehensive review on the recent advances in membrane-based processes for fruit juice concentration,” *Food Bioprod. Process.*, vol. 145, pp. 42–66, 2024, doi: 10.1016/j.fbp.2024.02.010

[5] M. Cheryan and J. R. Alvarez, “Food and beverage industry applications,” *Membr. Sci. Technol.*, vol. 2, pp. 415–465, 1995, doi: 10.1016/S0927-5193(06)80011-2

[6] A. P. Echavarría, C. Torras, J. Pagán, and A. Ibarz, “Fruit juice processing and membrane technology application,” *Food Eng. Rev.*, vol. 3, pp. 136–158, 2011, doi: 10.1007/s12393-011-9042-8

[7] C. Charcosset, “Classical and recent applications of membrane processes in the food industry,” *Food Eng. Rev.*, vol. 13, no. 2, pp. 322–343, 2021, doi: 10.1007/s12393-020-09262-9

[8] B. T. McKinnon and K. E. Avis, “Membrane filtration of pharmaceutical solutions,” *Am. J. Hosp. Pharm.*, vol. 50, no. 9, pp. 1921–1936, 1993, doi: 10.1093/ajhp/50.9.1921

[9] K. Staszak, “Membrane processes,” *Phys. Sci. Rev.*, vol. 2, no. 12, pp. 20170142, 2017, doi: 10.1515/psr-2017-0142

[10] C. Charcosset, “Membrane processes in biotechnology: An overview,” *Biotechnol. Adv.*, vol. 24, no. 5, pp. 482–492, 2006, doi: 10.1016/j.biotechadv.2006.03.002

[11] R. Castro-Muñoz and V. Fíla, "Membrane-based technologies as an emerging tool for separating high-added-value compounds from natural products," *Trends Food Sci. Technol.*, vol. 82, pp. 8–20, 2018, doi: 10.1016/j.tifs.2018.09.017

[12] A. Hausmann, M. C. Duke, and T. Demmer, "Principles of Membrane Filtration," *Membr. Process. Dairy Beverage Appl.*, pp. 17–51, 2012, doi: 10.1002/9781118457009.ch2

[13] M. Cai, W. Hou, Z. Li, Y. Lv, and P. Sun, "Understanding nanofiltration fouling of phenolic compounds in model juice solution with two membranes," *Food Bioprocess Technol.*, vol. 10, no. 12, pp. 2123–2131, 2017, doi: 10.1007/s11947-017-1970-8

[14] M. Shibuya *et al.*, "Experimental and theoretical study of a forward osmosis hollow fiber membrane module with a cross-wound configuration," *J. Memb. Sci.*, vol. 504, pp. 10–19, 2016, doi: 10.1016/j.memsci.2015.12.040

[15] A. K. Tiwari and M. Jain, "A novel process for rutin recovery from model solutions using nanofiltration: Experimental study, mathematical modeling, and scale-up design," *J. Food Process Eng.*, vol. 47, no. 3, pp. e14592, 2024, doi: 10.1111/jfpe.14592

[16] A. K. Tiwari and M. Jain, "Concentration of betanin from model beetroot extracts using nanofiltration: parameter estimation and sensitivity analysis," *J. Chem. Technol. Biotechnol.*, vol. 99, no. 9, pp. 1976–1983, 2024, doi: 10.1002/jctb.7698

[17] A. Boubakri, S. Elgharbi, I. Dhaouadi, D. Mansour, and S. Al-Tahar Bouguecha, "Optimization and prediction of lead removal from aqueous solution using FO–MD hybrid process: Statistical and artificial intelligence analysis," *J. Environ. Manage.*, vol. 337. pp. 117731, 2023, doi: 10.1016/j.jenvman.2023.117731

[18] A. Akhtar, M. Singh, S. Subbiah, and K. Mohanty, "Modelling, experimental validation and process design of forward osmosis process for sugarcane juice concentration," *Lwt*, vol. 141, pp. 110852, 2021, doi: 10.1016/j.lwt.2021.110852

[19] M. Jain, D. Attarde, and S. K. Gupta, "Removal of thiophene from n-heptane/thiophene mixtures by spiral wound pervaporation module: Modelling, validation and influence of operating conditions," *J. Memb. Sci.*, vol. 490, pp. 328–345, 2015, doi: 10.1016/j.memsci.2015.05.004

[20] L. Y. Ng *et al.*, "Advancements and limitations in nanofiltration transport models: A comprehensive review of predictive approaches and future directions," *J. Water Process Eng.*, vol. 69, pp. 106646, 2025, doi: 10.1016/j.jwpe.2024.106646

[21] E. Vellenga and G. Trägårdh, "Nanofiltration of combined salt and sugar solutions: Coupling between retentions," *Desalination*, vol. 120, no. 3, pp. 211–220, 1998, doi: 10.1016/S0011-9164(98)00219-7

[22] M. Hadian and M. Hadian, "Comparison of Spiegler–Kedem combined with film theory model and original SK model," *Desalin. Water Treat.*, vol. 272, pp. 1–5, 2022, doi: 10.5004/dwt.2022.28823

[23] S. S. Wadekar and R. D. Vidic, "Insights into the rejection of barium and strontium by nanofiltration membrane from experimental and modeling analysis," *J. Memb. Sci.*, vol. 564, pp. 742–752, 2018, doi: 10.1016/j.memsci.2018.07.060

[24] D. Attarde, M. Jain, and S. K. Gupta, "Modeling of a forward osmosis and a pressure-retarded osmosis spiral wound module using the Spiegler-Kedem model and experimental validation," *Sep. Purif. Technol.*, vol. 164, pp. 182–197, 2016, doi: 10.1016/j.seppur.2016.03.039

[25] M. F. J. Dijkstra, S. Bach, and K. Ebert, "A transport model for organophilic nanofiltration," *J. Memb. Sci.*, vol. 286, no. 1–2, pp. 60–68, 2006, doi: 10.1016/j.memsci.2006.09.012

[26] L. G. Peeva, E. Gibbins, S. S. Luthra, L. S. White, R. P. Stateva, and A. G. Livingston, "Effect of concentration polarisation and osmotic pressure on flux in organic solvent nanofiltration," *J. Memb. Sci.*, vol. 236, no. 1–2, pp. 121–136, 2004, doi: 10.1016/j.memsci.2004.03.004

[27] P. Marchetti and A. G. Livingston, "Predictive membrane transport models for organic solvent nanofiltration: How complex do we need to be?" *J. Memb. Sci.*, vol. 476, pp. 530–553, 2015, doi: 10.1016/j.memsci.2014.10.030

[28] W. R. Bowen and J. S. Welfoot, "Modelling the performance of membrane nanofiltration-critical assessment and model development," *Chem. Eng. Sci.*, vol. 57, no. 7, pp. 1121–1137, 2002, doi: 10.1016/S0009-2509(01)00413-4

[29] J. H. Kim, J. G. Na, H. J. Shim, and Y. K. Chang, "Modeling of ammonium lactate recovery and impurity removal from simulated fermentation broth by nanofiltration," *J. Memb. Sci.*, vol. 396, pp. 110–118, 2012, doi: 10.1016/j.memsci.2012.01.003

[30] F. Wu, L. Feng, and L. Zhang, "Rejection prediction of isopropylantipyrine and antipyrine by nanofiltration membranes based on the Spiegler-Kedem-Katchalsky model," *Desalination*, vol. 362, pp. 11–17, 2015, doi: 10.1016/j.desal.2015.01.046

[31] A. M. Hidalgo, G. León, M. Gómez, M. D. Murcia, E. Gómez, and J. L. Gómez, "Application of the Spiegler – Kedem – Kachalsky model to the removal of 4-chlorophenol by different nano filtration membranes," *Desalination*, vol. 315, pp. 70–75, 2013, doi: 10.1016/j.desal.2012.10.008

[32] A. Chatterjee, A. Ahluwalia, S. Senthilmurugan, and S. K. Gupta, "Modeling of a radial flow hollow fiber module and estimation of model parameters using numerical techniques," *J. Memb. Sci.*, vol. 236, no. 1–2, pp. 1–16, 2004, doi: 10.1016/j.memsci.2004.01.006

[33] A. Achilli, T. Y. Cath, and A. E. Childress, "Power generation with pressure retarded osmosis : An experimental and theoretical investigation," vol. 343, pp. 42–52, 2009, doi: 10.1016/j.memsci.2009.07.006

[34] B. Gu, D. Y. Kim, J. H. Kim, and D. R. Yang, "Mathematical model of flat sheet membrane modules for FO process : Plate-and-frame module and spiral-wound module," vol. 379, pp. 403–415, 2011, doi: 10.1016/j.memsci.2011.06.012

[35] J. R. Mccutcheon and M. Elimelech, "Influence of concentrative and dilutive internal concentration polarization on flux behavior in forward osmosis," vol. 284, pp. 237–247, 2006, doi: 10.1016/j.memsci.2006.07.049

[36] Y. Xu, X. Peng, C. Y. Tang, Q. S. Fu, and S. Nie, "Effect of draw solution concentration and operating conditions on forward osmosis and pressure retarded osmosis performance in a spiral wound module," vol. 348, pp. 298–309, 2010, doi: 10.1016/j.memsci.2009.11.013

[37] E. Sivertsen, T. Holt, W. Thelin, and G. Brekke, "Modelling mass transport in hollow fibre membranes used for pressure retarded osmosis," *J. Memb. Sci.*, vol. 417–418, pp. 69–79, 2012, doi: 10.1016/j.memsci.2012.06.014

[38] R. Sharma and M. Jain, "Variance-based sensitivity analysis and statistical optimization of design and operating parameters of spiral wound pervaporation modules for thiophene removal from FCC gasoline," *Comput. Chem. Eng.*, vol. 141, pp. 106987, 2020, doi: 10.1016/j.compchemeng.2020.106987

[39] I. M. Sobol', "Sobol 1990_1993," *Mmce*, vol. 1, no. 4. pp. 407–414, 1993

[40] A. Saltelli, P. Annoni, I. Azzini, F. Campolongo, M. Ratto, and S. Tarantola, "Variance-based sensitivity analysis of model output. Design and estimator for the total sensitivity index," *Comput. Phys. Commun.*, vol. 181, no. 2, pp. 259–270, 2010, doi: 10.1016/j.cpc.2009.09.018

Chapter – 3
Instrumentation and Experimental Procedures

CHAPTER – 3

INSTRUMENTATION AND EXPERIMENTAL PROCEDURES

3.1 Introduction

This chapter serves as the methodological backbone of this research, systematically detailing the key instrumentation and experimental methodologies employed. The chapter describes the primary characterization instruments, their fundamental principles, specifications, and calibration protocols. Following the instrumentation overview, the chapter elaborates upon the fabrication of the experimental setup at the laboratory scale, including a brief description of its components. Along with descriptions of the instruments, this chapter explains the experimental procedures, including membrane filtration and systematic data collection at each level. The chapter concludes by elaborating on the theoretical framework employed to optimize different membrane parameters. This detailed description of the instrumentation and experimental procedures provides the necessary foundation for understanding the results presented in subsequent chapters.

3.2 Instrumentation

Different instruments have been used at different stages of this research work, including an Ultraviolet-Visible (UV-Vis) spectrophotometer to measure the absorbance of permeate samples, a Scanning Electron Microscope (SEM) to examine membrane morphology, and MATLAB software to estimate parameters. The following sub-section gives a brief overview of all characterization techniques and methodologies used in the entire period of the thesis work.

3.2.1 Ultraviolet-Visible Spectroscopy (UV-Vis)

UV-Vis Spectroscopy is one of the most fundamental analytical techniques that investigates electron interactions among atoms, ions, and molecules using ultraviolet (180-390 nm) and visible (390-780 nm) wavelengths of electromagnetic radiation [1]. When electromagnetic radiation passes through a sample, absorption occurs at specific wavelengths, causing electrons to transition to higher-energy states [2]. As stated in

Beer-Lambert Law, the solution's absorption is directly related to the concentration of solute in the solution and the distance the light travels through the sample (equation (3.1)).

$$A = \varepsilon c l \ldots (3.1)$$

Where A indicates the absorbance, ε is the molar absorptivity coefficient, c is the concentration, and l is the path length.

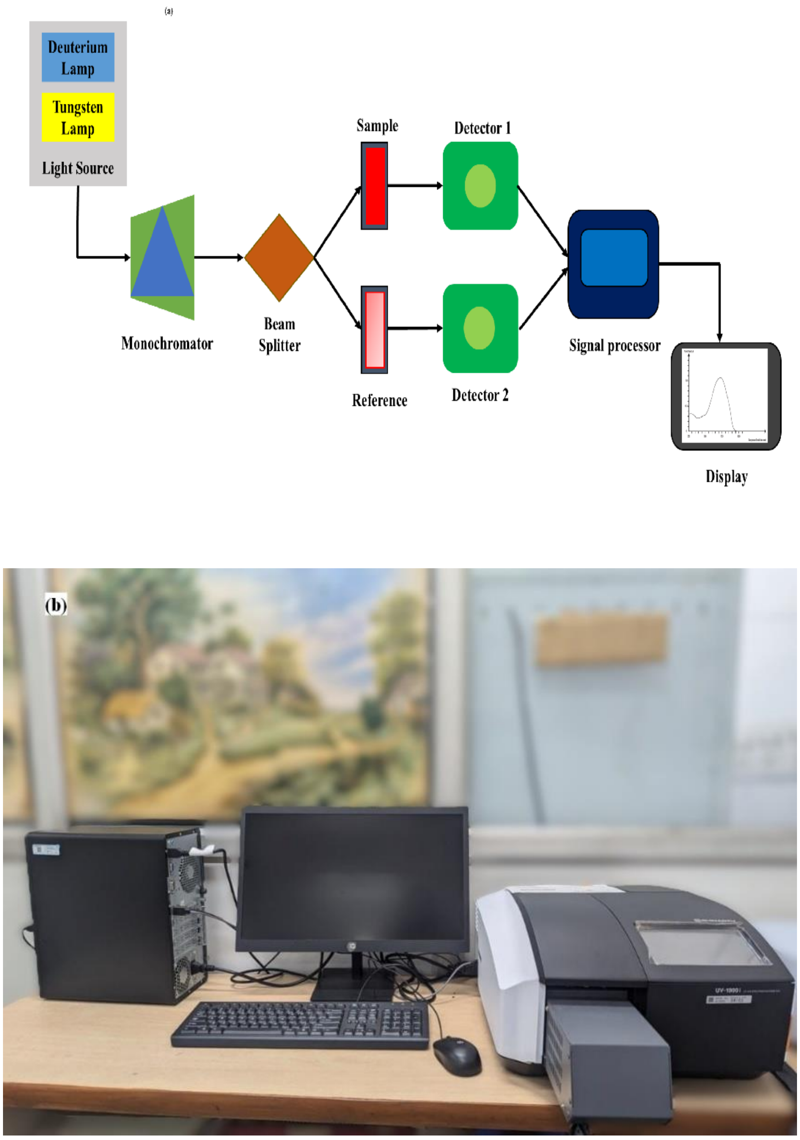

Figure 3.1 UV-Vis Spectrophotometer (a) block diagram, and (b) analytical instrument

Each molecule absorbs specific wavelengths of light characteristic of it. In this manner, the sample concentration can be determined by measuring the compound's absorbance at its characteristic wavelength. UV-Vis Spectroscopy has been widely used in chemistry, biochemistry, biotechnology, and material science to determine and analyze various substances based on their absorption properties.

A spectrometer uses a source of light (a deuterium lamp for UV light and a tungsten or halogen lamp for visible light), followed by a monochromator, a sample holder, a detector, and then a digital screen, as illustrated in Figure 3.1(a). SHIMADZU UV-1800 was employed for absorbance measurement (Figure 3.1(b)) for this research work. Calibration ensures the accuracy of a device and establishes measurement traceability [3]. Standard solutions with known concentrations are prepared to calibrate the UV-Vis spectrophotometer. The absorbance of each standard at the target wavelength is measured, and a calibration curve is generated plotting absorbance against concentration [4].

3.2.2 Scanning Electron Microscopy (SEM)

SEM is an advanced imaging tool for examining surface morphologies with excellent resolution. Instead of light, SEM uses a focused beam of electrons that scans the sample's surface, generating several signals that can be used to analyze its topography, composition, and other properties [5]. The main components of SEM include an electron source (i.e., an electron gun), a sample stage, lenses and scanning coils, an electron detector, and a display system for viewing images (Figure 3.2(a)). By directing a beam of high-energy electrons, SEM can produce large volumes of information at the solid surfaces.

SEM is widely used in materials science, biology, engineering, geology, and other fields. High-energy electrons are generated at the uppermost part of the column and accelerate downward, passing through multiple lenses to produce a focused beam that strikes the specimen's surface. During interaction between the specimen and the electron, signals are created and captured by detectors [6], [7]. ZEISS EVO 18 SEM with 2.0 nm resolution, shown in Figure 3.2(b), was employed in this particular study.

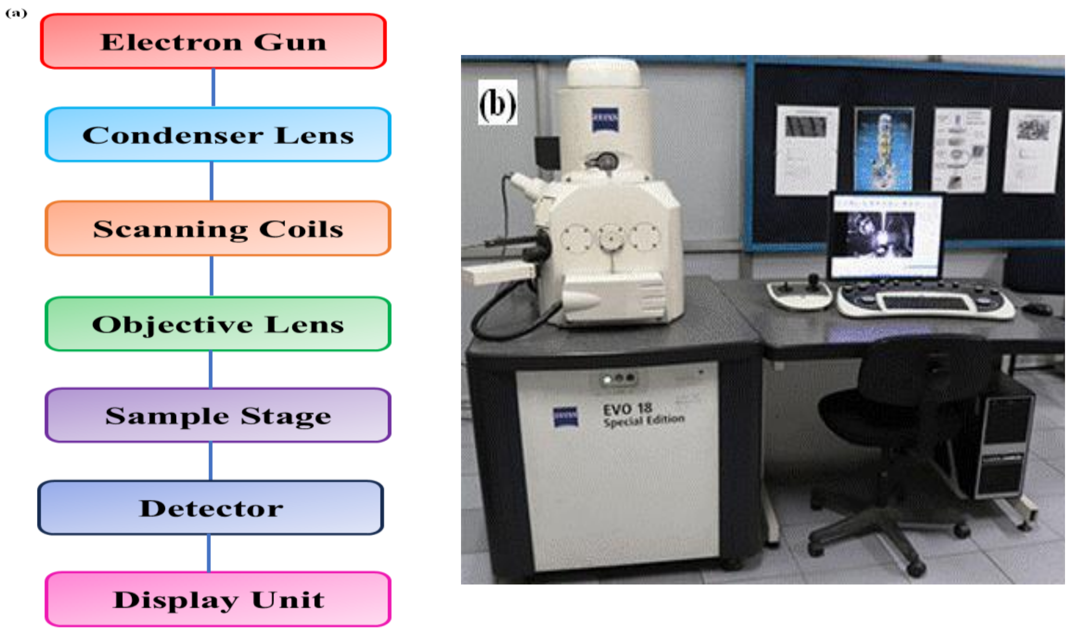

Figure 3.2 SEM (a) block diagram and (b) analytical instrument

3.2.3 Matrix Laboratory (MATLAB)

MATLAB R2018a software is a high-level programming language and computing environment developed by MathWorks, famous for its use in science, engineering, and math. It is well known for numerical calculation, data processing, analysis, visualization, and algorithm development. Its extensive library of built-in functions and toolboxes, including Signal Processing, Image Processing, Machine Learning, Control Systems, and Optimization Tools, makes it versatile across a wide range of applications. Because of its user-friendly interface and powerful computational capabilities, it has become an essential part of the research in multiple domains.

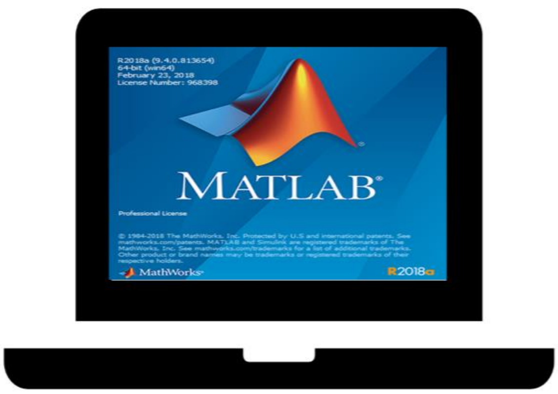

Figure 3.3 Matrix Laboratory

3.3 Fabrication of the Setup

The experimental setup primarily comprised a stainless-steel membrane test cell capable of withstanding pressures up to 40 bar, as illustrated in Figure 3.4(a), which shows the self-assembled nanofiltration (NF) system.

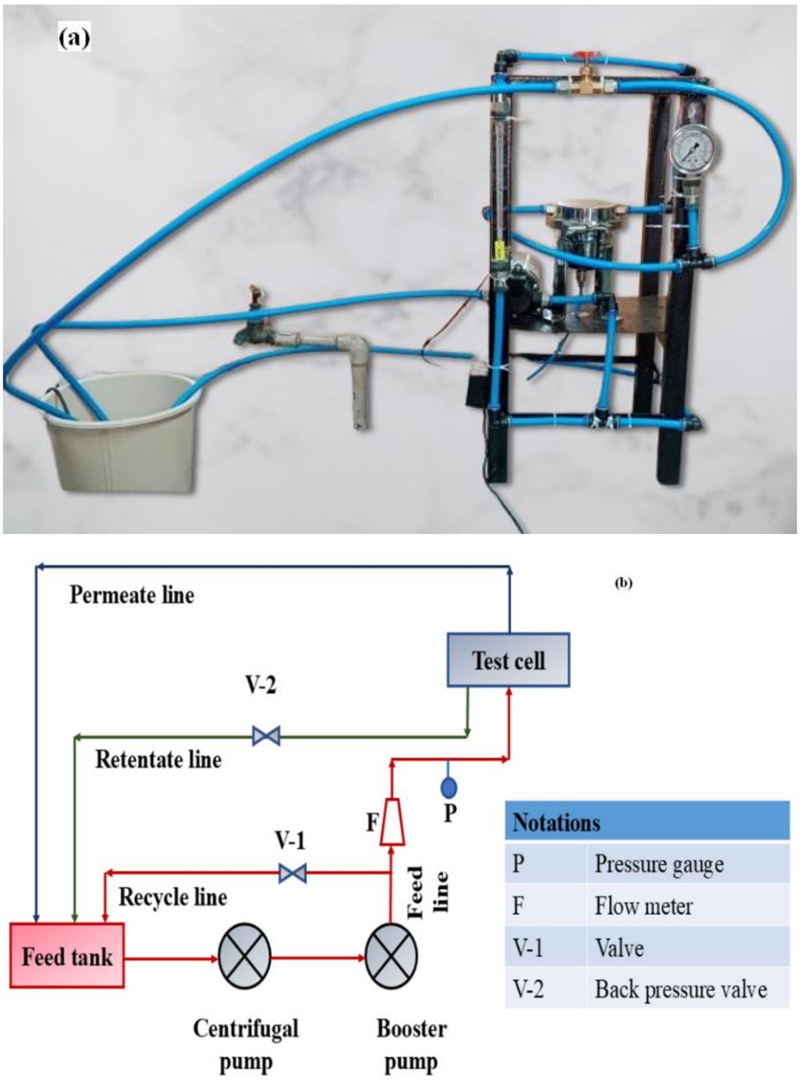

Figure 3.4 (a) Lab-prepared setup and (b) block diagram of the setup

The bulk feed solution was supplied from a 10 L feed tank to the membrane test cell using a centrifugal pump (0.25 hp) in combination with a booster pump having a nominal flow rate of 100 GPD and a maximum operating pressure of 12 bar. The system operated in cross-flow mode, with the feed continuously circulated through the membrane module and the permeate and retentate streams collected separately. The test cell housed a flat-sheet polyamide NF membrane with a molecular weight cut-off

(MWCO) of 150 Da, corresponding to an approximate pore size range of 0.1–10 nm. The effective membrane area used for all experiments was 0.007856 m².

Feed flow rate and pressure were monitored and controlled using a flow meter with a measurement range of 100–1200 mL/min and a glycerine-filled pressure gauge with a range of 0–9 bar. Needle valves installed on the feed and bypass lines were used to regulate both the cross-flow velocity and the operating pressure. The operating temperature was maintained at ambient conditions (25 ± 2 °C), and the system was allowed to reach steady state prior to data acquisition to ensure stable flux and rejection measurements. Permeate flux was determined gravimetrically at fixed time intervals, while retentate samples were collected in a separate tank for concentration.

3.4 Experimental Procedure

The experiments were conducted under standard procedures to ensure the reliability of the results. First, the membrane was washed with distilled water to remove surface contaminants from manufacturing and preservation processes [8], [9]. Water was then circulated through the membrane test cell under high pressure to compact and stabilize the washed membrane in position. The feed solution, prepared for the experiment, was then pumped into the membrane test cell by operating two specified pumps. The feed flow rates and pressures were regulated and maintained by valves and controllers along the feed and bypass lines. After each experimental run, a digital thermometer was employed to monitor the feed solution temperature. The retentate stream was then pumped back into the feed tank to maintain the feed solution's concentration. The permeate stream was collected at specific intervals, and permeate fluxes and flow rates were calculated by measuring the volume accumulated over a uniform time interval. Five different feed concentrations, feed flow rates, and pressures were used for the sampling.

3.5 Permeate Sample Analysis Technique

Permeate flux measures the amount of permeate that passes through the membrane per unit area per unit time. The mathematical equation (3.2) calculates the permeate flow rate.

$$\text{Permeate flux} = \frac{\text{Permeate volume}}{\text{Area} \times \text{Time}} \quad \ldots (3.2)$$

Permeate concentration was calculated using the Beer-Lambert Law (equation (3.1)). The permeate concentration measurement involved two stages. The first stage was the formation of the calibration curve, which involved plotting an absorbance versus concentration curve using standard solutions of known concentration. The value of the molar absorptivity constant was calculated from the slope of the calibration curve. The second stage involved measuring the absorbance of the permeate samples and then calculating the permeate concentration using the calculated molar absorptivity constant.

3.6 Parameter Estimation Technique

The above model contains five unknown parameters: the hydraulic permeability (L_p), solute permeability (B_m), reflection coefficient (σ), and two mass transfer coefficients, a and b. More accurate values of these unknown parameters are required to evaluate membrane performance.

An initial assumption for every model parameter is used to start the parameter estimation for the model. The predicted values of output characteristics, such as permeate flow rates (Q_p) and permeate concentrations (C_p), obtained from the model equations, were then compared with experimental values under different feed and operating conditions. The overall error between the theoretical and experimental characteristics was then minimized by formulating it as an objective function and adjusting the parameter values. The estimation was terminated if the computed error was below the desired tolerance limit and the obtained parameter values were correct. If the overall error was significant, the chosen parameter values were refined using optimization techniques. The above procedure was repeated until the experimental and predicted permeate characteristics were as close as possible and the error was minimized. The method, dependent on the Simplex search technique, was applied to estimate the parameters from a given set of experimental data. Once the actual parameters were received, the parameter set was used for model validation and prior simulation [10].

Algorithm: Figure 3.5 represents the general algorithm for the parameter estimation.

- Firstly, obtain the initial predictions for the parameters.
- Compute the values of error at all experimental data points. The expression for error is defined in equation (3.2)

$$\text{Error} = \sum_{i=1}^{t} \sqrt{\left(1 - \frac{Q_{pcal}}{Q_{pexp}}\right)^2 + \left(1 - \frac{C_{pcal}}{C_{pexp}}\right)^2} \quad \ldots (3.2)$$

Here, t is the number of experimental data points and their corresponding theoretical values used for the error calculation. Hence, the overall error is an optimization function dependent on all unknown model parameters.

- Parameter values are then adjusted to minimize the error by use of an optimization technique till the error is below a tolerance value.

  Minimize overall error = f (L_p, B_m, σ, a, b).

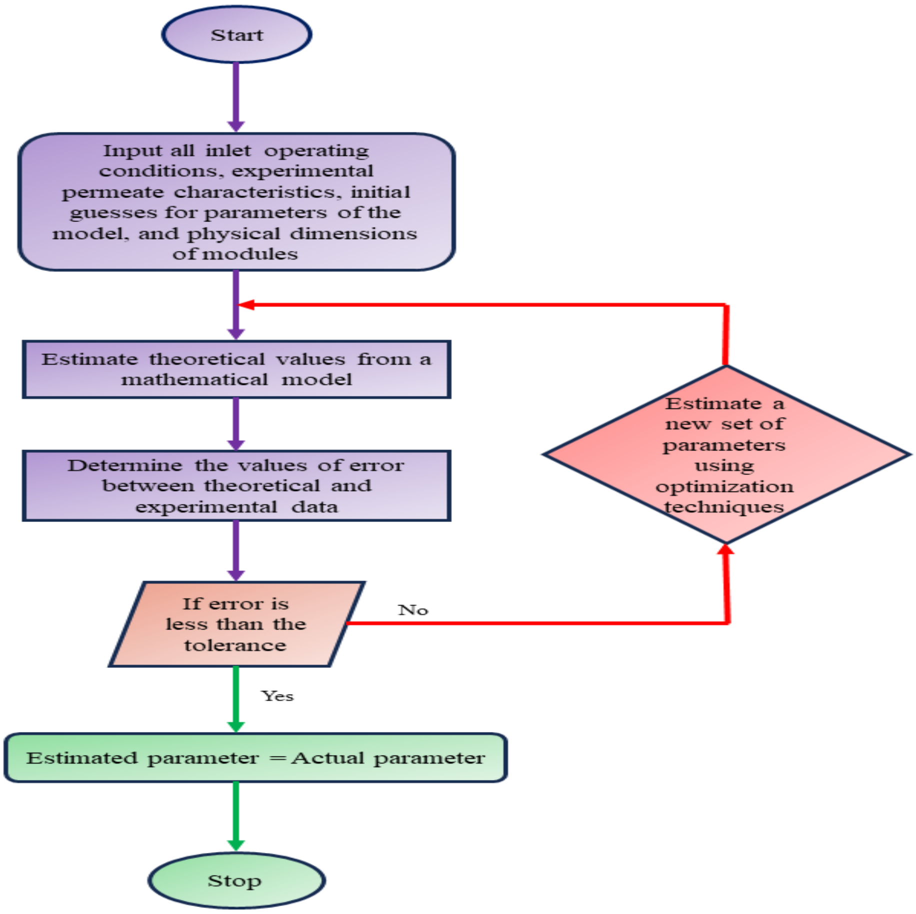

Figure 3.5 Algorithm flow chart for parameter estimation

In earlier literature, the unconstrained optimization method was applied to calibrate the unknown parameters. In unconstrained optimization, the parameter values are not restricted. Still, the values of unknown parameters cannot be negative, so a constrained optimization technique was used.

References

[1] F. Sánchez Rojas and J. M. Cano Pavón, “Spectrophotometry | Biochemical applications,” *Enc. Anal. Sci. (Second Edition)*, pp. 366–372, 2005, doi: 10.1016/B0-12-369397-7/00722-6

[2] P. J. Worsfold, “Spectrophotometry | Overview,” *Enc. Anal. Sci. (Second Edition)*, pp. 318–321, 2005, doi: 10.1016/B0-12-369397-7/00714-7

[3] J. Harshika, C. Chetan, and S. Leena, “Review : Calibration and validation of UV visible spectroscopy and method development of Letrozole by UV,” *Int. J. Res. Publ. Rev.*, vol. 4, no. 10, pp. 1990–1999, 2023

[4] S. Arshadi-Rastabi, J. Moghaddam, and M. Reza Eskandarian, “Synthesis, characterization, and stability of Cu_2O nanoparticles produced via supersaturation method considering operational parameters effect,” *J. Ind. Eng. Chem.*, vol. 22, pp. 34–40, 2015, doi: 10.1016/j.jiec.2014.06.022

[5] P. Raghavendra and T. Pullaiah, “Biomedical imaging role in cellular and molecular diagnostics,” *Adv. Cell Mol. Diagn.*, pp. 85–111, 2018, doi: 10.1016/b978-0-12-813679-9.00004-x

[6] T. S. Sampath Kumar, “Physical and Chemical Characterization of Biomaterials,” *Biomater. Charact.*, 2013, pp. 11-47, doi: https://doi.org/10.1016/B978-0-12-415800-9.00002-4

[7] M. Omidi *et al.*, “Characterization of biomaterials,” *Biomat. Oral and Dental Tissue Eng.*, 2017, pp. 97-115, doi: 10.1016/B978-0-08-100961-1.00007-4

[8] A. K. Tiwari and M. Jain, “Concentration of betanin from model beetroot extracts using nanofiltration: parameter estimation and sensitivity analysis,” *J. Chem. Technol. Biotechnol.*, 2024, vol. 99, no. 9, pp. 1976–1983, 2024, doi: 10.1002/jctb.7698

[9] A. K. Tiwari and M. Jain, “A novel process for rutin recovery from model solutions using nanofiltration: Experimental study, mathematical modeling, and scale-up design,” *J. Food Process Eng.*, vol. 47, no. 3, pp. e14592, 2024, doi: 10.1111/jfpe.14592

[10] S. Senthilmurugan and S. K. Gupta, "Modeling of a radial flow hollow fiber module and estimation of model parameters for aqueous multi-component mixture using numerical techniques," *J. Membr. Sci.*, vol. 279, no. 1–2, pp. 466–478, 2006, doi: 10.1016/j.memsci.2005.12.041

Chapter – 4

Recovery of Rutin From Model Solutions Using Nanofiltration

CHAPTER – 4

RECOVERY OF RUTIN FROM MODEL SOLUTIONS USING NANOFILTRATION

4.1 Introduction

Phenolics are the most abundant secondary metabolites in plants [1]. They are generally found in various plant and vegetable matrices. Based on their functional derivatives, more than 8000 structures are currently known. Phenolics are usually categorized by aromatic rings containing one or more hydroxyl groups [2]. The various classes of phenolics include flavonoids, stilbenes, phenolic acids, coumarins, tannins, lignins, and lignans [3]. These groups perform different plant functions, such as protection against ultraviolet radiation, pathogens, and other predators, and provide flavor, odor, taste, color, and oxidative stability [4], [5]. The physiological activities of these compounds include anti-infective, anti-aging, anti-inflammatory, and anti-proliferative properties [6].

Phenolics also impart various health benefits and become a vital ingredient of the human diet [7]. These phenolics are responsible for inhibitory activity against serious problems such as cancer, diabetes, and others [6], [8]. These beneficial effects are attributed to their antioxidant properties and ability to absorb generated free radicals. Many studies have reported their efficacy as pharmaceutical agents, either as alternatives or in synergy with aggressive treatments for diverse ailments. Other than the pharmaceutical industry, various industries such as food, textile, cosmetic, and packaging [9].

Rutin (quercetin 3-β-D-rutinoside; IUPAC name: 3′,4′,5,7-Tetrahydroxy-3-[α-L-rhamnopyranosyl-(1→6)-β-D-glucopyranosyloxy]flavone) is a slightly water-soluble crystalline powder that is yellow in color. The molecular structure of rutin is shown in Figure 4.1. It is the primary coloring matter found in the leaves and blossoms of buckwheat and many other plants [10]. Rutin is a beneficial pharmaceutical product due to its excellent antioxidant, antiviral, and estrogenic properties [11]. It is also called vitamin P. Rutin has a protective effect against harmful X-rays and is therefore used to treat people exposed to atomic radiation. The buckwheat plant is a prospective commercial source of rutin. It is a perennial plant with a height of 1–1.75 m and pinkish-white blooms, belonging to Central Asia. It is used as a fodder crop in several nations. As a small-scale grain crop, it is widely cultivated in Kashmir, Manipur, Sikkim, and Tamil Nadu. Rutin is mainly found in the plant's leaves and blooms (80–90%); it isn't found in any quantity in the stems or fruits. Rutin concentration varies with plant age, reaching a peak in the early stages of flowering.

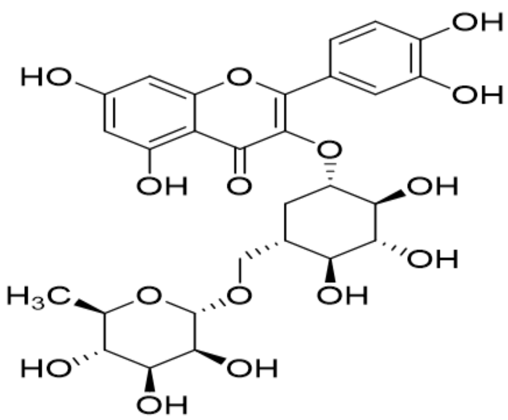

Figure 4.1 Rutin

The extraction and recovery of these bioactive phenolics are tedious tasks. Therefore, the extraction method must be carefully selected to prevent chemical changes to the target molecules [12]. Moreover, traditional extraction methods for separating phenolics use organic solvents, which makes them expensive. Also, the extract recovered from these processes may contain undesirable residual solvents for food applications. Therefore, there is a need for a new, cost-effective method for phenolic recovery and extraction [1], [13]. Membrane filtration has become a promising technology for concentrating phenolics. The principle behind the membrane-based processes is the permeation of selective particles through membranes. This filtration process offers various benefits, such as low-temperature requirements, low energy consumption, reduced operational costs and time, reduced waste disposal, continuous operation, and easy scalability for commercial upgradation [14]-[16]. Hydrostatic pressure is the driving force behind mass transfer in membrane processes [16], [17].

Membrane filtration expedites many applications, such as wine concentration, solvent exchange in the chemical industry, and clarification and concentration of various juices in the food industry [18]-[24]. Of all the processes, nanofiltration (NF) has the highest retention rate for a molecular weight range of 100 Da to 1000 Da [25].

Carmela Conidi *et al.* [26] used three commercially available NF membranes (NFPES 10, N30F, and NF270) to concentrate phenolic compounds from bergamot juice. The investigations revealed that the NF270 membrane showed the highest rejection of 82% towards phenolics and 90–97.7% towards flavonoids. Payel Ghosh *et al.* [23] concentrated the anthocyanidin from Indian blackberry by combining ultrafiltration (UF) and NF. A spiral-wound polysulfone NF membrane (MWCO of 300 Da) with an effective area of 0.3 m^2 was used to concentrate UF-clarified juice. This investigation observed a high permeate flux of 366 L/hm^2 and a 74% rejection of polyphenols at 2.5 mPa. Swallow Wei *et al.* [2] have concentrated the single-component rutin model solution and the binary mixture of rutin and glucose using UF. They used Pellicon-2 regenerated cellulose UF membrane with an active membrane area of 0.1 m^2 and a MWCO of 1000 Da. The single-component UF showed concentration factors of 1.32 for rutin and 1.02 for glucose at 4 bar, 35°C, and a feed flow rate of 1 L/min. The best performance of the dual component (sugar + rutin) was observed when the rutin concentration factor and recovery in the retentate were 2.9 and 72.5%, respectively.

Only a few papers were found on the concentration of rutin using NF. A detailed analysis of the membrane transport phenomenon to assess the process's viability on a larger scale was not reported. Hence, this research aims to focus on different model-rutin solutions, analyze the effects of operating conditions, and optimize transport parameters to assess the performance of the NF150 membrane for scale-up viability.

4.2 Materials and Methods

4.2.1 Materials

The laboratory-grade Rutin (molecular weight of 610.517 g/mol) was purchased from CDH Chemicals, New Delhi, India. The RO water was collected from a purification machine at Delhi Technological University, Delhi. The HFT-NF150 membrane was purchased from Permionics Pvt. Ltd., Gujarat, India.

4.2.2 Experimental Procedure and Conditions

As discussed in Chapter 3, the self-assembled NF Setup was used to perform all experiments. The concentration range of 20–100 mg/L for rutin was selected to reflect realistic levels reported in plant-derived extracts. In particular, extracts from buckwheat (Fagopyrum esculentum) milling fractions have been reported to contain rutin in the range of approximately 19-168 ppm, with many flour fractions falling within the ~20-100 ppm window. This concentration span directly overlaps with the 20-100 mg/L range commonly employed in nanofiltration model feed studies and represents moderately concentrated botanical extracts obtained after primary extraction and clarification. Therefore, the chosen range is both literature-supported and practically relevant, ensuring that the experimental conditions closely mimic real feed compositions while maintaining reliable analytical quantification and stable membrane operation.

The experiments for the model rutin solutions were conducted at low pressures, as the highest feasible pressure for the NF experimental setup is 6×10^5 Pa. Feed flow rates in the moderate range were preferred for the experimental studies due to the smaller area of the experimental setup. Regarding higher feed flow rates, variations in velocity and concentration in the permeate and feed channels may be imperceptible or negligible. Hence, the test cell performance cannot be adequately examined. Experiments were performed for different operating conditions, as depicted in Table 4.1

Table 4.1 Experimental conditions for different model solutions of rutin

Operating conditions	Value/Ranges
Feed concentration, mg/L	20 - 100
Pressure, Pa	2×10^5 - 6×10^5
Feed flow rate, L/h	12 - 36
Temperature, °C	22 ± 1
Time, min	5

4.3 Results and Discussion

The experiments were performed with a water/rutin mixture at varying feed concentrations under different operating conditions. The various operating parameters and their variation range are shown in Table 4.1. The system behavior was analyzed by varying one operating condition at a time while keeping the others constant.

4.3.1 Estimation of Unknown Model Parameters and Validation

4.3.1.1 Estimation of Hydraulic Permeability

The pure water flux tests were conducted under different conditions with feed flow rates ranging from 12 L/h to 36 L/h at an ambient temperature of 22 ± 1°C. The pressure was the variable under control in these tests. The tests were conducted by varying the pressure from 2×10^5 Pa to 6×10^5 Pa at a fixed feed flow rate of 30 L/h. A linear increase in flux values with increased pressure was observed (Figure 4.2). Table 4.2 presents the theoretical and experimental pure water permeability data, along with the percentage error. Conversely, the feed flow rates had a negligible impact on pure water flux at a fixed pressure. This indicates the absence of concentration polarization.

Table 4.2 Data for estimating the hydraulic permeability of the membrane before experiments on the rutin model solutions

Pressure (Pa)	Q_w the (L/h)	Q_w exp (L/h)	Error (%)
2×10^5	0.31	0.32	3.33
3×10^5	0.47	0.48	2.12
4×10^5	0.62	0.64	3.13
5×10^5	0.78	0.80	2.50
6×10^5	0.94	0.95	1.05
Predicted hydraulic permeability, $L_p = 5.52\times10^{-11}$ m^3/m^2sPa.			

The slope of the graph of pure water flux versus pressure difference gives the hydraulic permeability. The equation (4.1) relates hydraulic permeability, pressure difference, and flux.

$$L_P = \frac{J_w}{\Delta P} \quad \dots (4.1)$$

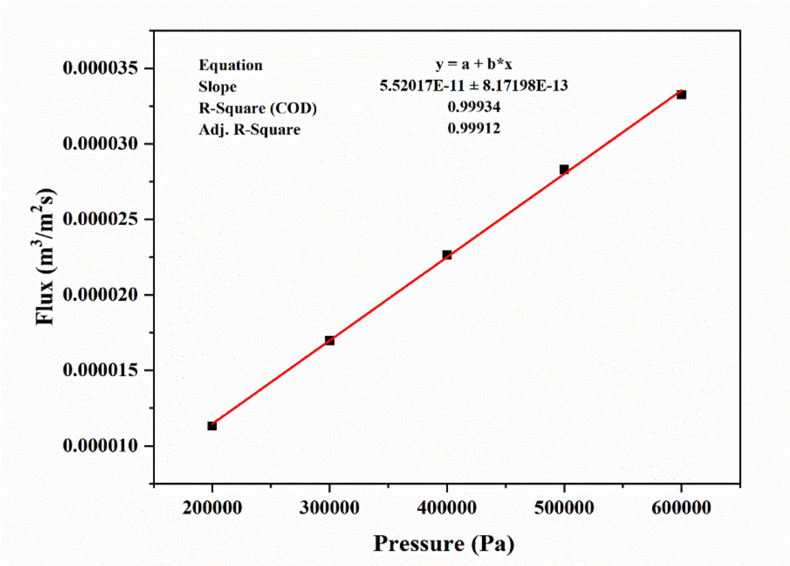

Figure 4.2 Pure water flux vs. pressure at a constant feed flow rate of 30 L/h

For validation of the experimental results with the theoretical results, the mean absolute percentage error was calculated by using the mathematical equation (4.2)

$$\mathrm{MAPE} = \frac{100}{n}\sum_{i=1}^{n}\left|\frac{Ev - Tv}{Ev}\right| \dots (4.2)$$

Here, E_v is the experimental value, T_v is the theoretical value, and n is the total number of experimental sets. For pure water permeability data, the MAPE for water flow rate was 2.43, with a maximum absolute percentage error (mAPE) of 3.33%. The calculated hydraulic permeability is then used to estimate other unknown parameters.

4.3.1.2 Estimation of Solute Permeability (B_m), Reflection Coefficient (σ), and Mass Transfer Coefficients (a & b)

Different sets of experimental runs were used to estimate solute permeability (B_m), reflection coefficient (σ), and mass transfer coefficients (a and b). The experimental values were obtained by fixing the value of two condition variables and varying the value of one. The pressure and concentration varied from 2×10^5 Pa to 6×10^5 Pa and from 20 mg/L to 100 mg/L, respectively. An ambient temperature of 22 ± 1 °C was selected for the experiment. Feed flow rate varies from 12 L/h to 36 L/h, with a 6 L/h range. The remaining parameters were estimated by fixing the calculated hydraulic permeability 5.52×10^{-11} m^3/m^2sPa and optimizing the others using the fminsearch optimization method in the MATLAB platform. The complete data on experimental and theoretical values, along with their validation, are tabulated in Appendix A1. The predicted average parameters were: Solute permeability (B_m) $= 2.15\times10^{-7}$ m/s; reflection coefficient (σ) = 0.98; mass transfer coefficients, a = 1.755×10^{-2}, b = 0.0809;

The above equation (4.2) is then used to calculate the MAPE for permeate flow rate, permeate concentration, and rejection percentage. The MAPEs for permeate flow rate, permeate concentration, and rejection were 16.6%, 14.85%, and 0.46%, respectively. The results also showed that the permeate concentration exhibited the greatest deviation between theoretical and experimental values, with a maximum percentage error of 54.04%. Table 4.3 represents the error analysis for permeate characteristics.

Table 4.3 Permeate characteristics error analysis for the model solutions of rutin

Permeate Characteristics	MAPE (%)	mAPE (%)
Permeate flow rate, L/h	16.6	36
Permeate concentration, mg/L	14.85	54
Rejection, %	0.46	1.8

4.3.2 Effects of Various Operating Conditions

The performance of the membrane test cell is greatly affected by various operating conditions. The roles of feed concentration, pressure, and feed flow rate were studied in this work using the HFT-NF150 membrane.

4.3.2.1 Effects of Pressure

The permeate flux increases with pressure at a fixed feed concentration and feed flow rate. An increase in permeate flux from 1.27×10^{-5} m^3/m^2s to 3.04×10^{-5} m^3/m^2s was observed as pressure increased from 2×10^5 Pa to 6×10^5 Pa at a fixed concentration of 20 mg/L and a feed flow rate of 36 L/h. This is because pressure is a driving force responsible for mass transfer. A similar trend was seen for other values of feed flow rates and feed concentrations, as depicted in Figure 4.3(a). Also, a slight increase in rejection percentage from 98 to 98.5% was observed with increased pressure at a fixed feed flow rate of 36 L/h and a 20 mg/L concentration. Figure 4.3(b) represents the influence of pressure on percentage rejection. This is generally due to decreased solute permeation due to the accumulation or agglomeration of solute particles on the membrane at higher pressure.

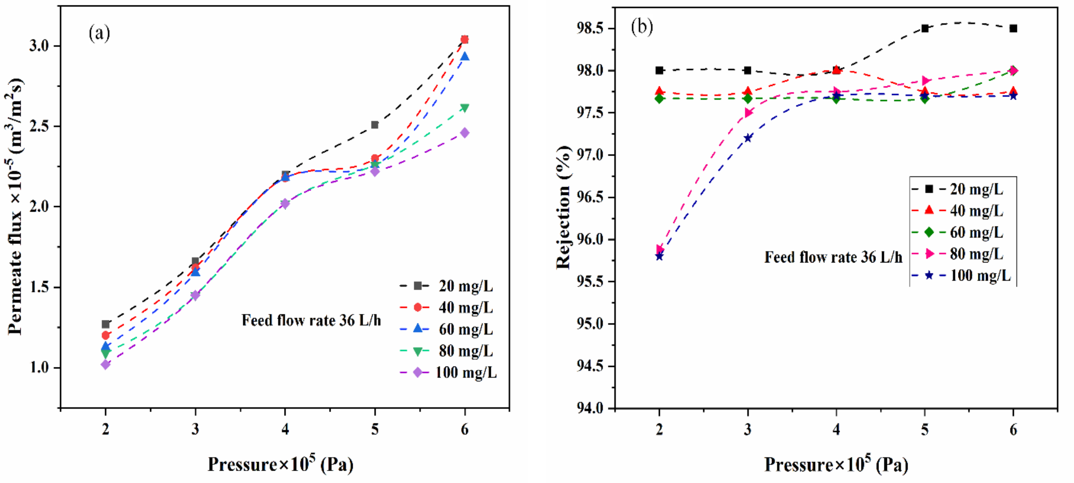

Figure 4.3 Effect of pressure on (a) permeate flux and (b) rejection percentage, for rutin model solutions, at a fixed flow rate of 36 L/h

4.3.2.2 Effect of Feed Concentration

Feed concentration plays a vital role in the mass transfer of molecules through membranes, as membranes are susceptible to the critical concentrations of compounds with higher molecular weight [27]. The permeate flux decreases as the feed concentration increases. This is caused by increased osmotic pressure, which reduces the driving forces for mass transfer. It was seen in Figure 4.4(a) that the value of permeate flux decreases from 1.27×10^{-5} m^3/m^2s to 1.02×10^{-5} m^3/m^2s as the feed concentration increases from 20 mg/L to 100 mg/L at a fixed feed flow rate of 36 L/h and pressure of 2×10^5 Pa. The same pattern was observed for other pressure values and feed flow rates. Also, a minimal decrease in rejection percentage was observed with increasing rutin concentration in the feed solution [28]. This may be because, at higher concentrations, a thin concentration layer forms near the membrane interface, resulting in a decrease in permeate flux. This decrease in flux results in an overall increase in permeate concentration. Figure 4.4(b) shows that at a fixed flow rate of 36 L/h and a pressure of 6×10^5 Pa, the percentage rejection decreased from 98.5% to 97.9% as the feed concentration increased from 20 mg/L to 100 mg/L.

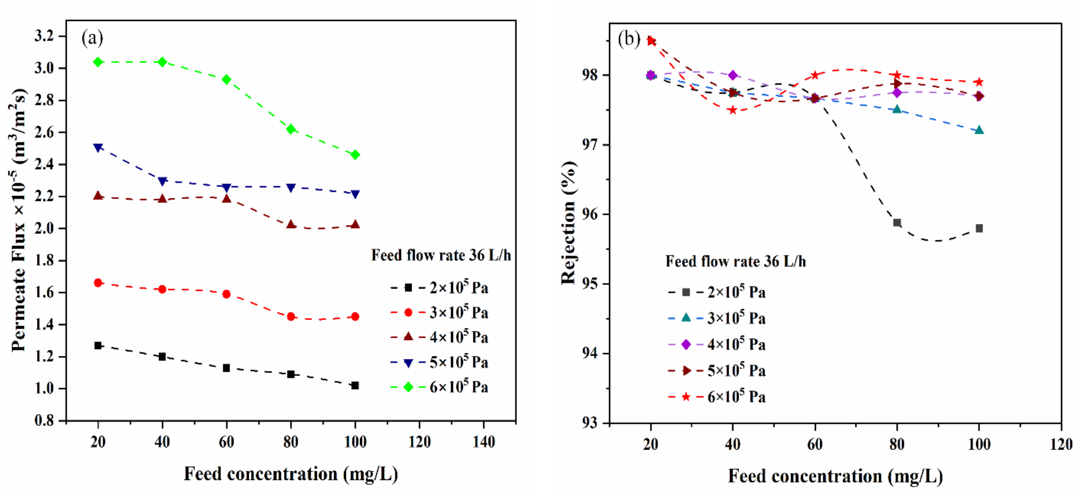

Figure 4.4 Effect of feed concentration on (a) permeate flux and (b) rejection percentage, for rutin model solutions, at a fixed flow rate of 36 L/h

4.3.2.3 Effects of Feed Flow Rate

The experimental results showed that the permeate flux increases with feed flow rates at a constant concentration and pressure. This is because removing solute molecules accumulating near the membrane surface reduces concentration polarization. Increasing feed flow rates also increases the rejection percentage. Figure 4.5(a) presents the variation of permeate flux as a function of feed flow rates. It was observed that the value of permeate flux increases from 0.99×10^{-6} m^3/m^2s to 1.27×10^{-5} m^3/m^2s at a fixed pressure of 2×10^5 Pa and fixed concentration of 20 mg/L. A similar trend was also observed for other pressure and concentration values. The results, as depicted in Figure 4.5(b), also show that the percentage rejection for the 20 mg/L feed solution increases from 98% to 98.5% with increasing feed flow rate from 12 L/h to 36 L/h at a fixed pressure of 6×10^5 Pa. This is due to a decrease in the concentration gradient caused by the turbulence in the stream at higher feed flow rates.

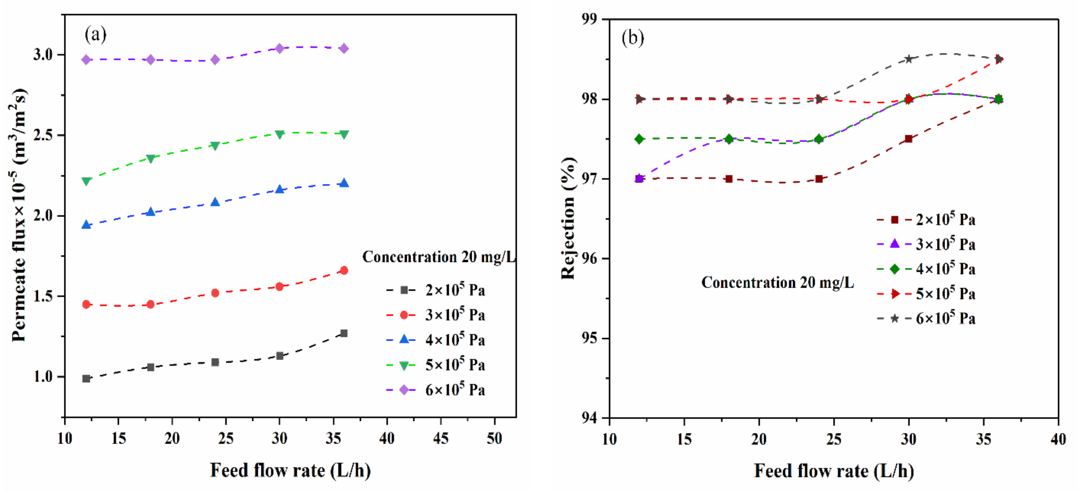

Figure 4.5 Effect of feed flow rate on (a) permeate flux and (b) rejection percentage, for rutin model solutions, at a feed concentration of 20 mg/L

4.3.3 Variation Analysis

The theoretical values of the permeate characteristics were investigated using the estimated parameters. At constant feed concentration and feed flow rate, the experimental variation of permeate flux and rejection percentage with respect to pressure was seen clearly in Figures 4.3(a) and 4.3(b), in accordance with the mathematical equations (2.12) and (2.8), respectively (as discussed in Chapter 2). The experimental data for analyzing the effect of feed concentration on permeate flux showed a trend per equation (2.12), discussed in Chapter 2, as depicted in Figure 4.4(a). However, the variation in theoretical data for permeate flux and rejection percentage was not observed with changes in concentration. This may be due to the minimal variation in feed concentration (parts per million), which showed no visible effect on the osmotic pressure term in equation (2.3) of Chapter 2. The experimental variation in permeate flux and rejection percentage with feed flow rate was clearly evident, as depicted in Figures 4.5(a) and 4.5(b). The mathematical equations (2.5) and (2.6) discussed in Chapter 2 for concentration polarization validate the same trend. As the feed flow rate increases, the mass transfer coefficient increases, ultimately decreasing the concentration polarization. Hence, the theoretical equations validate the observed experimental trend. However, the theoretical data for permeate flux and rejection percentage showed no apparent variation and remained almost constant with respect to the feed flow rate. This may be due to a negligible increase in the mass transfer coefficient, attributed to the tiny membrane test cell area of 0.007856 m^2. The regression curve in Figure 4.6 showed the deviation of experimental data from the theoretical data. The regression curve showed that the error variation for permeate flow rate, permeate concentration, and rejection percentage is between ±30%, ±30%, and ±3%, respectively. The maximum number of data points is found from the error bars of permeate concentration, as shown in Figure 4.6(b).

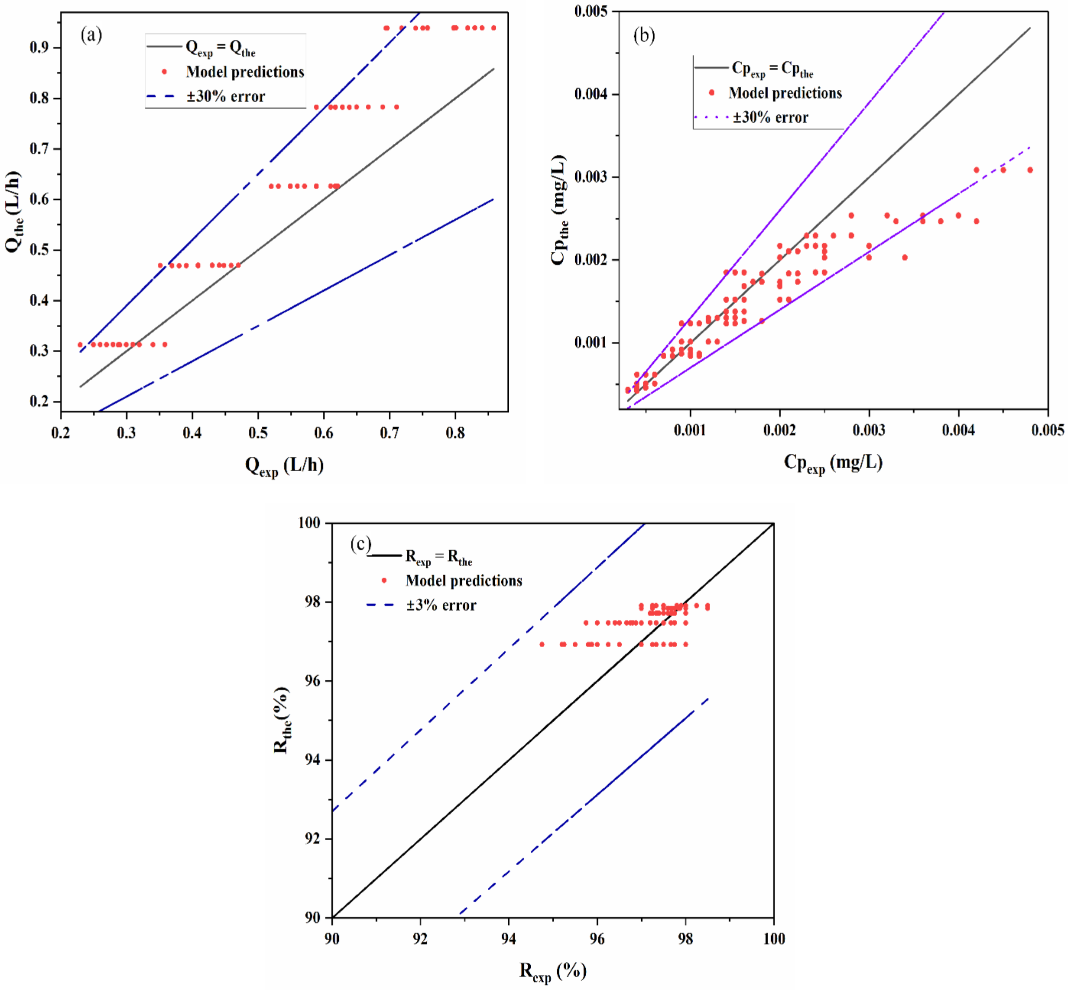

Figure 4.6 Regression curve of rutin model solutions for (a) permeate flux, (b) permeate concentration, and (c) rejection percentage.

4.3.4 Selectivity Analysis

Based on the experimental conditions and optimized parameter values, a suitable range of operating conditions and membrane parameters was selected for the variance-based sensitivity analysis and reported in Table 4.4.

Table 4.4 Ranges of different parameters for the sensitivity analysis for the model rutin solutions

Parameters	Range
Pressure, Pa	2×10^{5} - 6×10^{5}
Feed concentration, mg/L	20 - 100
Feed flow rate, L/h	6 - 36
Hydraulic permeability, kg/m^{2}sPa	5.5×10^{-9} - 5.5×10^{-7}
Solute permeability, m/s	2.15×10^{-6} - 2.15×10^{-8}
Reflection coefficient	0.7 - 1

As discussed in Chapter 2, a variance-based sensitivity analysis was used to assess the dependence and interdependence of module parameters and operating conditions on permeate flux and rejection percentage. The analysis requires the formulation of two independent matrices, each containing random values drawn from the given data ranges. The matrices should contain equal numbers of input parameters. All the model evaluations were performed in Google Colab. All the data were stored in a CSV file for further processing.

Figures 4.7 and 4.8 present the normalized sensitivities (first-order and total) for permeate flux and rejection percentage, respectively, under different operating conditions and membrane module parameters, with varying sample sizes. The convergence of the entire data set, sampled randomly, occurs slowly after a certain number of samples. The results showed that the first-order and total-order sensitivity indexes fluctuated initially, then varied marginally. The negligible variance after a sample size of 80,000 provides confidence in the sensitivity estimates at 1,00,000.

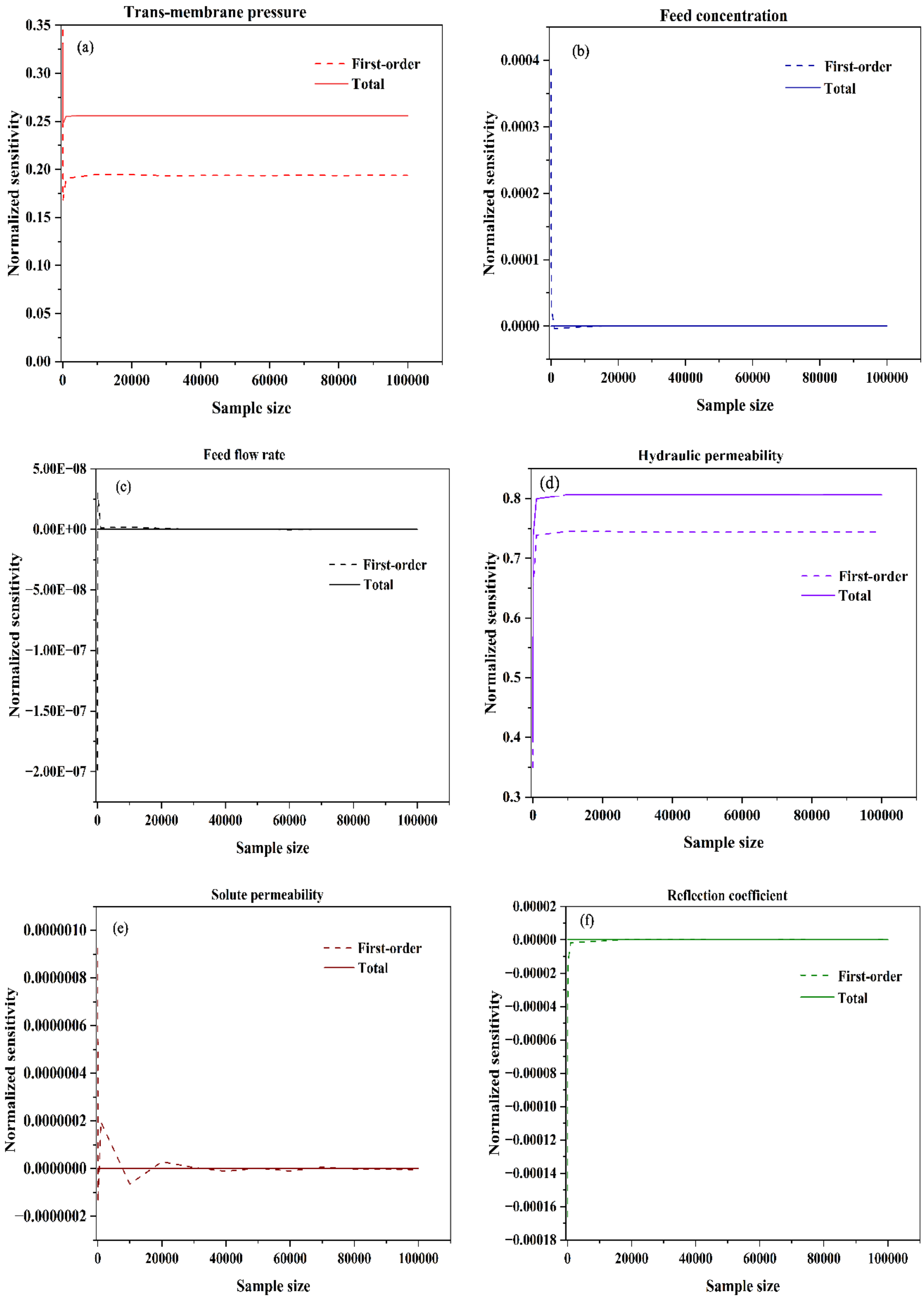

Figure 4.7 Values of first-order sensitivity and total sensitivity on total permeate flux of model rutin solutions with increasing sample size for (a) pressure, (b) feed concentration, (c) feed flow rate, (d) hydraulic permeability, (e) solute permeability, and (f) reflection coefficient.

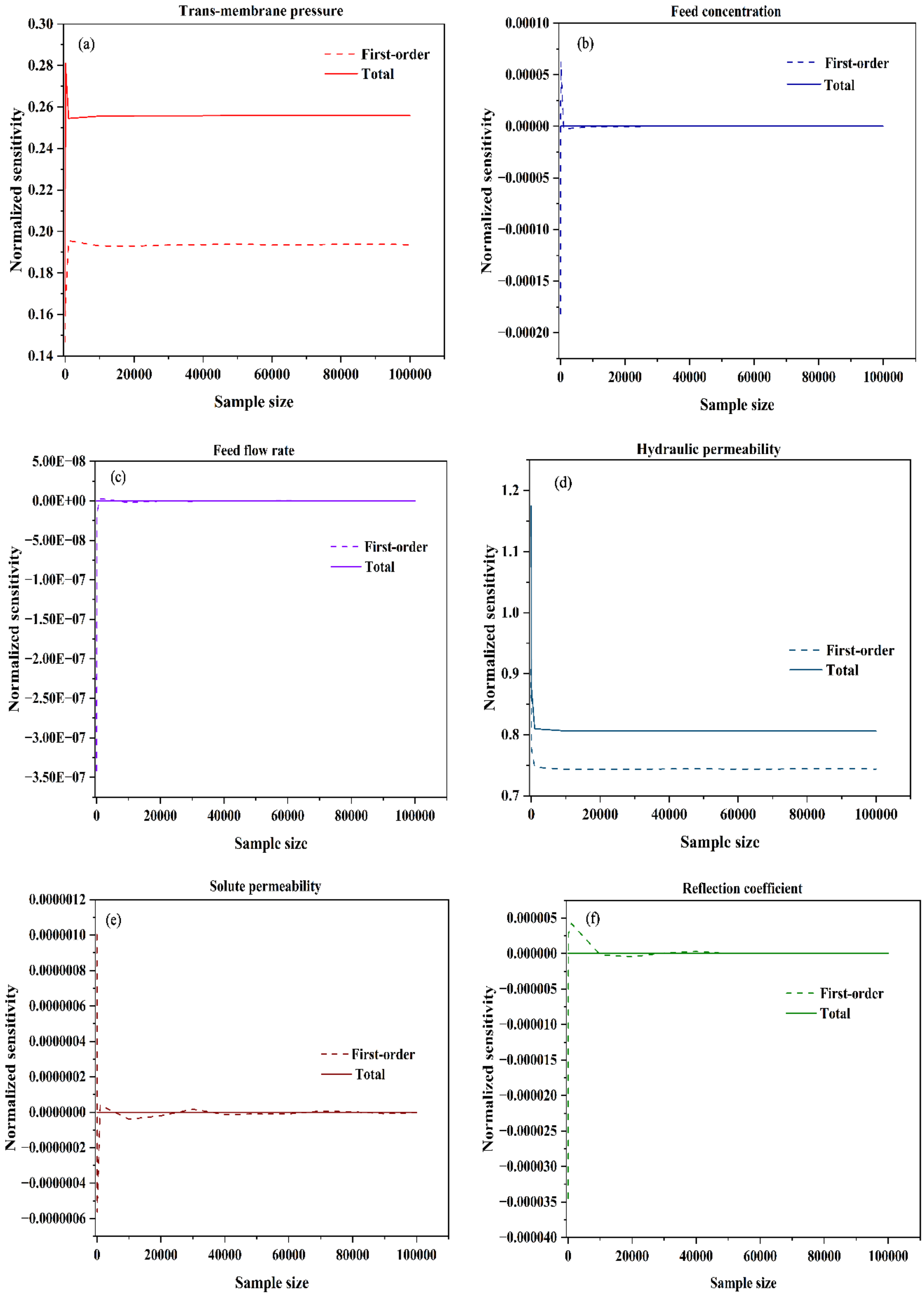

Figure 4.8 Values of the first-order and total sensitivity on rejection of rutin with increasing sample size for (a) pressure, (b) feed concentration, (c) feed flow rate, (d) hydraulic permeability, (e) solute permeability, and (f) reflection coefficient.

4.3.4.1 Sensitivities of Different Operating Variables and Membrane Parameters for Permeate Flux

Figure 4.9(a) represents the comparison of first-order sensitivity (S), total sensitivity (S_T), and their differences (S_T-S) for permeate flux. It was observed that the normalized sensitivities (S and S_T) of hydraulic permeability were the highest, followed by pressure, and the sensitivities of all other operating parameters, such as feed flow rate, feed concentration, solute permeability, and reflection coefficient, were comparatively negligible. Thus, it can be concluded that hydraulic permeability and pressure are the most controlling parameters for total volumetric permeate flux. Also, the value of (S_T-S) was low for L_p and ΔP. Therefore, the interactive effects of ΔP with other operating parameters are relatively insignificant on volumetric flux. Based on the sensitivity values (S_T and S), operating variables and membrane parameters can be sorted in decreasing order as $L_p > \Delta P > Cb > \sigma > B_m > Q$. The lower sensitivities of Cb and Q are due to low concentration polarization and a smaller test cell area.

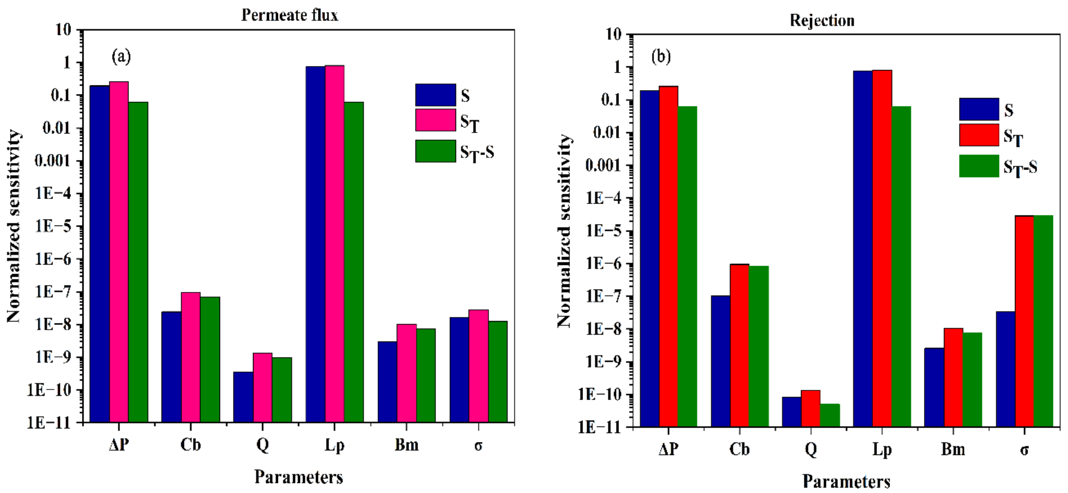

Figure 4.9 Sensitivity of different operating and membrane parameters for (a) permeate flux and (b) rejection, for rutin solutions.

4.3.4.2 Sensitivities of Different Operating Variables and Membrane Parameters for Rejection

As with permeate flux, hydraulic permeability (L_p) is the most influential parameter. A similar trend in (S_T-S) was observed, as seen earlier for permeate flux (Figure 4.9(b)).

4.3.5 Performance of Scale-up

The efficiency of membrane test cells depends largely on operating conditions. However, removing rutin to the desired limit also depends on the module's active membrane area. Not only this, but the higher membrane area may also lead to greater variations in pressure and temperature along the length of the flow channels in the module, thereby reducing the overall efficiency of the membrane module. Thus, using many smaller test cells in series is recommended rather than increasing the membrane area in a single test cell. Figure 4.10 represents the schematic diagram for the scale-up setup.

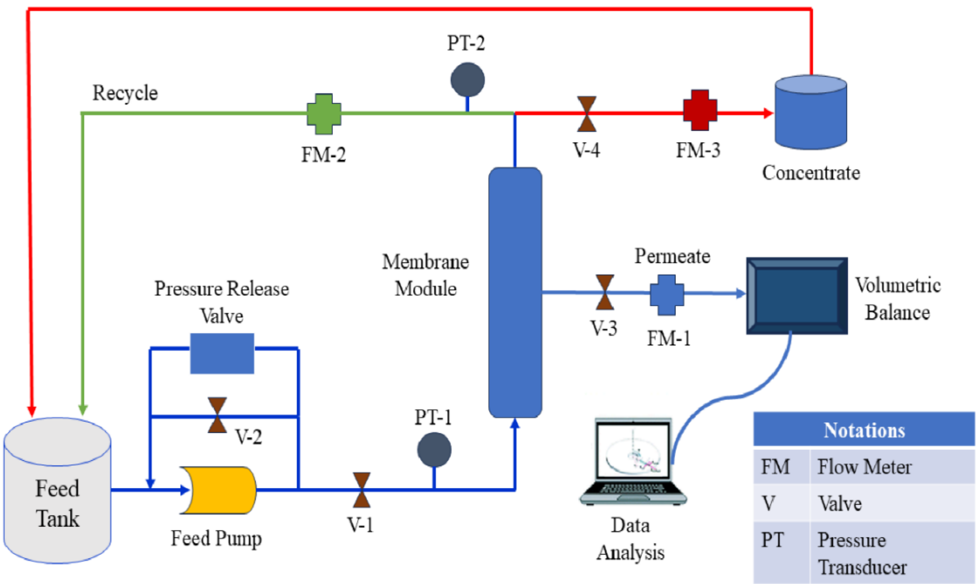

Figure 4.10 Schematic diagram for scale-up

Simulations were performed to treat 100 L of model compound solution at a feed concentration of 100 mg/L, a pressure of 2×10^5 Pa, and a feed flow rate of 36 L/h. Figure 4.11 shows the variation in feed concentration and volume over time. It was found that the feed concentration increases exponentially up to a specific limit and then becomes almost constant, whereas the feed volume decreases over time and eventually becomes constant. This may be due to the precipitation of the rutin in the feed solution, which almost stops water permeation. Other operating conditions, such as the feed flow rate and operating temperature, are held constant throughout the simulation. These simulations proved that the proposed scale-up setup can concentrate rutin to the desired limits.

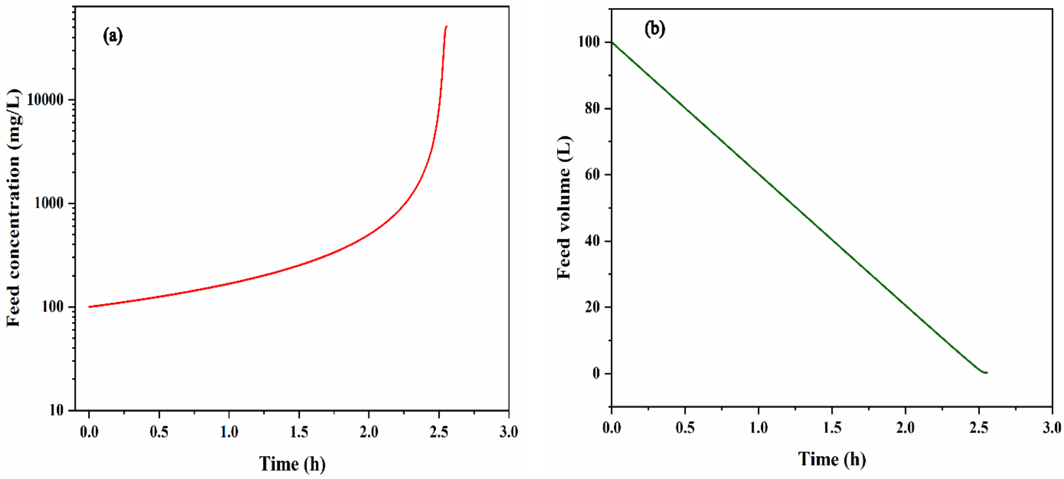

Figure 4.11 Variation analysis of (a) feed concentration and (b) feed volume concerning time for a 100 L rutin model solution having a 100 mg/L feed concentration.

Results were then analyzed to concentrate the rutin in the feed solution from 100 mg/L to 50000 mg/L at different pressures and active membrane areas. Figure 4.12(a) shows the time variation concerning pressure at a fixed feed flow rate of 36 L/h and an active membrane area of 1.0 m^2. This relationship is crucial for scale-up because it shows that increasing pressure can optimize process efficiency, but with diminishing returns above a certain level. This is because the permeation volume increases with pressure until a critical concentration is reached; at this point, solute precipitation starts at the membrane surface.

As shown in Figure 4.12(a), a significant decrease in filtration time from 2.55 h to 0.84 h was observed as the pressure increased from 2×10^5 Pa to 6×10^5 Pa. Simultaneously, the feed volume decreased from around 0.21 L to 0.08 L. The gradual decline suggests that rutin molecules interact moderately with the membrane surface, creating some resistance but not severe fouling.

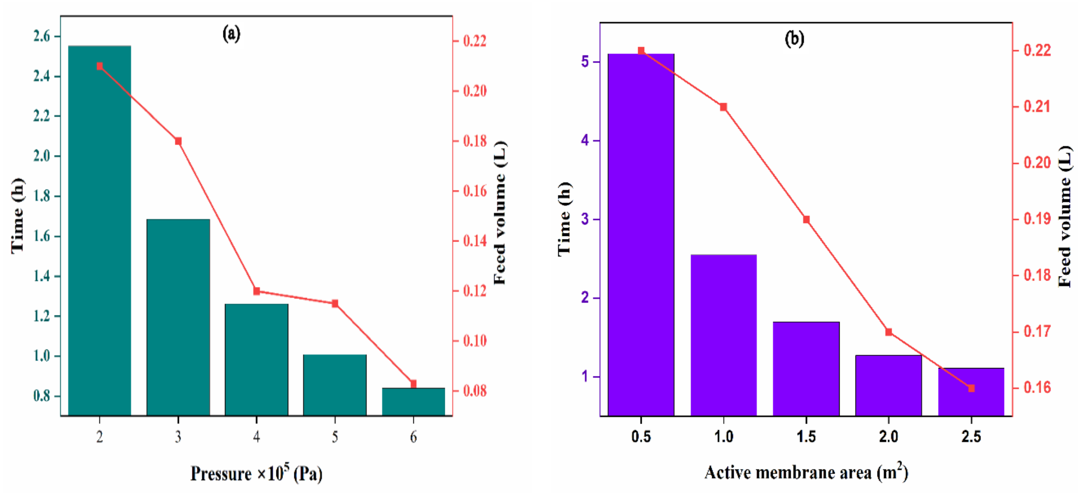

Figure 4.12 Time required to concentrate rutin from 100 mg/L to 50000 mg/L at (a) different operating pressures and (b) active membrane area.

The simulations with different membrane areas also showed the same trend as the pressure simulations. It can be seen from Figure 4.12(b) that the time required to concentrate the rutin feed solution from 100 mg/L to 50000 mg/L decreases from 5.10 h to 1.02 h with an increase in active membrane area from 0.5 m^2 to 2.5 m^2 at a fixed pressure of 2×10^5 Pa and feed flow rate of 36 L/h. Also, the rutin feed volume decreases gradually from 0.22 L to 0.16 L.

4.4 Conclusion

The attempt to investigate the separation of different model rutin solutions was successfully achieved in this study. The best performance of the HFT-NF150 membrane for rutin concentration was observed at a pressure of 6×10^5 Pa and a feed flow rate of 36 L/h, with a maximum permeate flux of 3.04×10^{-5} m^3/m^2s and a maximum separation of 98.5%. The theoretical studies of the transport parameters used to estimate membrane performance were also evaluated using equations from the Spiegler-Kedem model. The experimental and theoretical results for permeate flow rate, permeate concentration, and percentage rejection were well matched, with mean absolute errors of 16.6, 14.85, and 0.46, respectively. The lower MAPE value provides confidence in integrating this test cell at a larger scale. Simulations for the scale-up setup demonstrate that the HFT-NF 150 membrane analyzed in this study can concentrate rutin to the desired level. It was also found that pressure and active membrane area have a greater impact on the time required to concentrate rutin. In contrast, the feed flow rate had a negligible effect on the concentration time.

References

[1] H. Nawaz, J. Shi, G. S. Mittal, and Y. Kakuda, "Extraction of polyphenols from grape seeds and concentration by ultrafiltration," *Sep. Purif. Technol.*, vol. 48, no. 2, pp. 176–181, 2006, doi: 10.1016/j.seppur.2005.07.006

[2] S. Wei, M. M. Hossain, and Z. S. Saleh, "Concentration of rutin model solutions from their mixtures with glucose using ultrafiltration," *Int. J. Mol. Sci.*, vol. 11, no. 2, pp. 672–690, 2010, doi: 10.3390/ijms11020672

[3] M. Naczk and F. Shahidi, "Phenolics in cereals, fruits and vegetables: Occurrence, extraction and analysis," *J. Pharm. Biomed. Anal.*, vol. 41, no. 5, pp. 1523–1542, 2006, doi: 10.1016/j.jpba.2006.04.002.

[4] K. B. Pandey and S. I. Rizvi, "Plant polyphenols as dietary antioxidants in human health and disease," *Oxid. Med. Cell. Longev.*, vol. 2, no. 5, pp. 270–278, 2009, doi: 10.4161/oxim.2.5.9498

[5] O. R. Alara, N. H. Abdurahman, and C. I. Ukaegbu, "Extraction of phenolic compounds: A review," *Curr. Res. Food Sci.*, vol. 4, pp. 200–214, 2021, doi: 10.1016/j.crfs.2021.03.011

[6] A. Durazzo *et al.*, "Polyphenols: A concise overview on the chemistry, occurrence, and human health," *Phyther. Res.*, vol. 33, no. 9, pp. 2221–2243, 2019, doi: 10.1002/ptr.6419

[7] N. Balasundram, K. Sundram, and S. Samman, "Phenolic compounds in plants and agri-industrial by-products: Antioxidant activity, occurrence, and potential uses," *Food Chem.*, vol. 99, no. 1, pp. 191–203, 2006, doi: 10.1016/j.foodchem.2005.07.042

[8] M. L. Luna-Guevara, J. J. Luna-Guevara, P. Hernández-Carranza, H. Ruíz-Espinosa, and C. E. Ochoa-Velasco, "Phenolic compounds: A good choice against chronic degenerative diseases," *Stud. Nat. Prod. Chem.*, vol. 59, pp. 79–108, 2018, doi: 10.1016/B978-0-444-64179-3.00003-7

[9] B. R. Albuquerque, S. A. 8. Heleno, M. B. P. P. Oliveira, L. Barros, and I. C. F. R. Ferreira, "Phenolic compounds: Current industrial applications, limitations

and future challenges," *Food Funct.*, vol. 12, no. 1, pp. 14–29, 2021, doi: 10.1039/d0fo02324h

[10] L. R. Fitzpatrick and T. Woldemariam, "Small-Molecule Drugs for the Treatment of Inflammatory Bowel Disease," *CMC III*, pp. 495-510, 2017, doi: 10.1016/B978-0-12-409547-2.12404-7

[11] K. Patel and D. K. Patel, "The Beneficial Role of Rutin, A Naturally Occurring Flavonoid in Health Promotion and Disease Prevention: A Systematic Review and Update," *Bioactive Food as Dietary Interventions for Arthritis and Related Inflammatory Diseases*, pp. 457-479, 2019, doi: 10.1016/B978-0-12-813820-5.00026-X

[12] K. Bradley, " Book Review," *Companion Anim.*, vol. 23, no. 8, pp. 433–433, 2018, doi: 10.12968/coan.2018.23.8.433

[13] J. Shi, H. Nawaz, J. Pohorly, G. Mittal, Y. Kakuda, and Y. Jiang, "Extraction of polyphenolics from plant material for functional foods - Engineering and technology," *Food Rev. Int.*, vol. 21, no. 1, pp. 139–166, 2005, doi: 10.1081/FRI-200040606

[14] M. Mondor, B. Girard, and C. Moresoli, "Modeling flux behavior for membrane filtration of apple juice," *Food Res. Int.*, vol. 33, no. 7, pp. 539–548, 2000, doi: 10.1016/S0963-9969(00)00089-2

[15] J. P. F. De Bruijn, A. Venegas, J. A. Martínez, and R. Bórquez, "Ultrafiltration performance of Carbosep membranes for the clarification of apple juice," *LWT - Food Sci. Technol.*, vol. 36, no. 4, pp. 397–406, 2003, doi: 10.1016/S0023-6438(03)00015-X

[16] V. M. Matta, R. H. Moretti, and L. M. C. Cabral, "Microfiltration and reverse osmosis for clarification and concentration of acerola juice," *J. Food Eng.*, vol. 61, no. 3, pp. 477–482, 2004, doi: 10.1016/S0260-8774(03)00154-7

[17] A. S. Mujumdar, "A Review of: 'Food process design,'" *Dry. Technol.*, vol. 24, no. 1, pp. 117–117, 2006, doi: 10.1080/07373930500538915

[18] J. Geens, K. Boussu, C. Vandecasteele, and B. Van der Bruggen, "Modelling of

solute transport in non-aqueous nanofiltration," *J. Memb. Sci.*, vol. 281, no. 1–2, pp. 139–148, 2006, doi: 10.1016/j.memsci.2006.03.028

[19] S. Banvolgyi, I. Kiss, E. Bekassy-Molnar, and G. Vatai, "Concentration of red wine by nanofiltration," *Desalination*, vol. 198, no. 1–3, pp. 8–15, 2006, doi: 10.1016/j.desal.2006.09.003

[20] H. Mirsaeedghazi, Z. Emam-Djomeh, S. M. Mousavi, A. Aroujalian, and M. Navidbakhsh, "Clarification of pomegranate juice by microfiltration with PVDF membranes," *Desalination*, vol. 264, no. 3, pp. 243–248, 2010, doi: 10.1016/j.desal.2010.03.031

[21] G. T. Vladisavljević, P. Vukosavljević, and B. Bukvić, "Permeate flux and fouling resistance in ultrafiltration of depectinized apple juice using ceramic membranes," *J. Food Eng.*, vol. 60, no. 3, pp. 241–247, 2003, doi: 10.1016/S0260-8774(03)00044-X

[22] G. D. Arend *et al.*, "Concentration of phenolic compounds from strawberry (Fragaria X ananassa Duch) juice by nanofiltration membrane," *J. Food Eng.*, vol. 201, pp. 36–41, 2017, doi: 10.1016/j.jfoodeng.2017.01.014

[23] P. Ghosh, R. C. Pradhan, S. Mishra, and P. K. Rout, "Quantification and concentration of anthocyanidin from indian blackberry (*Jamun*) by combination of ultra- and nano-filtrations," *Food Bioprocess Technol.*, vol. 11, no. 12, pp. 2194–2203, 2018, doi: 10.1007/s11947-018-2176-4

[24] B. Girard and L. R. Fukumoto, "Membrane processing of fruit juices and beverages: A review," *Crit. Rev. Food Sci. Nutr.*, vol. 40, no. 2. pp. 91-157, 2000, doi: 10.1080/10408690091189293

[25] H. Dach, "Comparison of nanofiltration and reverse osmosis processes for a selective desalination of brackish water feeds," *Eng. Sci., Université d'Angers*, pp. 193, 2009

[26] C. Conidi and A. Cassano, "Recovery of phenolic compounds from bergamot juice by nanofiltration membranes," *Desalin. Water Treat.*, vol. 56, no. 13, pp. 3510–3518, 2015, doi: 10.1080/19443994.2014.968219

[27] S. K. Karode, B. B. Gupta, and T. Courtois, "Ultrafiltration of raw Indian sugar solution using polymeric and mineral membranes," *Sep. Sci. Technol.*, vol. 35, no. 15, pp. 2473–2483, 2000, doi: 10.1081/SS-100102350

[28] N. García-Vaquero Marín and J. A. López-Ramírez, "Influence of organic fouling and operating conditions on nanofiltration membranes to reduce phenol concentration in natural waters," *Water Sci. Technol. Water Supply*, vol. 11, no. 4, pp. 473–480, 2011, doi: 10.2166/ws.2011.077

Chapter – 5
Concentration of Betanin From Model Beetroot Using Nanofiltration

CHAPTER – 5

CONCENTRATION OF BETANIN FROM MODEL BEETROOT USING NANOFILTRATION

5.1 Introduction

Phenolic compounds are plants' most abundant secondary metabolites [1]. Over 8000 structures are known based on their functional derivatives and are found in various varieties of matrices in different vegetables and fruits. Phenolic compounds are generally characterized by one or more aromatic rings bearing one or more hydroxyl groups [2]. The phenolic compounds are classified into flavonoids, simple and condensed tannins, phenolic acids, stilbenes, lignans, coumarins, and lignins [3]. These phenolic compounds perform various functions in plants, including protection; they also provide flavor (astringency, odor, and taste), appearance (color), and oxidative stability [4]. Phenolics also exhibit physiological properties such as anti-aging, anti-infective, anti-inflammatory, and anti-proliferative [5].

Phenolic compounds also provide many human-health-related functional benefits. Their natural antioxidant properties prevent oxidation of high-density lipoproteins and remove low-density lipoproteins, which are helpful in human cellular processes [6]. Moreover, their free radical-scavenging properties reduce ulceration and counteract the harmful effects of mutagens, including carcinogens [1], [2]. The ability of these phenolic compounds to absorb generated free radicals is also responsible for inhibiting the progression of various inflammatory and degenerative diseases, such as cancer, Alzheimer's, and diabetes [5], [7]. Many scientific studies have shown the efficacy of these phenolic compounds as pharmaceutical agents, either as alternatives or in synergy with regular meditation for diverse ailments. Not only do pharmaceutical industries utilize these phenolic compounds, but they also have biotechnological applications in various other industries, such as food, packaging, cosmetic, and textile industries [8].

Betanin is a water-soluble vacuolar chromo-alkaloid with a molecular weight of approximately 550 Da and is found in *Beta Vulgaris L*, also known as beetroot and chukandar [9]. At mildly acidic to neutral pH, betanin predominantly exists in an ionized form, strongly influencing its transport by Donnan exclusion effects in addition to steric hindrance. Structurally, betanin possesses a relatively rigid, bulky molecular framework with multiple hydroxyl and carboxyl groups, resulting in a large hydrated radius and high hydrogen-bonding capacity. These features increase its effective size in aqueous solution, enhancing size-based rejection even by membranes with nominal molecular weight cut-offs close to its molecular weight. Collectively, these physicochemical attributes make betanin an ideal probe molecule for elucidating coupled steric and electrostatic transport mechanisms in nanofiltration, and for systematically studying the interplay between membrane pore size, surface charge, and operating conditions in the separation of natural bioactive compounds. Betanin has applications in various industries, including the food industry as a colorant and the pharmaceutical industry as an active ingredient in medicines. It is used for coloring meat substitutes, gelatin, desserts, summer sausage, and dairy products. The recovery of phenolic bioactive compounds from their natural sources is tedious due to the high enzyme activity in most foods and plants. Therefore, the choice of extraction method must be made with the utmost caution to prevent chemical changes to the target molecules [10]. Also, standard extraction and separation methods for phenolic compounds from natural sources often use organic solvents such as methanol and hexane. These solvent-based processes are very costly, and the phenolic extracts may contain residual solvents, which makes them unfit or undesirable for food applications [1]. Therefore, a new cost-effective technology is required to concentrate the phenolic fractions for nutraceutical use.

Membrane filtration is a promising technology for the concentration of phenolic compounds due to its benefits, such as the absence of high temperatures, the lack of phase transitions, low energy consumption, the absence of organic solvents, and low waste disposal. Moreover, other biological molecules, such as sugars and proteins, can be easily separated from phenolic solutions, and concentration and purification steps can be combined into a single step, reducing operational costs and time. Membrane-based processes can operate continuously and are easy to scale up to the commercial level [11]. Membrane-based processes rely on the selective permeation of different feed species through semipermeable membranes. The driving force for mass transfer in membrane processes such as microfiltration (MF), ultrafiltration (UF), nanofiltration (NF), and reverse osmosis (RO) is hydrostatic pressure [12]. Membrane filtration is used in many applications, such as solvent exchange in the chemical industry [13], concentration and purification of xanthophylls [14], concentration of wines [15], and concentration and clarification of juices [16]-[20] in the food industry.

Giordana D. Arend *et al.* [18] have concentrated the bioactive compounds from strawberry juice using a polyvinylidene difluoride (PVDF) NF membrane with a molecular weight cut-off of 150-300 Da. They found that the NF of natura juice has retention values above 95% for total phenolic content (TPC). In another similar work, Carmela Conidi *et al.* [21] concentrated the phenolic compounds from orange press liquor using four different membranes: NF-70 (polyamide+polysulfone), NF-200 (poly-piperazine amide), N30F (polyethersulfone), and NFPES10 (polyethersulfone) having MWCO of 180 Da, 300 Da, 400 Da, and 1000 Da, respectively. The investigations revealed that all the NF membranes showed a high average rejection percentage towards anthocyanins (89.2-95.9%) and flavonoids (70–95.4%). Beatriz C.B.S Mello *et al.* [22] have concentrated the flavonoids and phenolic compounds in aqueous and ethanolic propolis extract using NF90 membrane (polyamide and polysulfone). It was obtained that the aqueous solution of propolis retained almost 99% of flavonoids and 84% of phenolic compounds. However, the retention values were reduced to 90% for flavonoids and 53% for phenolic compounds during the filtration of ethanolic solutions.

In previous studies [16]-[19], [21], [23], [24], the authors have focused solely on different phenolic compounds, and a detailed investigation of membrane transport phenomena using mathematical models was not reported. Besides this, no literature has been found on the concentration of betanin using the HFT-NF 150 membrane. This study investigated the performance of the HFT-NF 150 membrane for the recovery of betanin from model beetroot extract. The Spiegler-Kedem model was used to describe the transport phenomenon and to assess the process's viability for industrial applications. A rigorous study was also conducted to analyze the effects of various operating conditions and transport parameters through a sensitivity analysis.

5.2 Materials and Methods

5.2.1 Materials

The laboratory-grade betanin (molecular weight: 550.47 g/mol) was bought from TCI Chemicals, Adambakkam, India. Figure 5.1 represents the molecular structure of the betanin compound. The RO water was collected from the RO water purification machine available at Delhi Technological University, Delhi. An NF membrane (HFT-NF 150) was supplied by Permionics Pvt. Ltd., Gorwa, Vadodara, India. The membrane surface was composed of polyamide and had a molecular weight cut-off of 150 Da.

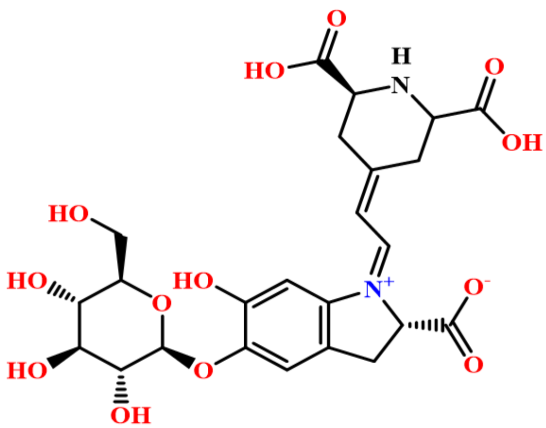

Figure 5.1 Betanin

5.2.2 Experimental Procedure and Conditions

All the experiments were performed on the self-assembled NF Setup, as discussed in Chapter 3. The experiments for the model betanin solutions were conducted at low pressures, as the highest feasible pressure for the NF experimental setup is 0.6 MPa. Flow rates in the moderate range were preferred for experimental studies due to the smaller area of the experimental setup. At higher flow rates, variations in velocity and concentration in the permeate and feed channels may be imperceptible or negligible. Hence, the test cell performance cannot be adequately examined. Experiments were performed for different operating conditions, as depicted in Table 5.1

Table 5.1 Experimental conditions for different model solutions of betanin

Operating conditions	**Values**
Pressure, MPa	0.2 – 0.6
Feed concentration, g/L	0.1 – 0.5
Feed flow rate, mL/min	200 – 600
Operating temperature, °C	25 ± 1
Operating time, min	5

5.3 Results and Discussion

All experiments and simulations were performed using model solutions of betanin with varying feed concentrations under different operating conditions. The system's behavior was examined by changing a single operating condition at a time and keeping others constant.

5.3.1 Unknown Parameter Estimation and Model Validation:

5.3.1.1 Estimation of Hydraulic Permeability (L_p):

The pure RO water flux tests were performed under various conditions using different feed flow rates (200 mL/min - 600 mL/min) at room temperature. The pressure was the variable under control in these trials. The experiments were performed by increasing the pressure from 0.2 to 0.6 MPa in increments of 0.1 MPa. Since there was no fouling, a linear increment in water flux with pressure was seen [25]. On the other hand, because there would be no concentration polarisation at the membrane surface, the feed flow rate had a very low impact on pure RO water flux at a single pressure [26]. Tap water, on the other hand, contains substances that can accumulate on the membrane surface, causing fouling; therefore, different flow behavior will be observed when tap water is used [2].

A numerical parameter estimation program determined the hydraulic permeability (L_p), which was matched to the value obtained from a graph of permeate flux versus the pressure difference across the membrane. The feed flow rate of 500 mL/min was kept constant for this particular investigation. Table 5.2 shows the pure water permeability data, and Figure 5.2 represents the pure water ($\rho \times J_w$) vs ΔP graph. The hydraulic permeability (L_p) of the membrane is calculated by the slope of the line and is given by the formula represented in equation (5.1)

$$L_p = \frac{J_w}{\Delta P} \times \rho \quad \ldots (5.1)$$

Table 5.2 Data for estimating the hydraulic permeability of the membrane before experiments on the betanin model solutions

Pressure (MPa)	J_w exp ($\times 10^{-5}$ m³/m²s)	J_w the ($\times 10^{-5}$ m³/m²s)	Error (%)
0.2	1.13	1.10	2.25
0.3	1.70	1.65	2.26
0.4	2.26	2.21	2.81
0.5	2.83	2.76	2.25
0.6	3.33	3.31	0.38
Predicted hydraulic permeability, $L_p = 5.52 \times 10^{-8}$ kg/m²sPa.			

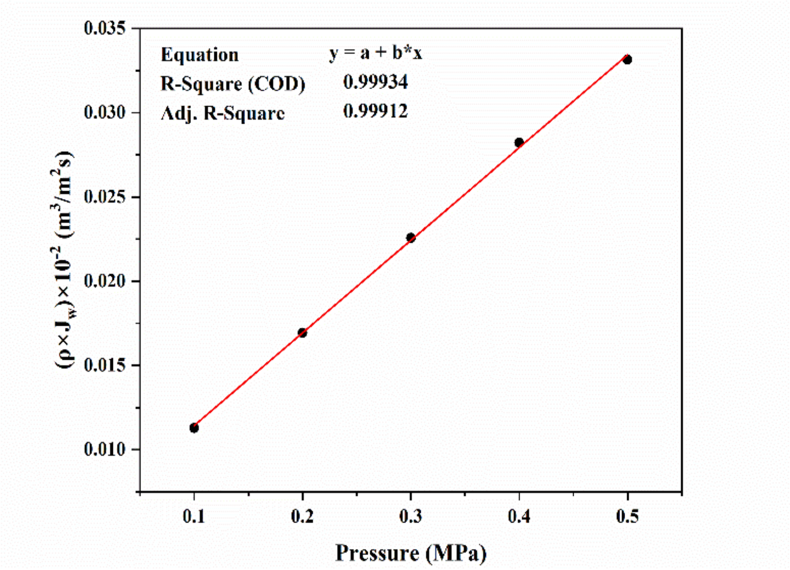

Figure 5.2 Pure water ($\rho \times J_w$) versus ΔP at a constant flow rate of 500 mL/min

The mean absolute percentage error (MAPE) can be calculated by equation (5.2)

$$\text{Mean absolute percentage error} = \frac{100}{n}\sum_{i=1}^{n}\left|1 - \frac{T_w}{E_w}\right| \quad \dots (5.2)$$

T_w represents the theoretical value, E_w represents the experimental value, and n represents the number of experimental sets performed. The mean absolute percentage error (MAPE) was 1.99 for pure water flux. The above set of equations now has only four unknown parameters: B_m, σ, a, and b.

5.3.1.2 Estimation of Solute Permeability (B_m), Reflection Coefficient (σ), and Mass Transfer Coefficient (a and b)

The values of solute permeability (B_m), reflection coefficient (σ), and mass transfer coefficients (a and b) were estimated using different experimental runs at various operating conditions. The pressure varied from 0.2 to 0.6 MPa, with increments of 0.1 MPa, and the feed concentration ranged from 0.1 to 0.5 g/L, with increments of 0.1 g/L. The temperature was maintained at 22 ± 1 °C for all experiments. The feed flow rates used for this investigation were 200, 300, 400, 500, and 600 mL/min.

In this experimental work, two optimization methods were used to analyze the effects of different model parameters on permeate flux and rejection. In the first optimization method (M1), the value of L_p was calculated from the slope of the pure water flux vs pressure graph. This value is then fixed for optimizing B_m, σ, a, and b. The complete data points used for optimization and their model validation data are shown in Appendix A2. In this case, the mean absolute percentage errors for permeate flux and rejection are 11.06% and 1.05%, respectively. All five parameters were optimized in the second optimization method (M2) to minimize the overall error between theoretical and experimental data points. The mean absolute error for permeate flux and rejection is 7.03% and 1.02%, respectively, for this case (Appendix A3). It was seen in Table 5.3 that the optimization of all five parameters (L_p, B_m, σ, a, and b) using theoretical and experimental data points showed the lowest value of MAPE for permeate flux and rejection than other methods of optimization. This may be because, in addition to the permeate flux for model solutions, the experimental pure water flux also showed some variation from the calculated fluxes; hence, the calculated L_p can be optimized to minimize the overall error, as L_p is the most influential parameter on permeate flux. Previous literature [27]-[30] showed that the membrane deforms at higher hydraulic pressures. Hence, applied pressure changes the value of hydraulic and solute permeability. The lower overall deviation at 0.6 MPa indicates that the membrane does not deform significantly.

Table 5.3 Comparison of the parameter estimation methods for the betanin model solutions

Method	Optimization technique	mAPE (%)		MAPE (%)	
		J_p	R	J_p	R
M1	B_m, σ, a, and b optimization using calculated L_p	29.49	2.68	11.06	1.05
M2	L_p, B_m, σ, a, and b optimization	26.40	2.68	7.03	1.02

5.3.2 Effects of Various Operating Conditions

Various operating conditions, such as feed concentration, pressure, and feed flow rate, can influence the performance of the membrane test cell. The roles of these operating conditions on the separation and concentration of betanin model solutions were investigated using the HFT-NF 150 membrane.

5.3.2.1 Effect of Pressure

The overall permeate flux at any time interval increases with increasing pressure for constant concentration and flow rate, as depicted in Figures 5.3(a) and 5.3(b). The results obtained showed that at a constant flow rate of 600 mL/min, the value of permeate flux increased from 1.37×10^{-5} m^3/m^2s to 3.14×10^{-5} m^3/m^2s for a concentration of 0.1 g/L and from 1.13×10^{-5} m^3/m^2s to 2.57×10^{-5} m^3/m^2s for a feed concentration of 0.5 g/L. This is generally due to an increase in the permeation force, as pressure is the primary driving force for mass transfer across the membrane. Similar patterns were observed for other concentration and feed flow rate values.

Moreover, the rejection percentage increases slightly from 96 to 99% as the pressure increases from 0.2 MPa to 0.6 MPa for a feed concentration of 0.1 g/L and from 94 to 96% for a 0.5 g/L feed concentration at a fixed flow rate of 600 mL/min, as depicted in Figure 5.3(c). This may be because increased pressure increases hydraulic flux.

However, solute flux does not vary much with pressure, as diffusive mass transport dominates over convective mass transport ($\sigma = 0.969$), leading to an overall decline in permeate concentration and a slight increase in rejection.

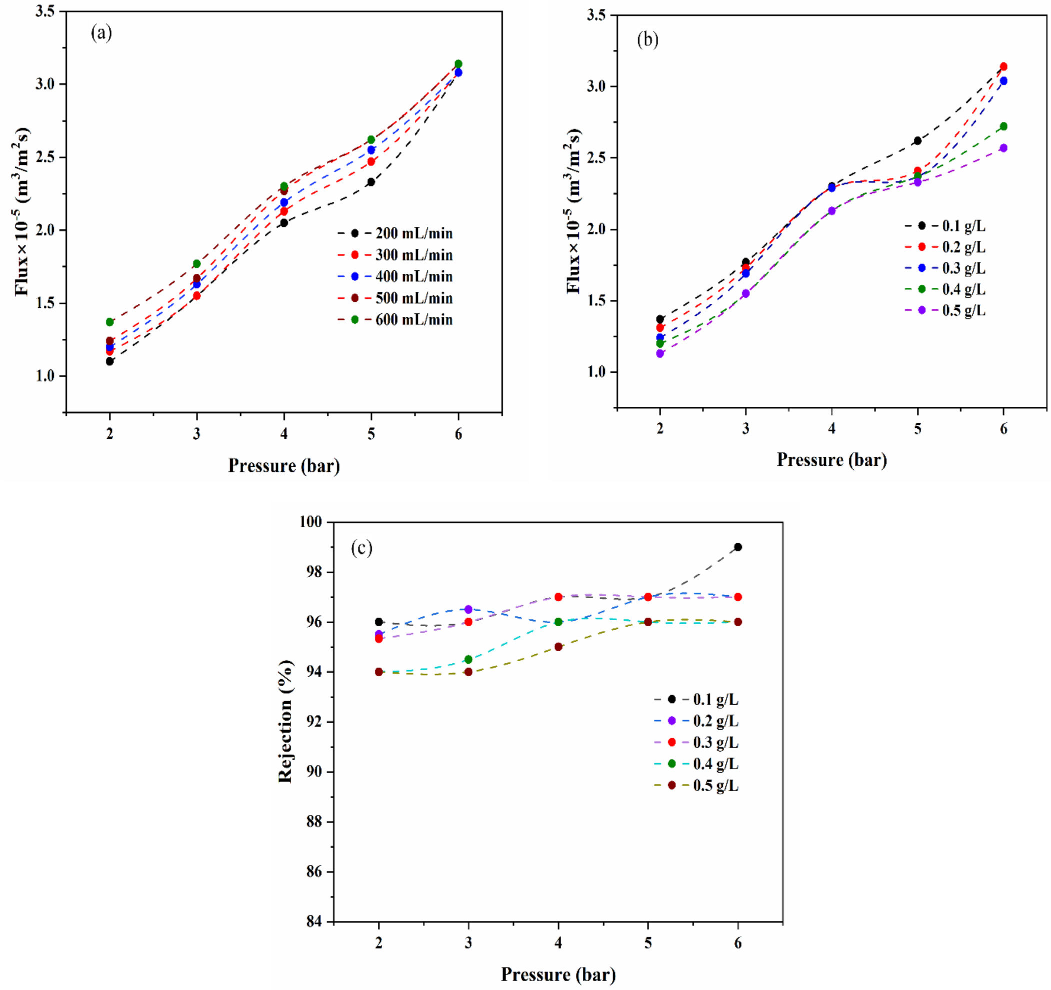

Figure 5.3 Influence of pressure on permeate flux (a) at a constant feed concentration of 0.1 g/L, (b) at a constant feed flow rate of 600 mL/min, (c) influence of pressure on percentage rejection at a constant feed flow rate of 600 mL/min, for betanin model solutions.

5.3.2.2 Effect of Feed Flow Rates

The experimental results showed that increasing feed flow rate increased permeate flux at constant concentration (Figure 5.4(a)) and at constant pressure (Figure 5.4(b). This is because a high feed flow rate removes solute particles from the membrane surface, thereby reducing concentration polarization. Figures 5.4(a) and 5.4(b) depict a variation of permeate flux as a function of feed flow rates ranging from 200 mL/min to 600 mL/min at different pressure variations of 0.2 MPa to 0.6 MPa and concentration variation from 0.1 g/L to 0.5 g/L. The graph shows that the permeate flux increases from 1.10×10^{-5} m^3/m^2s to 1.37×10^{-5} m^3/m^2s at a constant pressure of 0.2 MPa and a constant concentration of 0.1 g/L. The same trend was observed for other pressure and concentration values.

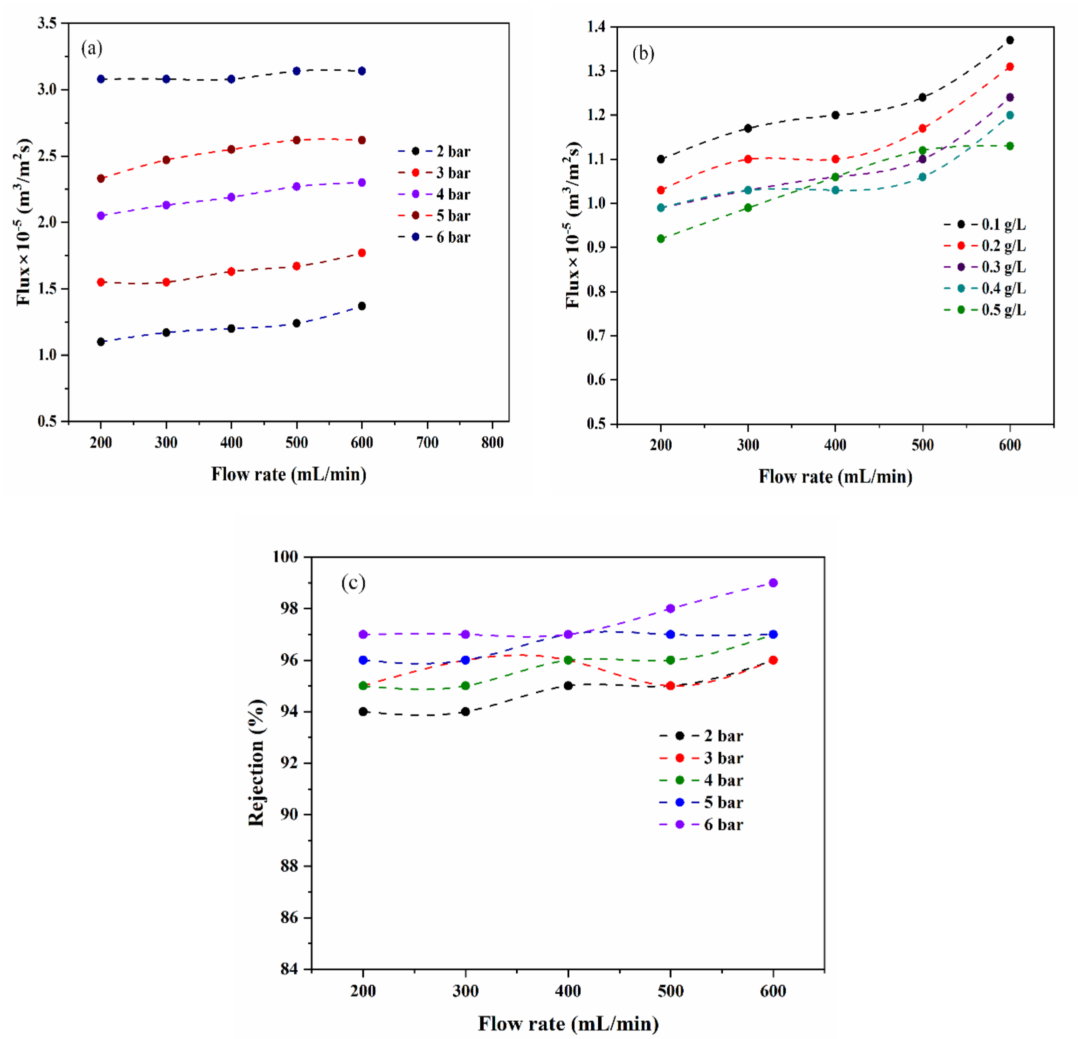

Figure 5.4 Influence of feed flow rate on permeate flux (a) at a constant feed concentration of 0.1 g/L, (b) at a constant pressure of 0.2 MPa, (c) influence of feed flow rate on percentage rejection at a constant feed concentration of 0.1 g/L, for betanin model solutions.

Also, the solute rejection percentage increases from 97 to 99% as the feed flow rate increases from 200 mL/min to 600 mL/min at a constant pressure of 0.6 MPa and a constant concentration of 0.1 g/L (Figure 5.4(c)). A similar trend was observed for other concentration and pressure values (Figure 5.4(c)). This may be because a reduction in concentration polarization at higher flow rates lowers solute concentration at the membrane surface, leading to lower solute flux and higher rejection.

5.3.2.3 Effects of Feed Concentration

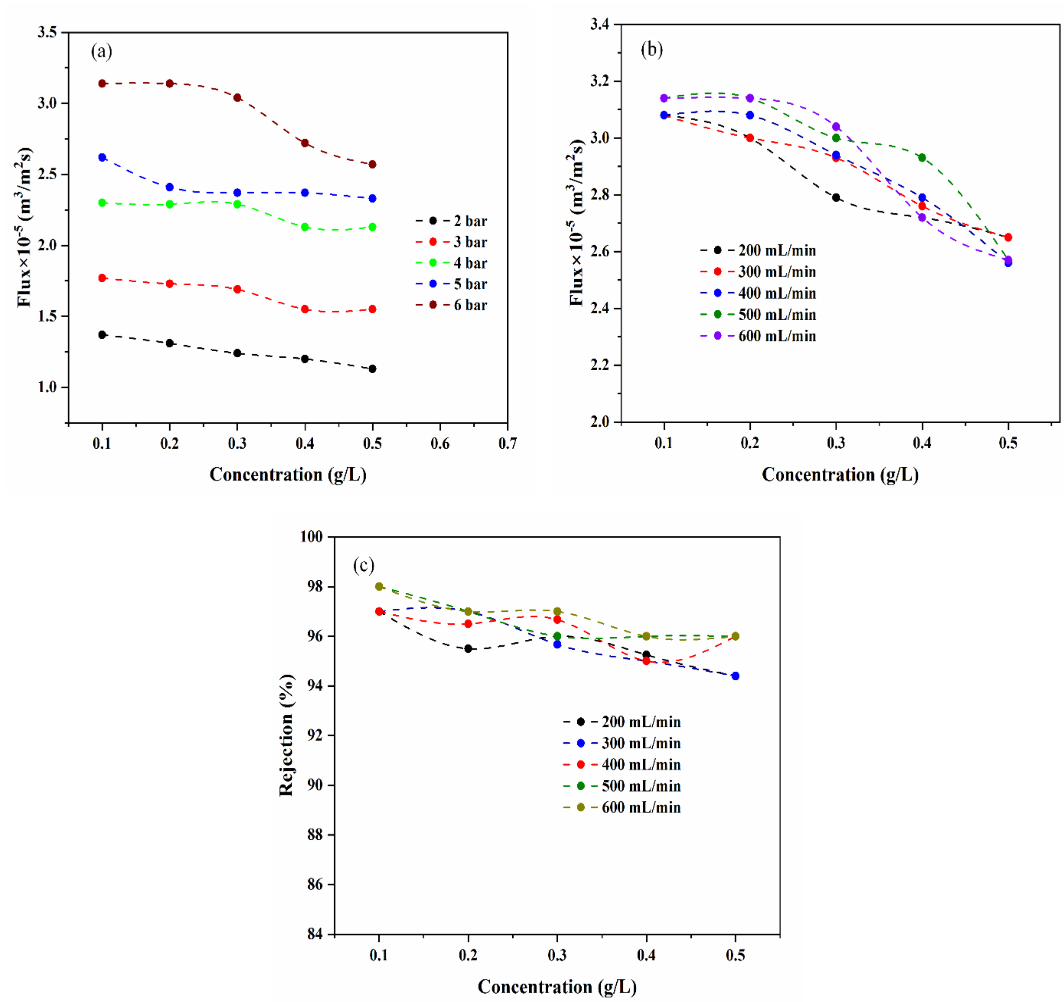

Figure 5.5 Influence of feed concentration on permeate flux (a) at a constant feed flow rate of 600 mL/min, (b) at a constant pressure of 0.6 MPa, (c) influence of feed concentration on percentage rejection at a constant pressure of 0.6 MPa, for betanin model solutions.

Feed concentration plays a vital role in membrane fouling. As mass transfer in membrane processes depends on the membrane's molecular weight cut-off, concentration by membrane processing is highly sensitive to the critical concentration for moderately high-molecular-weight compounds [31]. The permeate flux and permeate flow rate decrease with increasing betanin feed concentration, as higher concentrations increase osmotic pressure, thereby reducing the driving force for mass transfer. Figure 5.5(b) represents the decline in permeate flux value from 3.14×10^{-5} m^3/m^2s to 2.57×10^{-5} m^3/m^2s as the feed concentration increases from 0.1 g/L to 0.5 g/L at a feed flow rate of 600 mL/min and a constant pressure of 0.6 MPa. A similar trend was observed for other flow rates and pressures, as shown in Figure 5.5(a). Also, Figure 5.5(c) shows a decrease in the rejection percentage from 97 to 94.4% as the feed concentration increased from 0.1 g/L to 0.5 g/L at 0.6 MPa pressure and a feed flow rate of 200 mL/min. This is due to the lower water flux and higher solute flux at higher solute concentrations in the feed.

5.3.3 Regression Curve Analysis

The regression curve showed the variation between the experimental data points and the theoretical values calculated from the model equations. Figure 5.6(a) shows that all the permeate flux data points obtained experimentally lie within the band range of -30 to 30% of the theoretical values of permeate flux obtained through model equations. The rejection regression curve (Figure 5.6(b)) showed the lowest errors, with all the rejection data points obtained experimentally falling within ±5 % of the theoretical rejection values calculated from the model equations.

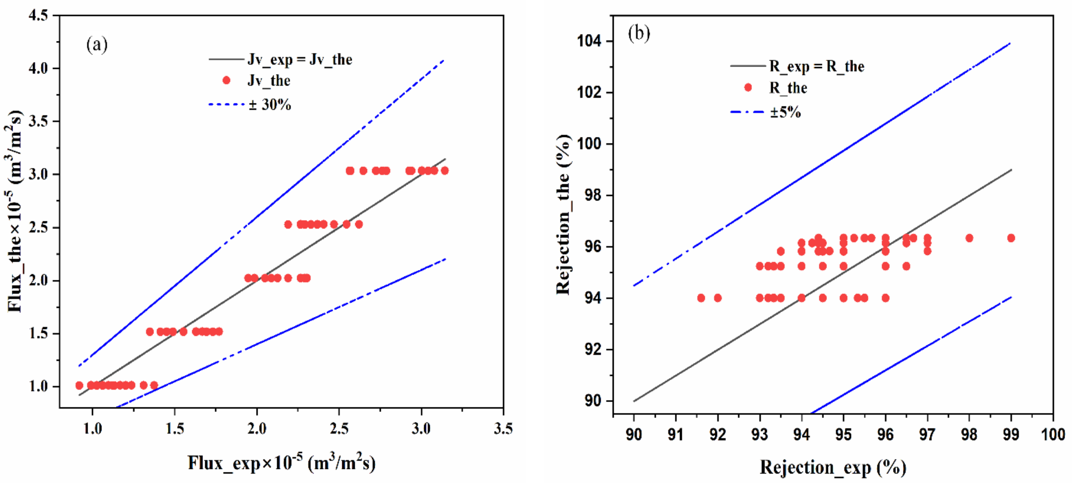

Figure 5.6 Regression curves of betanin model solutions for (a) permeate flux and (b) rejection percentage.

5.3.4 Selectivity Analysis

The sensitivities of different module parameters and operating conditions were analyzed using a suitable range for each input parameter and are reported in Table 5.4. As discussed in Chapter 2, variance-based sensitivity analysis requires the formulation of two independent matrices (*P* and *Q*) containing equal numbers of input parameter sets. All the model evaluations were performed in Google Colab. All the data were stored in a CSV file for further processing.

Table 5.4 Ranges of different parameters for sensitivity analysis of model betanin solutions

Parameters	**Range**
Pressure, MPa	0.2 – 0.6
Feed concentration, kg/m^3	0.1- 0.5
Feed flow rate, m^3/s	3.3×10^{-6} - 10×10^{-6}
Hydraulic permeability, kg/m^{2}sPa	5.5×10^{-9} - 5.5×10^{-7}
Solute permeability, m/s	4.03×10^{-6} – 4.03×10^{-8}
Reflection coefficient	0.8 - 1

Normalized sensitivities (first-order and total) for different operating conditions and membrane module parameters to permeate flux and rejection percentage, with variation in sample size, are shown in Figure 5.7 and Figure 5.8, respectively. As S_i and S_{Ti} are computed after every batch (containing 100 random samples) selected from the whole dataset, convergence occurs slowly after a certain number of samples. The results showed that the first-order sensitivity and total order sensitivity index fluctuated initially until 5000 samples, then varied marginally. This provides confidence in evaluating the sensitivity values at a sample size of 50000.

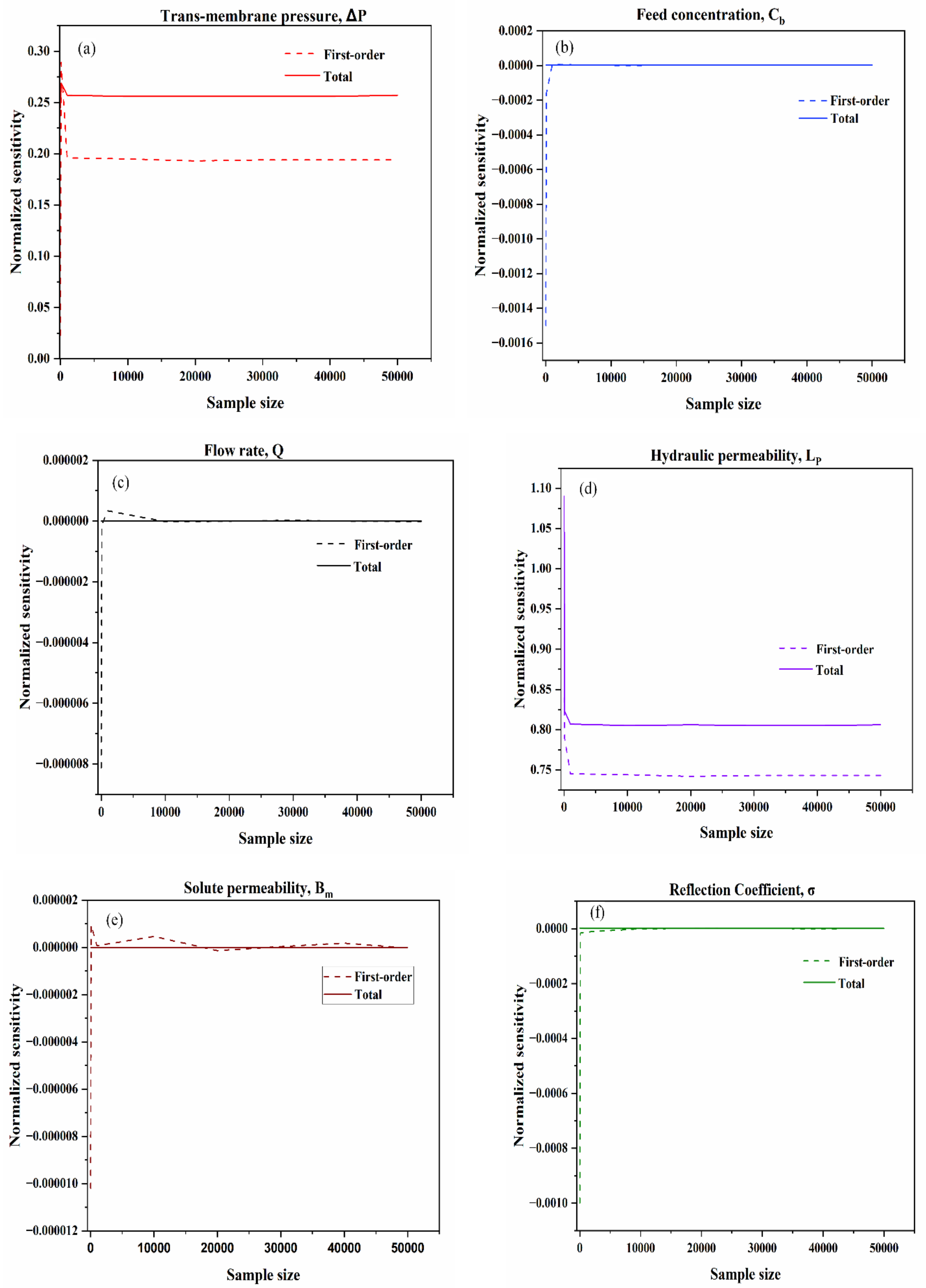

Figure 5.7 Values of first-order and total sensitivity on total permeate flux of model betanin solutions with increasing sample size for (a) pressure, (b) feed concentration, (c) feed flow rate, (d) hydraulic permeability, (e) solute permeability, and (f) reflection coefficient.

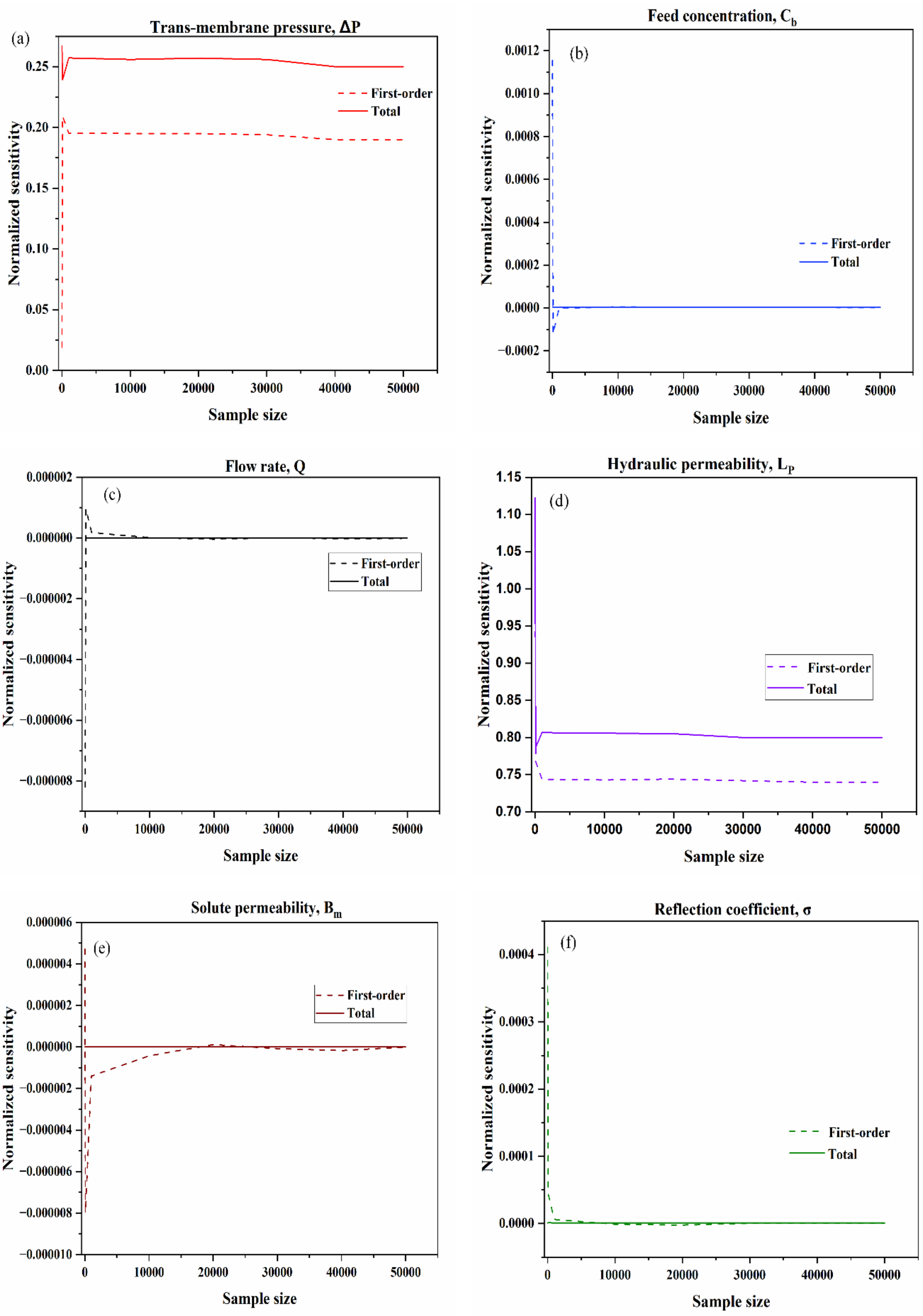

Figure 5.8 Values of the first-order and total sensitivity on rejection of betanin with increasing sample size for (a) pressure, (b) feed concentration, (c) feed flow rate, (d) hydraulic permeability, (e) solute permeability, and (f) reflection coefficient.

5.3.4.1 Sensitivities of Different Operating Variables and Membrane Parameters for Permeate Flux

Table 5.5 presents a comparison of first-order sensitivity (S), total sensitivity (S_T), and their difference (S_T-S) for permeate flux. It was observed that the normalized sensitivities of hydraulic permeability were the highest, followed by pressure, and the sensitivities of all other operating parameters, such as feed flow rate, feed concentration, solute permeability, and reflection coefficient, were comparatively negligible. Thus, it can be concluded that for total volumetric permeate flux, hydraulic permeability, and pressure are the most controlling parameters. Pressure is the main driving force for mass transfer across the membrane. Also, the value of (S_T-S) was low for L_p and ΔP. Therefore, the interactive effects of ΔP with other operating parameters are relatively insignificant on volumetric flux. Based on the sensitivity values (S_T and S), operating variables and membrane parameters can be sorted in decreasing order as $L_p > \Delta P > Cb > \sigma > B_m > Q$, as represented in Figure 5.9(a). The lower sensitivity of C_b and Q is due to lower concentration polarization and a smaller test cell area.

Table 5.5 Normalized sensitivities of different operating and membrane parameters for total permeate flux at a 50000 sample size

Parameter	S	S_T	S_T-S
Pressure, MPa	1.940×10^{-1}	2.560×10^{-1}	6.20×10^{-2}
Feed concentration, kg/m^3	2.620×10^{-6}	3.150×10^{-6}	5.30×10^{-7}
Feed flow rate, m^3/s	2.260×10^{-9}	1.740×10^{-8}	1.51×10^{-8}
Hydraulic permeability, kg/m^{2}sPa	7.430×10^{-1}	8.050×10^{-1}	6.20×10^{-2}
Solute permeability, m/s	3.530×10^{-8}	7.150×10^{-8}	3.62×10^{-8}
Reflection coefficient	4.960×10^{-7}	9.870×10^{-7}	4.91×10^{-7}

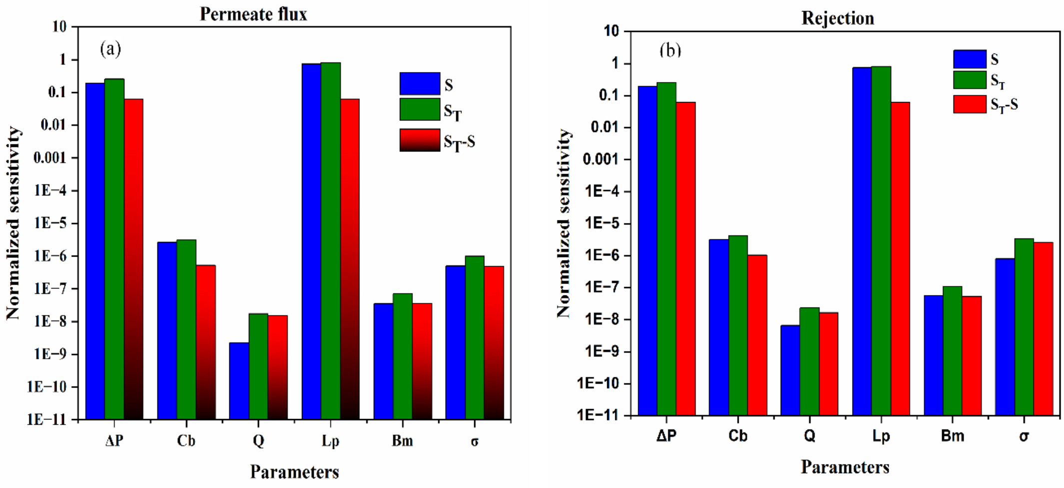

Figure 5.9 Sensitivity of different operating and membrane parameters for (a) permeate flux and (b) rejection, for betanin solutions.

5.3.4.2 Sensitivities of Different Operating Variables and Membrane Parameters for Rejection

First-order sensitivity (S), total sensitivity (S_T), and their difference (S_T-S) for operating variables and membrane parameters related to rejection are tabulated in Table 5.6

Table 5.6 Normalized sensitivities of different operating and membrane parameters for rejection at the sample size of 50000.

Parameter	S	S_T	S_T-S
Pressure, MPa	1.949×10^{-1}	2.566×10^{-1}	6.17×10^{-2}
Feed concentration, kg/m^3	3.207×10^{-6}	4.256×10^{-6}	1.05×10^{-6}
Feed flow rate, m^3/s	6.573×10^{-9}	2.320×10^{-8}	1.66×10^{-8}
Hydraulic permeability, kg/m^{2}sPa	7.430×10^{-1}	8.047×10^{-1}	6.17×10^{-2}
Solute permeability, m/s	5.732×10^{-8}	1.101×10^{-7}	5.29×10^{-8}
Reflection coefficient	7.992×10^{-7}	3.430×10^{-6}	2.63×10^{-6}

As with permeate flux, hydraulic permeability (L_p) is the most influential parameter. A similar trend in (S_T-S) was observed, as seen earlier for permeate flux (Figure 5.9(b)).

5.3.5 Performance of Scale-up Setup

Operating conditions primarily influence the efficiency of membrane test cells, while betanin removal's effectiveness depends on the test cells' active membrane area. However, an increase in membrane area can lead to substantial variations in pressure and temperature along the length of the flow channels, thereby reducing overall module efficiency. To mitigate these effects, employing multiple smaller test cells in series is recommended over expanding the membrane area in a single test cell.

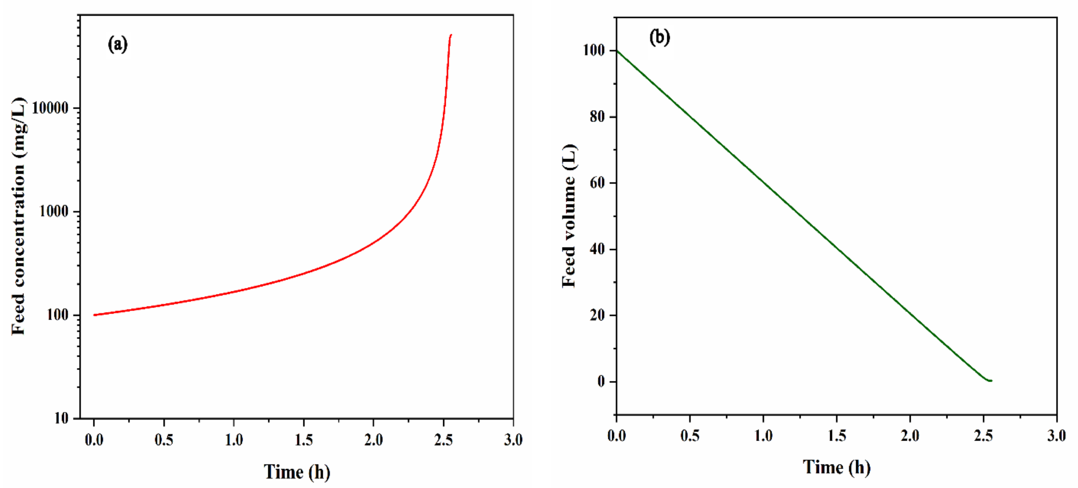

Figure 5.10 Variation analysis of (a) feed concentration and (b) feed volume concerning time for a 100 L model solution of betanin having a 100 mg/L feed concentration.

Simulations were conducted to process 100 liters of model betanin solution with an initial feed concentration of 100 mg/L, applying a pressure of 2×10^5 Pa and a feed flow rate of 36 L/h. Figure 5.10 illustrates the variation in feed concentration and volume over time. The results indicate that feed concentration increases exponentially up to a threshold, beyond which it stabilizes, while feed volume decreases over time until reaching a steady state. This phenomenon is likely attributed to the precipitation of betanin within the feed solution, which significantly impairs water permeation. The simulation maintained other operational parameters, including feed flow rate and operating temperature, at constant values.

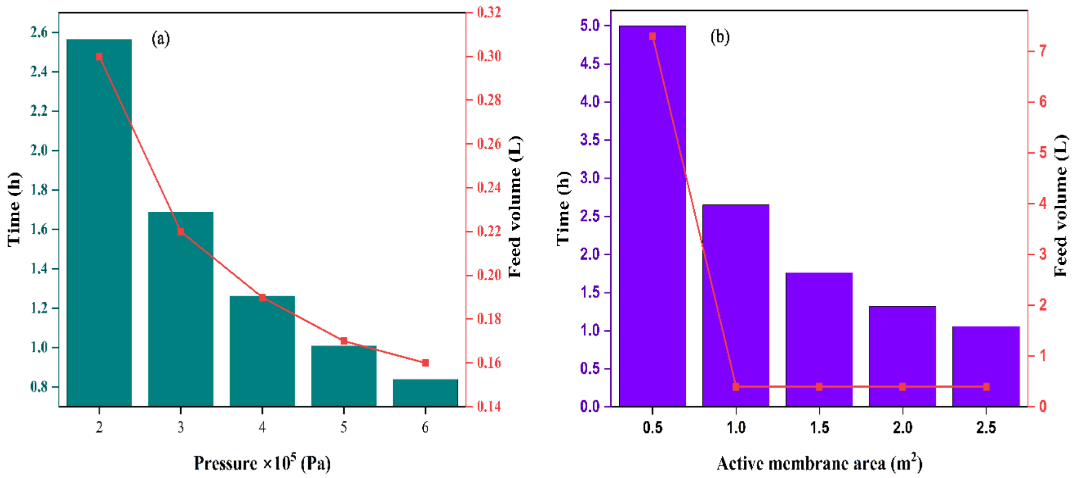

Figure 5.11 Time required to concentrate betanin from 100 mg/L to 50000 mg/L at (a) different operating pressures and (b) active membrane area.

Results were then analyzed to concentrate betanin from 100 mg/L to 50000 mg/L in the feed solution at different pressures and active membrane areas. Figure 5.11(a) shows the time variation in response to pressure at a fixed feed flow rate of 36 L/h and an active membrane area of 1.0 m^2. This relationship is crucial for scale-up because it demonstrates that increasing pressure can optimize process efficiency, but with diminishing returns above certain levels. This is because the permeation volume increases with pressure until a critical concentration is reached; at this point, solute precipitation starts at the membrane surface.

As shown in Figure 5.11(a), a significant decrease in filtration time from 2.57 h to 0.84 h was observed as the pressure increased from 2×10^5 Pa to 6×10^5 Pa. Simultaneously, the feed volume shows a much steeper initial decline from about 0.30 L to 0.16 L. This steeper decline suggests that betanin molecules may be more susceptible to pressure-induced conformational changes or aggregation. Figure 5.11(b) shows the simulation results for the filtration time required to concentrate betanin feed solution from 100 mg/L to 50000 mg/L. The time decreased from 5.00 h to 1.06 h, with an increase in active membrane area from 0.5 m^2 to 2.5 m^2 at a fixed pressure of 2×10^5 Pa and a feed flow rate of 36 L/h. However, betanin feed solutions exhibit a much more dramatic response to changes in membrane area. The feed volume drops sharply from about 7.26 L to nearly 0.43 L as the area increases from 0.5 m^2 to 1.0 m^2, then stabilizes. This dramatic change suggests that betanin is more sensitive to surface area effects.

5.4 Conclusions

In this work, the membrane test cell performance of HFT-NF 150 was investigated experimentally and theoretically for the separation of model betanin feed solutions of different concentrations. The theoretical predictions of the Spiegler-Kedem model for output characteristics are well matched to the experimental results. Low mean absolute percentage error (MAPE) values for output characteristics, such as permeate flux and rejection percentage, provide confidence in integrating the HFT-NF 150 membrane test cell into the design of a commercial-scale NF unit. Also, the effects of various operating parameters were analyzed in this work. The permeate flux increases with pressure and flow rate, but decreases with concentration. The maximum permeate flux of 3.14×10^{-5} m^3/m^2s and a percentage rejection of 99% was obtained at a high flow rate of 600 mL/min and high pressure of 0.6 MPa, but at a low feed concentration of 0.1 g/L.

Variance-based sensitivity analysis was also used to assess the influence and interdependence of operating and membrane module parameters on permeate flux and rejection. The indices began to converge after 5000 and remained almost stable at a sample size of 50000. The hydraulic permeability and pressure were the most influential parameters for permeate flux and rejection, respectively.

Simulations for the scale-up setup demonstrate that the HFT-NF 150 membrane analyzed in this study can concentrate betanin to the desired level. It was also found that pressure and active membrane area have a greater impact on the time required to concentrate rutin. In contrast, the feed flow rate had a negligible effect on the concentration time.

References

[1] H. Nawaz, J. Shi, G. S. Mittal, and Y. Kakuda, "Extraction of polyphenols from grape seeds and concentration by ultrafiltration," *Sep. Purif. Technol.*, vol. 48, no. 2, pp. 176–181, 2006, doi: 10.1016/j.seppur.2005.07.006.

[2] S. Wei, M. M. Hossain, and Z. S. Saleh, "Concentration of rutin model solutions from their mixtures with glucose using ultrafiltration," *Int. J. Mol. Sci.*, vol. 11, no. 2, pp. 672–690, 2010, doi: 10.3390/ijms11020672.

[3] M. Naczk and F. Shahidi, "Phenolics in cereals, fruits and vegetables: Occurrence, extraction and analysis," *J. Pharm. Biomed. Anal.*, vol. 41, no. 5, pp. 1523–1542, 2006, doi: 10.1016/j.jpba.2006.04.002.

[4] K. B. Pandey and S. I. Rizvi, "Plant polyphenols as dietary antioxidants in human health and disease," *Oxid. Med. Cell. Longev.*, vol. 2, no. 5, pp. 270–278, 2009, doi: 10.4161/oxim.2.5.9498.

[5] A. Durazzo *et al.*, "Polyphenols: A concise overview on the chemistry, occurrence, and human health," *Phyther. Res.*, vol. 33, no. 9, pp. 2221–2243, 2019, doi: 10.1002/ptr.6419.

[6] R. Mark, X. Lyu, J. J. L. Lee, R. Parra-Saldívar, and W. N. Chen, "Sustainable production of natural phenolics for functional food applications," *J. Funct. Foods*, vol. 57, no. 0, pp. 233–254, 2019, doi: 10.1016/j.jff.2019.04.008.

[7] M. L. Luna-Guevara, J. J. Luna-Guevara, P. Hernández-Carranza, H. Ruíz-Espinosa, and C. E. Ochoa-Velasco, "Phenolic compounds: A good choice against chronic degenerative diseases," *Stud. Nat. Prod. Chem.*, vol. 59, no. 0, pp. 79–108, 2018, doi: 10.1016/B978-0-444-64179-3.00003-7.

[8] B. R. Albuquerque, S. A. Heleno, M. B. P. P. Oliveira, L. Barros, and I. C. F. R. Ferreira, "Phenolic compounds: Current industrial applications, limitations and future challenges," *Food Funct.*, vol. 12, no. 1, pp. 14–29, 2021, doi: 10.1039/d0fo02324h.

[9] L. C. P. Gonalves *et al.*, "A comparative study of the purification of betanin," *Food Chem.*, vol. 131, no. 1, pp. 231–238, 2012, doi:

10.1016/j.foodchem.2011.08.067.

[10] K. Bradley, " Book Review ," *Companion Anim.*, vol. 23, no. 8, pp. 433–433, 2018, doi: 10.12968/coan.2018.23.8.433.

[11] V. M. Matta, R. H. Moretti, and L. M. C. Cabral, "Microfiltration and reverse osmosis for clarification and concentration of acerola juice," *J. Food Eng.*, vol. 61, no. 3, pp. 477–482, 2004, doi: 10.1016/S0260-8774(03)00154-7.

[12] A. S. Mujumdar, "A Review of: 'Food process design,'" *Dry. Technol.*, vol. 24, no. 1, pp. 117–117, 2006, doi: 10.1080/07373930500538915.

[13] J. Geens, K. Boussu, C. Vandecasteele, and B. Van der Bruggen, "Modelling of solute transport in non-aqueous nanofiltration*," J. Memb. Sci.*, vol. 281, no. 1–2, pp. 139–148, 2006, doi: 10.1016/j.memsci.2006.03.028.

[14] E. M. Tsui and M. Cheryan, "Membrane processing of xanthophylls in ethanol extracts of corn," *J. Food Eng.*, vol. 83, no. 4, pp. 590–595, 2007, doi: 10.1016/j.jfoodeng.2007.03.041.

[15] S. Banvolgyi, I. Kiss, E. Bekassy-Molnar, and G. Vatai, "Concentration of red wine by nanofiltration," *Desalination*, vol. 198, no. 1–3, pp. 8–15, 2006, doi: 10.1016/j.desal.2006.09.003.

[16] H. Mirsaeedghazi, Z. Emam-Djomeh, S. M. Mousavi, A. Aroujalian, and M. Navidbakhsh, "Clarification of pomegranate juice by microfiltration with PVDF membranes," *Desalination*, vol. 264, no. 3, pp. 243–248, 2010, doi: 10.1016/j.desal.2010.03.031.

[17] G. T. Vladisavljević, P. Vukosavljević, and B. Bukvić, "Permeate flux and fouling resistance in ultrafiltration of depectinized apple juice using ceramic membranes," *J. Food Eng.*, vol. 60, no. 3, pp. 241–247, 2003, doi: 10.1016/S0260-8774(03)00044-X.

[18] G. D. Arend *et al.*, "Concentration of phenolic compounds from strawberry (*Fragaria X ananassa Duch*) juice by nanofiltration membrane," *J. Food Eng.*, vol. 201, pp. 36–41, 2017, doi: 10.1016/j.jfoodeng.2017.01.014.

[19] P. Ghosh, R. C. Pradhan, S. Mishra, and P. K. Rout, "Quantification and

concentration of anthocyanidin from Indian blackberry (*Jamun*) by combination of ultra- and nano-filtrations," *Food Bioprocess Technol.*, vol. 11, no. 12, pp. 2194–2203, 2018, doi: 10.1007/s11947-018-2176-4.

[20] B. Girard and L. R. Fukumoto, "Membrane processing of fruit juices and beverages: A review," *Crit. Rev. Food Sci. Nutr.*, vol. 40, no. 2, pp. 91- 157, 2010, doi:10.1080/10408690091189293

[21] C. Conidi, A. Cassano, and E. Drioli, "Recovery of phenolic compounds from orange press liquor by nanofiltration," *Food Bioprod. Process.*, vol. 90, no. 4, pp. 867–874, 2012, doi: 10.1016/j.fbp.2012.07.005.

[22] B. C. B. S. Mello, J. Carlos, C. Petrus, and M. Dupas, "Concentration of flavonoids and phenolic compounds in aqueous and ethanolic propolis extracts through nanofiltration," *J. Food Eng.*, vol. 96, no. 4, pp. 533–539, 2010, doi: 10.1016/j.jfoodeng.2009.08.040.

[23] A. Cassano, C. Conidi, R. Ruby-Figueroa, and R. Castro-Muñoz, "Nanofiltration and tight ultrafiltration membranes for the recovery of polyphenols from agro-food by-products," *Int. J. Mol. Sci.*, vol. 19, no. 2, pp. 351, 2018, doi: 10.3390/ijms19020351.

[24] C. Conidi and A. Cassano, "Recovery of phenolic compounds from bergamot juice by nanofiltration membranes," *Desalin. Water Treat.*, vol. 56, no. 13, pp. 3510–3518, 2015, doi: 10.1080/19443994.2014.968219.

[25] N. S. Krishna Kumar, M. K. Yea, and M. Cheryan, "Soy protein concentrates by ultrafiltration," *J. Food Sci.*, vol. 68, no. 7, pp. 2278–2283, 2003, doi: 10.1111/j.1365-2621.2003.tb05759.x.

[26] J. L. Acero, F. J. Benítez, A. I. Leal, and F. J. Real, "Removal of phenolic compounds in water by ultrafiltration membrane treatments," *J. Environ. Sci. Heal. - Part A Toxic/Hazardous Subst. Environ. Eng.*, vol. 40, no. 8, pp. 1585–1603, 2005, doi: 10.1081/ESE-200060651.

[27] E. Sivertsen, T. Holt, W. Thelin, and G. Brekke, "Modelling mass transport in hollow fibre membranes used for pressure retarded osmosis," *J. Memb. Sci.*,

vol. 417–418, no. 0, pp. 69–79, 2012, doi: 10.1016/j.memsci.2012.06.014.

[28] D. Attarde, M. Jain, K. Chaudhary, and S. K. Gupta, "Osmotically driven membrane processes by using a spiral wound module - Modeling, experimentation and numerical parameter estimation," *Desalination*, vol. 361, no. 0, pp. 81–94, 2015, doi: 10.1016/j.desal.2015.01.025.

[29] A. Chatterjee, A. Ahluwalia, S. Senthilmurugan, and S. K. Gupta, "Modeling of a radial flow hollow fiber module and estimation of model parameters using numerical techniques," *J. Memb. Sci.*, vol. 236, no. 1–2, pp. 1–16, 2004, doi: 10.1016/j.memsci.2004.01.006.

[30] D. Attarde, M. Jain, and S. K. Gupta, "Modeling of a forward osmosis and a pressure-retarded osmosis spiral wound module using the Spiegler-Kedem model and experimental validation," *Sep. Purif. Technol.*, vol. 164, no. 0, pp. 182–197, 2016, doi: 10.1016/j.seppur.2016.03.039.

[31] S. K. Karode, B. B. Gupta, and T. Courtois, "Ultrafiltration of raw Indian sugar solution using polymeric and mineral membranes," *Sep. Sci. Technol.*, vol. 35, no. 15, pp. 2473–2483, 2000, doi: 10.1081/SS-100102350.

Chapter – 6
Concentration of Betanin From Beetroot Juice

CHAPTER – 6

CONCENTRATION OF BETANIN FROM BEETROOT JUICE

6.1 Introduction

Natural foods and bioactives have been part of the human diet for ages [1]. However, in the last few decades, the demand for natural food colors and bioactives has grown significantly as people have shown interest in healthier options over artificial additives [2]. Research indicates that plant-derived ingredients make food more appealing and offer health benefits, such as helping fight aging, infections, inflammation, and abnormal cell growth [3]-[5]. Phenolics are a highly prevalent secondary metabolite in plants, contributing to their health and sensory qualities. These compounds, identified by their unique aromatic rings with hydroxyl groups, boast over 8000 known varieties in many vegetables and fruits [6]-[8]. Phenolic compounds come in diverse forms, including flavonoids, tannins (both simple and condensed), phenolic acids, stilbenes, lignans, coumarins, and lignins. Each of these has a function in plants, providing defense and contributing to the plant's flavor, color, and even its oxidative stability.

Regarding human health, these compounds are nothing short of remarkable. These compounds offer numerous health benefits in humans due to their antioxidant properties. They play a critical role in preventing the oxidation of high-density lipids, neutralizing free radicals, and reducing the adverse effects of mutagens and carcinogens. They act as the body's cleanup crew, neutralizing free radicals that cause cell damage and exhibiting anti-aging, anti-infective, anti-inflammatory, and anti-proliferative properties [9]-[12]. As a result, these compounds are gaining attention for their potential use in the pharmaceuticals, food, cosmetics, packaging, and textile industries.

Betanin is a water-soluble vacuolar chromo-alkaloid found in *Beta vulgaris L.* (commonly known as beetroot or chukandar) [13]. In the food industry, it's used to color a wide range of products, including meat substitutes, gelatins, dairy products, juices, and desserts [14]. However, recovering these valuable phenolic compounds is challenging due to enzymatic activity in most foods and crops. The standard conventional methods for isolation and concentration are liquid-liquid extraction, evaporation, or crystallization. These often require organic solvents such as methanol and hexane, which can be prohibitively expensive and leave unwanted residues, mainly when used in food products [15], [16]. New, cutting-edge, cost-effective technologies are required to address this, and one of them is membrane filtration. Scientists have already proven the potential of membrane filtration in many applications [17], [18].

Due to its efficiency and eco-friendliness, membrane filtration has solved the challenge of extracting phenolic compounds. Precise separation of molecules can be achieved using techniques such as microfiltration (MF), ultrafiltration (UF), nanofiltration (NF), and reverse osmosis (RO). This technology has many advantages over traditional methods: it operates at low temperatures, undergoes no phase transition, consumes low energy, and uses no organic solvents. It can easily overcome the hurdles posed by other biological molecules, such as sugars and proteins, and achieve concentration and purification in a single step. On top of all that, membrane-based methods are on a continuous and commercial scale. Researchers have used different membrane technologies to concentrate phenolic compounds from strawberry juice, orange press liquor, and propolis extracts [19]-[23].

Tamba A. *et al.* [24] employed an integrated coupling process to separate betacyanins in cactus pear juice using four different MF membranes. The investigations showed retention values of 0.81-1 for betacyanins. Arend G.D. *et al.* [19] used a polyvinylidene difluoride NF membrane with a molecular weight cut-off (MWCO) of 150-300 Da to concentrate the bioactive compounds in strawberry juice. They discovered that the natura juice's NF had total phenolic content (TPC) retention values greater than 95%. Conidi C. *et al.* [20] used four distinct membranes: NF-70 (polyamide+polysulfone), NF-200 (poly-piperazine amide), N30F (polyethersulfone), and NFPES10 (polyethersulfone) - with MWCOs of 180, 300, 400, and 1000 Da, respectively, to concentrate the phenolic compounds from orange press liquor in a related study. According to the investigations, these NF membranes exhibited a high average rejection percentage towards flavonoids (70-95.4%) and anthocyanins (89.2-95.9%).

Studies have shown that different membranes for concentrating phenolic compounds exhibit high retention values and industrial potential.

This investigation aimed to check the separation efficiency of a hybrid system comprised of UF and NF for the concentration of betanin in beetroot juice. It assessed the effects of different operating conditions concerning permeate flux and rejection. Later, the fouling mechanism was evaluated using the experimental data obtained.

6.2 Materials and Methods

6.2.1 Materials

The red beetroot was purchased from Ajadpur mandi, Delhi, India. Reverse osmosis (RO) water was collected from the RO purification machine at Delhi Technological University, Delhi. Flat sheet NF membranes (HFT-NF 150) were supplied by Permionics Pvt. Ltd, Gorwa Vadodara, India.

6.2.2 Experimental Setup

The hybrid system was designed to integrate ultrafiltration (UF) and nanofiltration (NF) processes for the efficient separation and concentration of bioactive compounds (Figure 6.1). The system incorporated two stainless-steel membrane housings for UF and NF membranes. The system also consisted of two feed tanks (UF feed tank and NF feed tank) and four electric motors (¼ horsepower centrifugal pumps, followed by booster pumps (Konvio Neer 100 GPD RO diaphragm booster pump, input power suitable for 24V DC). Needle valves, rotameters (100–1200 mL/min), and glycerine-filled pressure gauges (0–16 bar) were also installed to monitor and control the feed flow rate and maintain hydraulic pressure. Separate tanks were used to collect the retentate and permeate streams, with the retentate recirculated into the feed tank during single-component experiments involving betanin.

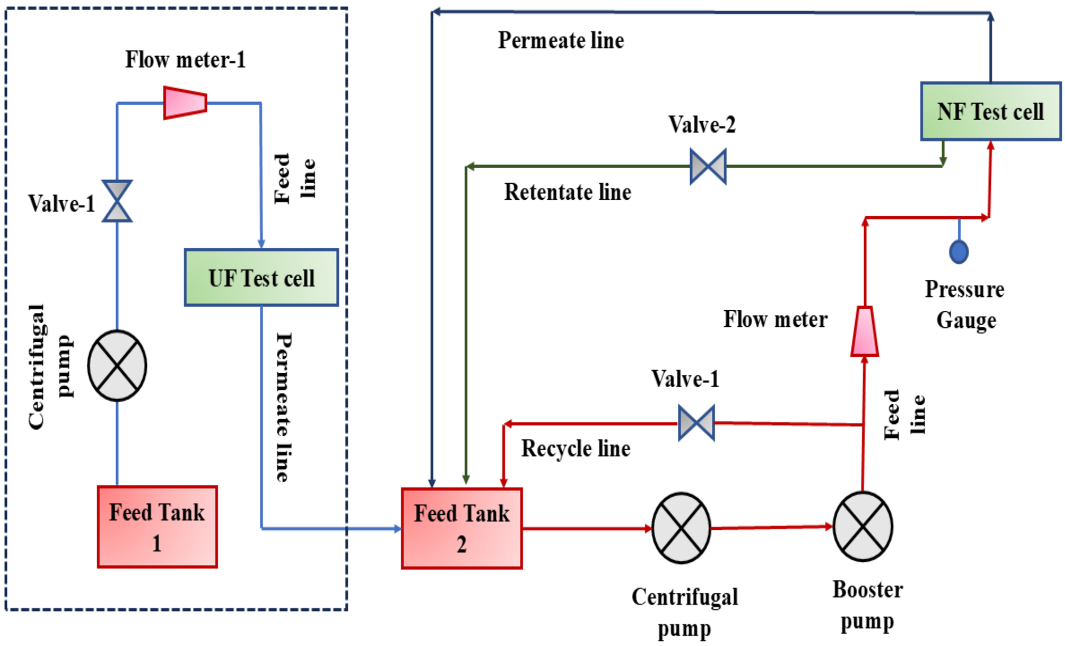

Figure 6.1 Block diagram of self-assembled hybrid system (UF+NF)

6.2.3 Experimental Procedure

6.2.3.1 Juice Extraction

The red beetroot obtained from the Ajadpur mandi was thoroughly washed with RO water to remove natural microflora, dirt, and other impurities. After washing, the beetroot was peeled cautiously and segmented into uniform small pieces. A domestic fruit juicer (Bajaj Neo JX4 450-Watt Juicer Mixer Grinder With 2 Jars, Delhi, India) was employed to extract juice from the fragmented beetroots. The extracted juice was immediately filtered through a standard filter and temporarily stored at 4°C before clarification. The freshly extracted beetroot juice used as the feed solution was characterised to establish its physicochemical properties prior to membrane filtration. The juice exhibited a pH of 6.5, providing a mildly acidic nature. The dynamic viscosity was measured at approximately 1.5-2.2 mPa.s at 25 °C, which is higher than that of distilled water due to dissolved sugars, pigments, and colloidal solids. The betanin concentration in the raw juice was determined spectrophotometrically and ranged from 300 to 800 mg/L, depending on the beetroot variety and extraction conditions.

6.2.3.2 Membrane Filtration

Other polysaccharides and proteins present in raw beetroot juice strongly influence betanin NF behavior by modifying both the physicochemical properties of the feed and the fouling dynamics at the membrane surface. The elevated viscosity and high molecular weight polysaccharides enhance concentration polarization and form a compressible gel or cake layer on the membrane, increasing hydraulic resistance and reducing permeate flux, while sometimes increasing the apparent rejection of betanin due to secondary filtration effects. Proteins further exacerbate fouling through adsorption and pore blocking via electrostatic and hydrophobic interactions, and they can alter the effective membrane surface charge, thereby changing solute-membrane interactions that govern betanin transmission. Together, these matrix components lead to greater flux decline, higher operating pressures, and less stable long-term performance, underscoring the importance of upstream clarification or pretreatment (e.g., ultrafiltration or centrifugation) to improve the efficiency and reproducibility of betanin nanofiltration.

Before experiments, the UF and NF membranes were rinsed with distilled water for 24 hours to remove residual preservatives from the surfaces used to manufacture and preserve the membranes. High-pressure water circulation was used for 1-2 hours to ensure membrane compaction and stabilization in the test cells. The feed solution was circulated through the setup for 15–20 minutes to precondition the system.

The system begins with the UF stage, introducing 10 liters of diluted juice into the system using two electric pumps at a constant temperature of 25 ± 2 °C. The valve installed on the feed line was used to regulate the feed flow rate, as observed by the provided flow meter. During UF, the feed stream was converted into two streams: the permeate stream, which passes through the membrane, and the retentate stream, which does not pass through the membrane. The permeate stream was collected in a tank for further processing, while the retentate stream was recycled into the feed tank. The permeate stream of the UF setup was then transferred to the feed tank of the NF setup.

The NF experiments were carried out by pumping clarified juice into the NF test cell using a centrifugal pump and a booster pump. The NF test cell has an HFT-NF membrane composed of polyamide with an active membrane area of 0.00785 m^2. The clarified juice was pumped into the test cell using electric pumps. Similar to the UF stage, the retentate stream was reprocessed into the feed tank to maintain the feed solution concentration, and the permeate stream was collected in a separate tank for analysis. The tests were performed at varying times (5 - 25 min), pressures (2 - 6 bar), and feed flow rates (200 - 600 mL/min), aiming to evaluate the influence of these operating conditions on permeate flux and rejection. The different valves and controllers at the feed and bypass lines maintained and controlled the feed flow rates and pressures. The average temperature maintained for NF experiments was room temperature. A digital thermometer was also employed to check the temperature of the feed solution after each run. The collected permeate stream was used to calculate permeate fluxes by measuring the volume collected after a constant period (equation (6.1)). The concentration of betanin in the feed and permeate was determined using a UV-1800 spectrophotometer (SHIMADZU). Experiments were conducted over varying times, pressures, and feed flow rates to ensure consistent, reproducible results.

$$J_p = \frac{V_p}{A_m \times t} \quad \dots (6.1)$$

J_p is the permeate flux, V_p is the permeate volume, A_m is the active membrane area, and t is the time.

6.2.3.3 Membrane Fouling

Fouling accumulates unwanted materials on the membrane surface or within its pores over time during a separation process. It is one of the significant problems in membrane technology that leads to degradation of membrane performance, increased energy consumption, and reduced membrane lifetime [25]-[27]. Fouling also affects the efficiency and selectivity of various membrane processes by reducing permeability; thus, it is a critical factor in membrane selection for membrane filtration.

For this investigation, the membranes underwent a two-step cleaning process after filtration, combining a 30-minute rinse with pure RO water at a higher feed flow rate of 600 mL/min, followed by a 60-minute exposure to 0.125 M NaOH solution. Pure water permeability tests were performed before and after the experiments to evaluate the membrane's fouling index (FI) using equation (6.2) [23].

$$FI = \left(1 - \frac{W_a}{W_b}\right) \times 100 \quad \ldots (6.2)$$

Here, W_a and W_b are pure water permeability before and after filtration.

6.2.3.4 Fouling Mechanism

The deposition of foulants on the membrane surface can be described using four mechanistic models: complete blocking, intermediate blocking, standard blocking, and cake filtration. The complete blocking model conjecture posits that particles block the entry points to membrane pores entirely because their sizes exceed the pores' diameters. This results in an immediate reduction in the membrane filtration area, preventing the flow into the system. Equation (6.3) represents the normalized flux as a function of time for the complete blocking model. The intermediate blocking model assumes that some particles block pores and others accumulate on top of other deposited particles (equation (6.4)). Cake filtration occurs when particles accumulate on membrane surfaces, forming a thick, permeable cake that adds resistance to flow by acting as a secondary filtration layer (equation (6.5)). Standard blocking assumes that particles accumulate on the pore walls, gradually decreasing the pore size and, hence, reducing the permeate flux (equation (6.6)). These models help predict filtration behavior, optimize membrane-cleaning strategies, and enhance system design to improve efficiency and longevity.

$$\frac{J}{J_o} = \exp(-k't) \quad \ldots. (6.3)$$

$$\frac{J}{J_o} = \frac{1}{1+k't} \quad \ldots. (6.4)$$

$$\frac{J}{J_o} = \frac{1}{(1+k't)^{0.5}} \quad \ldots. (6.5)$$

$$\frac{J}{J_o} = \frac{1}{(1+k't)^{2}} \quad \ldots. (6.6)$$

J is the permeate flux at time t, and J_o is the initial flux. The fouling rate constant is represented by k'.

6.3. Results and Discussion

The beetroot juice experiments were performed at various times under various operational conditions. At room temperature, the feed flow rates were increased from

200 mL/min to 600 mL/min, and the pressure was raised from 2 bar to 6 bar. A smaller range of feed flow rates was chosen for experimental studies due to the small size of the membrane test cell. A total of 125 data points were recorded by varying these operating parameters.

6.3.1 Estimation of Membrane's Hydraulic Permeability

The pure water flux tests were performed under various conditions using different feed flow rates (200 mL/min - 600 mL/min) at room temperature. The pressure was the variable under control in these trials. The experiment was performed by changing the pressure from 1 to 6 bar with increments of 1 bar. Since there was no fouling, a linear increment in water flux with pressure was seen. On the other hand, because there was no concentration polarisation at the membrane surface, the feed flow rate had a negligible impact on pure RO water flux at a single pressure.

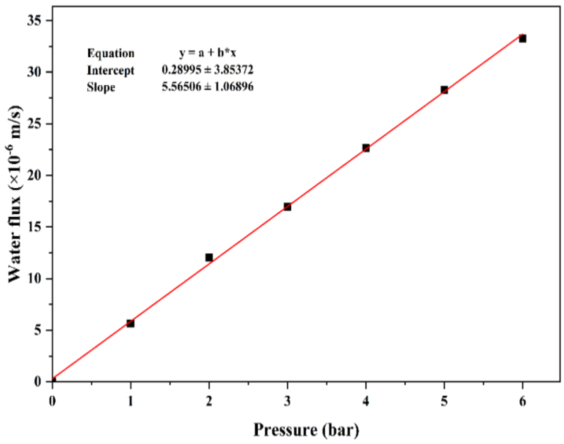

Figure 6.2 Water flux vs. pressure

A numerical parameter estimation program determined the hydraulic permeability (L_P), which was matched to the value obtained from a graph of permeate flux versus the pressure difference across the membrane. The feed flow rate of 500 mL/min was kept constant for this investigation. Table 6.1 shows the pure water permeability data, and Figure 6.2 represents the pure water flux vs pressure graph.

The membrane's hydraulic permeability (L_P) was calculated from the slope of the line and was obtained as 5.57×10^{-6} $ms^{-1}bar^{-1}$.

Table 6.1 Data for estimating the hydraulic permeability of the membrane before experiments on beetroot juice

Pressure (bar)	J_w exp ($\times 10^{-6}$ m^3/m^2s)	J_w the ($\times 10^{-6}$ m^3/m^2s)	Error (%)
1.0	5.66	5.57	1.59
2.0	12.03	11.14	7.40
3.0	16.99	16.71	1.65
4.0	22.65	22.28	1.63
5.0	28.31	27.85	1.62
6.0	33.26	33.42	-0.48

The formula represented in equation (6.7) was used to calculate the theoretical water fluxes, and equation (6.8) was used to calculate the mean absolute percentage error (MAPE) [28], [29].

$$L_p = \frac{J_w}{\Delta P} \quad \dots (6.7)$$

$$\mathrm{MAPE} = \frac{100}{n}\sum_{i=1}^{n}\left|1 - \frac{T_w}{E_w}\right| \quad \dots (6.8)$$

T_w and E_w represent the theoretical and experimental water flux, respectively, and n represents the number of experiments performed. The MAPE was 2.26 for water flux.

6.3.2 Operating Parameters Effect Analysis

6.3.2.1 Effect of Operating Time

As the feed solution is beetroot juice containing high-molecular-weight compounds, operating time is a key factor in concentration polarization and fouling. The permeate flux decreases with increasing operating time. This may be due to either concentration polarization or the accumulation of particles near the membrane surface or in the pores, which reduces the water transport across the membrane. As shown in Figure 6.3(a), the permeate flux decreases from 6.94×10^{-6} m/s to 3.33×10^{-6} m/s as the operating time increases from 5 minutes to 25 minutes at a fixed feed flow rate of 600 mL/min and a pressure of 6 bar. Also, a very slight decrease in rejection percentage was observed with increasing operating time. Figure 6.3(b) shows that at a fixed flow rate of 600 mL/min and a pressure of 6 bar, the percentage rejection decreased from 94% to 93% with an increase in operating time from 5 minutes to 25 minutes. This may be because a decline in the diffusive flux of water results in less dilution of the permeate and slightly increases its concentration.

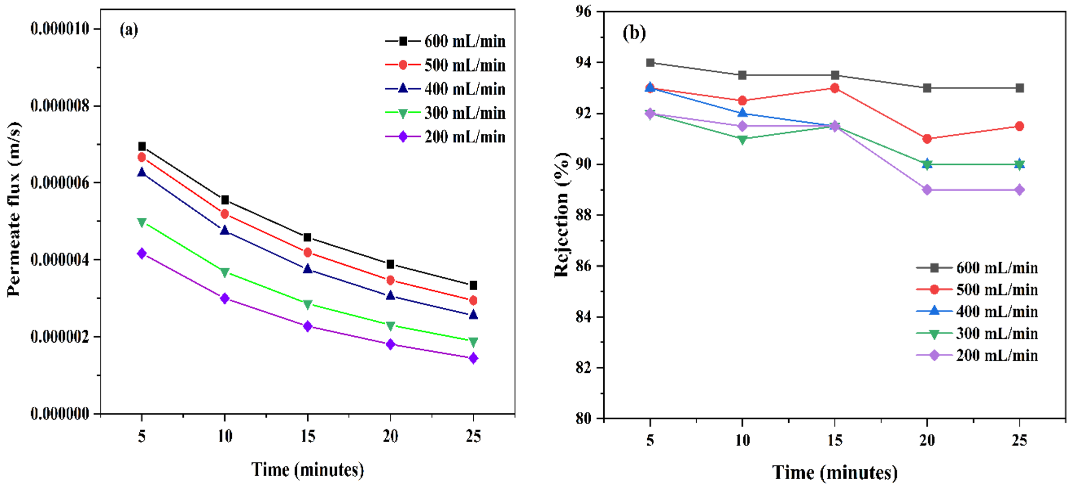

Figure 6.3 Influence of time on (a) permeate flux and (b) percentage rejection, for beetroot juice

6.3.2.2 Effects of Pressure

The permeate flux increases with increasing pressure at a fixed feed flow rate. An increase in permeate flux for 5 minutes was observed from 2.31×10^{-6} m/s to 6.94×10^{-6} m/s as the pressure was increased from 2 bar to 6 bar at a feed flow rate of 600 mL/min (Figure 6.4(a)). This is because pressure is the driving force for water transport across the membrane. A similar trend was observed for other feed flow rates. The rejection percentage increased slightly from 92% to 95% as pressure increased from 2 bar to 6 bar, at a fixed feed flow rate of 600 mL/min and a duration of 5 minutes (Figure 6.4(b)). This is because increased pressure increases the diffusive water flux rather than the convective solute flux, leading to greater dilution of the permeate and higher rejection values.

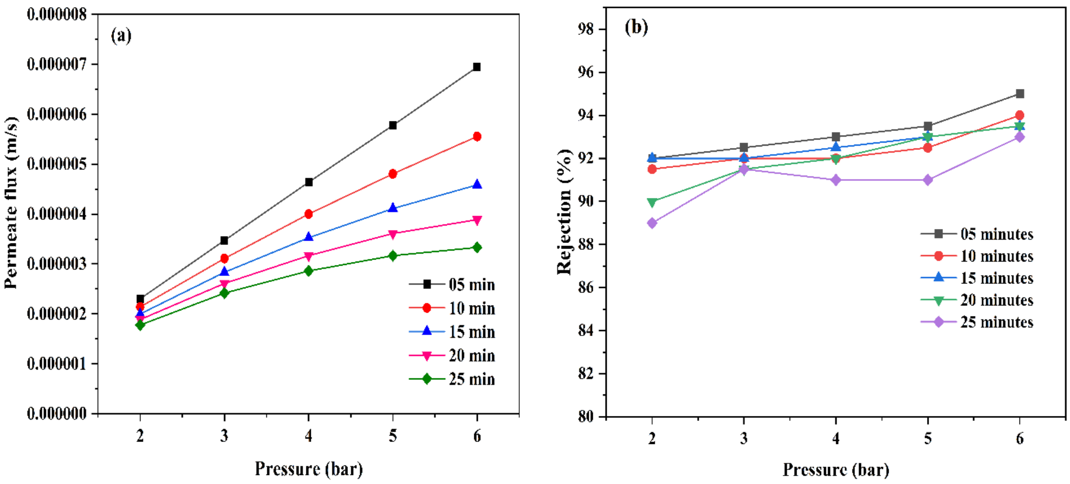

Figure 6.4 Pressure influence on (a) permeate flux and (b) percentage rejection, for beetroot juice

6.3.2.3 Effects of Feed Flow Rate:

Figure 6.5(a) presents the variation of permeate flux as a function of feed flow rates. The experimental results showed that the permeate flux increased from 4.17×10^{-6} m/s to 6.94×10^{-6} m/s over 5 minutes at a fixed pressure of 6 bar. Higher feed flow rates reduce the thickness of the concentration polarization layer and remove accumulated solute molecules near the membrane by increasing turbulence. This enables more water to be transported across the membrane, causing higher permeate flux. A similar trend was also observed for other pressure and time values. Figure 6.5(b) shows that increasing the feed flow rate from 200 mL/min to 600 mL/min slightly increases the rejection percentage from 92% to 94% at 5 minutes and 6 bar. As discussed earlier, a higher feed flow rate reduces concentration polarization by increasing mixing in the feed section, thereby lowering the osmotic pressure, which is the driving force for solute transport. Thus, lower osmotic pressure reduces solute transport across the membrane and enhances solute rejection. A similar trend was observed for other concentrations and pressures.

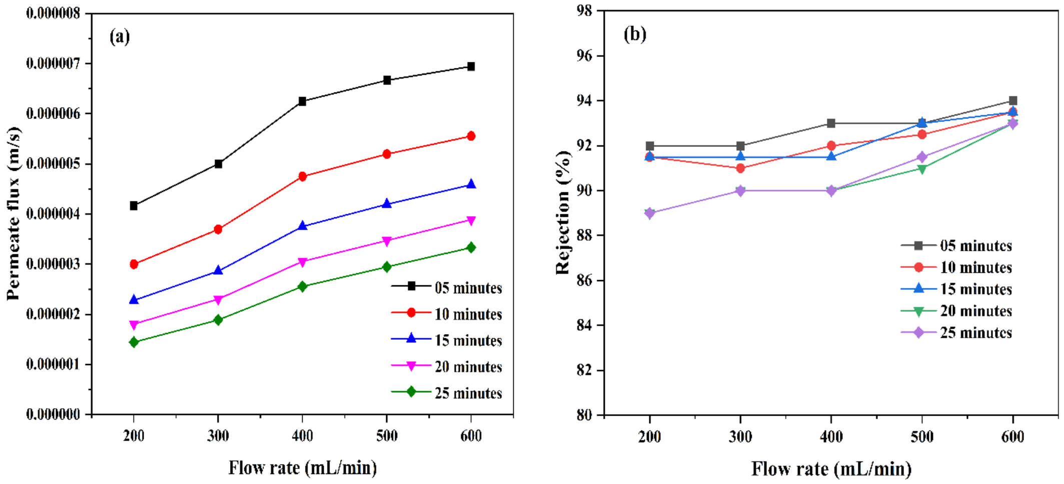

Figure 6.5 Influence of feed flow rate on (a) permeate flux and (b) percentage rejection, for beetroot juice

6.3.3 Fouling Analysis

Equation (6.2) was used to report the membrane fouling index. The pure water hydraulic permeability was measured following the chemical cleaning process. The hydraulic permeability of the membrane decreased from 5.57×10^{-6} $ms^{-1}bar^{-1}$ to 4.73×10^{-6} $ms^{-1}bar^{-1}$ with the FI of 15.1%. The cleaning method proved efficient at preserving membrane operational capabilities for extended filtration.

The comprehensive membrane fouling analysis across varying operating conditions revealed complex interactions between pressure, flow rate, and fouling mechanisms. At 6.0 bar pressure, severe flux decline patterns were observed, ranging from 52% at 600 mL/min to 65% at 200 mL/min, indicating that lower flow rates exacerbate fouling due to increased particle residence time and enhanced concentration polarization effects. In contrast, at a low pressure of 2.0 bar, the flux decline was more moderate, ranging from 23% at 600 mL/min to 42% at 200 mL/min, suggesting that reduced pressure leads to lower particle deposition rates and more sustainable operation (Appendix A5).

Table 6.2 The fouling rate constant (*k'*) and R^2 of different fouling models

Press. (bar)	Flowrate (mL/min)	Cake layer		Complete blocking		Intermediate blocking		Standard blocking	
		k'	**R^2**	**k'**	**R^2**	**k'**	**R^2**	**k'**	**R^2**
6	500	0.095	0.744	0.030	0.885	0.038	0.818	0.017	0.853
6	200	0.134	0.696	0.038	0.872	0.051	0.786	0.022	0.831
5	600	0.064	0.795	0.022	0.898	0.027	0.850	0.012	0.875
5	500	0.075	0.779	0.025	0.894	0.031	0.840	0.014	0.869
5	400	0.087	0.758	0.028	0.889	0.035	0.827	0.016	0.854
4	400	0.070	0.785	0.024	0.895	0.029	0.844	0.013	0.871
3	600	0.034	0.849	0.013	0.910	0.015	0.881	0.077	0.896
3	300	0.064	0.792	0.022	0.897	0.027	0.847	0.012	0.873
2	600	0.023	0.869	0.096	0.912	0.010	0.892	0.005	0.902
2	200	0.056	0.812	0.020	0.903	0.024	0.861	0.011	0.883

Figure 6.6 shows the experimental data fit to different models. In addition, mathematical modeling of fouling mechanisms revealed that the R^2 for the complete blocking model was highest across various pressures and feed flow rates, indicating it as the best-fit model. Table 6.2 represents different models' R-squared (R^2) and fouling rate constant (k') at various pressures and feed flow rates, with Appendix A4 representing the complete table. This underscores that surface-based fouling mechanisms predominate under these conditions, a physical effect supported by the increasing particle drag forces at higher pressure. The fouling rate constant increased exponentially with pressure, quantitatively confirming the pressure-dependent nature of fouling mechanisms.

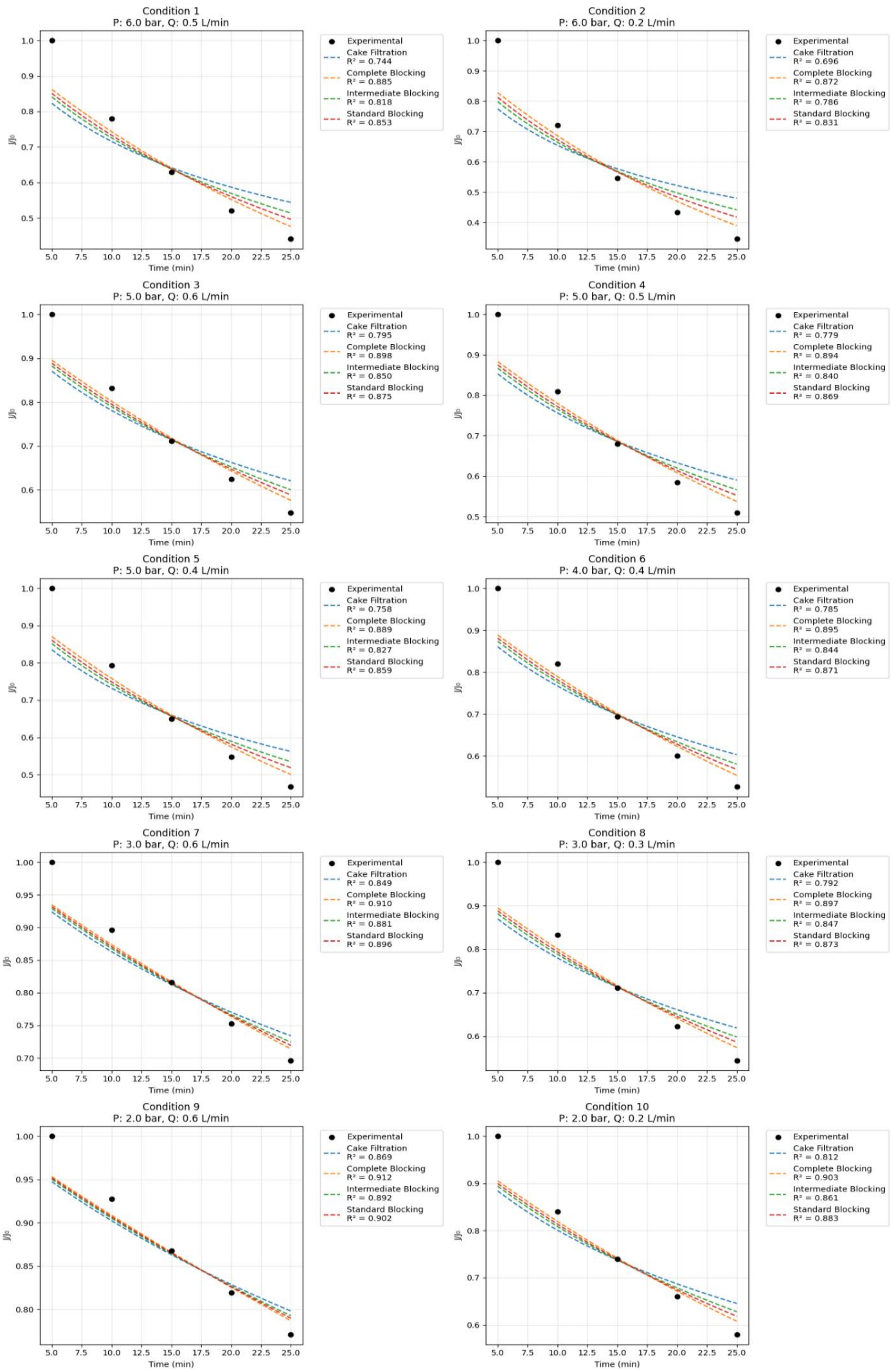

Figure 6.6 Model fitting graphs for fouling analysis

6.3.4 Morphological Analysis

The morphological analysis of the membrane samples provides a qualitative indication of the fouling mechanism. The SEM micrographs revealed a significant transformation of membrane morphology from a pristine fibrous network to a heavily fouled surface (Figure 6.7).

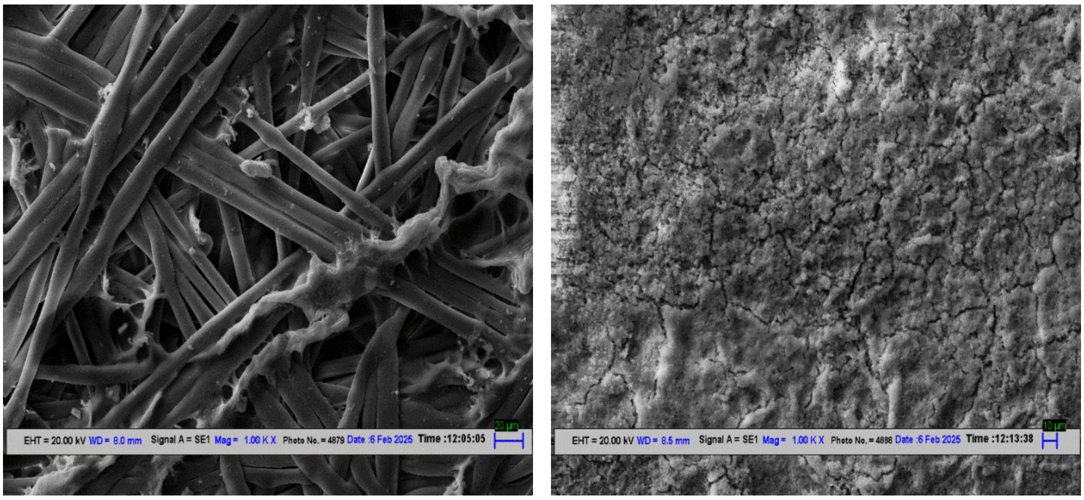

Figure 6.7 SEM micrographs of the HFT-NF 150 membrane (a) before and (b) after experiments

ImageJ was used to analyze SEM micrographs for morphological parameters, including size and surface roughness [30]. The quantitative measurements from ImageJ software, shown in Table 6.3, systematically documented this transition. The original HFT-NF 150 membrane exhibited a discrete, well-defined fiber structure characterized by smooth, uniformly thin fibers with high circularity and solidity. After the filtration of beetroot juice for 25 minutes at 6 bar pressure and 200 mL/min flow rate, the membrane underwent a significant morphological shift, evidenced by a substantial increase in particle count and a rise in surface area coverage. This indicated extensive foulant deposition that obscured the original fiber network, thereby supporting the observed decline in flux over time. The foulant particles showed larger average sizes, decreased circularity, and reduced solidity, thus quantitatively corroborating the visible, irregular, and complex aggregates covering the membrane surface. The measurements revealed an approximately fourfold increase in area coverage, with shape parameters showing meaningful decreases that reflected the more irregular deposit morphology.

Table 6.3 Comparison of the morphological parameters before and after fouling, using ImageJ software

Membrane	Original membrane	Fouled membrane
Count	2850	4263
Total Area	3180.03	13722.22
Average Size	1.116	3.219
% Area	3.325	12.201
Perimeter	2.816	5.415
Circularity	0.917	0.864
Solidity	0.925	0.888
Integrated intensity	273.57	770.705
Kurtosis	21.54	19.787

6.4 Conclusion

The study reported the separation efficiency of the UF+NF hybrid system in concentrating betanin from natural beetroot juice. The influence of different operating parameters, including operating time, feed flow rate, and pressure, was analyzed for the HFT-NF 150 membrane. The permeate flux declines over time from 52% to 65% as the feed flow rate is reduced from 600 mL/min to 200 mL/min at constant pressure, suggesting greater fouling at lower flow rates. The higher rejection percentages in the 87-94% range for different operating conditions indicate the applicability of NF membranes for concentrating betanin. The fouling study showed that the complete blocking model is the best bit model, with an R^2 ranging from 0.88 to 0.92. Also, the results showed that the fouling rate constant increases with pressure at constant feed flow rates. The SEM micrographs of fouled membranes also validated the results.

References

[1] C. Alasalvar, J. S. Salvadó, and E. Ros, "Bioactives and health benefits of nuts and dried fruits," *Food Chem.*, vol. 314, no. 0, pp. 126192, 2020, doi: 10.1016/j.foodchem.2020.126192

[2] D. Trishitman, P. S. Negi, and N. K. Rastogi, "Concentration of pomegranate juice by forward osmosis or thermal evaporation and its shelf-life kinetic studies," *Food Chem.*, vol. 399, no. 0, pp. 133972, 2023, doi: 10.1016/j.foodchem.2022.133972

[3] F. Delgado Vargas, A. R. Jimenez, and O. Paredes Lopez, "Natural pigments: Carotenoids, anthocyanins, and betalains - Characteristics, biosynthesis, processing, and stability," *Crit. Rev. Food Sci. Nutr.* , vol. 40, no. 3, pp. 173-289, 2010, doi: 10.1080/10408690091189257

[4] J. A. Vinson, X. Su, L. Zubik, and P. Bose, "Phenol antioxidant quantity and quality in foods: Fruits," *J. Agric. Food Chem.*, vol. 49, no. 11, pp. 5315–5321, 2001, doi: 10.1021/jf0009293

[5] I. Žitňanová, S. Ranostajová, H. Sobotová, D. Demelová, I. Pecháň, and Z. Ďuračková, "Antioxidative activity of selected fruits and vegetables," *Biologia (Bratisl).*, vol. 61, no. 3, pp. 279–284, 2006, doi: 10.2478/s11756-006-0051-7

[6] J. Shi, H. Nawaz, J. Pohorly, G. Mittal, Y. Kakuda, and Y. Jiang, "Extraction of polyphenolics from plant material for functional foods - Engineering and technology," *Food Rev. Int.*, vol. 21, no. 1, pp. 139–166, 2005, doi: 10.1081/FRI-200040606

[7] K. B. Pandey and S. I. Rizvi, "Plant polyphenols as dietary antioxidants in human health and disease," *Oxid. Med. Cell. Longev.*, vol. 2, no. 5, pp. 270–278, 2009, doi: 10.4161/oxim.2.5.9498

[8] A. K. Tiwari and M. Jain, "Concentration of betanin from model beetroot extracts using nanofiltration: parameter estimation and sensitivity analysis," *J. Chem. Technol. Biotechnol.*, vol. 99, no. 9, pp. 1976–1983, 2024, doi: 10.1002/jctb.7698

[9] A. Durazzo *et al.*, "Polyphenols: A concise overview on the chemistry, occurrence, and human health," *Phyther. Res.*, vol. 33, no. 9, pp. 2221–2243, 2019, doi: 10.1002/ptr.6419

[10] R. Mark, X. Lyu, J. J. L. Lee, R. Parra-Saldívar, and W. N. Chen, "Sustainable production of natural phenolics for functional food applications," *J. Funct. Foods*, vol. 57, no. 0, pp. 233–254, 2019, doi: 10.1016/j.jff.2019.04.008

[11] M. L. Luna-Guevara, J. J. Luna-Guevara, P. Hernández-Carranza, H. Ruíz-Espinosa, and C. E. Ochoa-Velasco, "Phenolic compounds: A good choice against chronic degenerative diseases," *Stud. Nat. Prod. Chem.*, vol. 59, no. 0, pp. 79–108, 2018, doi: 10.1016/B978-0-444-64179-3.00003-7

[12] B. R. Albuquerque, S. A. Heleno, M. B. P. P. Oliveira, L. Barros, and I. C. F. R. Ferreira, "Phenolic compounds: Current industrial applications, limitations, and future challenges," *Food Funct.*, vol. 12, no. 1, pp. 14–29, 2021, doi: 10.1039/d0fo02324h

[13] J. Kanner, S. Harel, and R. Granit, "Betalains - A new class of dietary cationized antioxidants," *J. Agric. Food Chem.*, vol. 49, no. 11, pp. 5178–5185, 2001, doi: 10.1021/jf010456f

[14] L. C. P. Gonalves *et al.*, "A comparative study of the purification of betanin," *Food Chem.*, vol. 131, no. 1, pp. 231–238, 2012, doi: 10.1016/j.foodchem.2011.08.067

[15] O. R. Alara, N. H. Abdurahman, and C. I. Ukaegbu, "Extraction of phenolic compounds: A review," *Curr. Res. Food Sci.*, vol. 4, no. 0, pp. 200–214, 2021, doi: 10.1016/j.crfs.2021.03.011

[16] Q. W. Zhang, L. G. Lin, and W. C. Ye, "Techniques for extraction and isolation of natural products: A comprehensive review," *Chinese Med. (United Kingdom)*, vol. 13, no. 1, pp. 1–26, 2018, doi: 10.1186/s13020-018-0177-x

[17] K. Lutchmiah, A. R. D. Verliefde, K. Roest, L. C. Rietveld, and E. R. Cornelissen, "Forward osmosis for application in wastewater treatment: A review," *Water Res.*, vol. 58, no. 0, pp. 179–197, 2014, doi:

10.1016/j.watres.2014.03.045

[18] R. Castro-Muñoz, B. E. Barragán-Huerta, V. Fíla, P. C. Denis, and R. Ruby-Figueroa, "Current role of membrane technology: From the treatment of agro-industrial by-products up to the valorization of valuable compounds," *Waste and Biomass Valori.*, vol. 9, no. 4, pp. 513–529, 2018, doi: 10.1007/s12649-017-0003-1

[19] G. D. Arend *et al.*, "Concentration of phenolic compounds from strawberry (*Fragaria X ananassa Duch*) juice by nanofiltration membrane," *J. Food Eng.*, vol. 201, no. 0, pp. 36–41, 2017, doi: 10.1016/j.jfoodeng.2017.01.014

[20] C. Conidi, A. Cassano, and E. Drioli, "Recovery of phenolic compounds from orange press liquor by nanofiltration," *Food Bioprod. Process.*, vol. 90, no. 4, pp. 867–874, 2012, doi: 10.1016/j.fbp.2012.07.005

[21] A. Cassano, M. Marchio, and E. Drioli, "Clarification of blood orange juice by ultrafiltration: analyses of operating parameters, membrane fouling, and juice quality," *Desalination*, vol. 212, no. 1–3, pp. 15–27, 2007, doi: 10.1016/j.desal.2006.08.013

[22] Z. S. Saleh, R. Stanley, and R. Wibisono, "Separation and concentration of health compounds by membrane filtration," *Handb. Environ. Chem. Water Pollut.*, vol. 2, no. 3, pp. 1–14, 2006, doi: 10.2202/1556-3758.1125

[23] A. P. Echavarría, V. Falguera, C. Torras, C. Berdún, J. Pagán, and A. Ibarz, "Ultrafiltration and reverse osmosis for clarification and concentration of fruit juices at pilot plant scale," *Lwt*, vol. 46, no. 1, pp. 189–195, 2012, doi: 10.1016/j.lwt.2011.10.008

[24] A. Tamba, A. Servent, C. Mertz, M. Cissé, and M. Dornier, "Coupling of pressure-driven membrane technologies for concentrating, purifying and fractionizing betacyanins in cactus pear (*Opuntia dillenii Haw.*) juice," *Innov. Food Sci. Emerg. Technol.*, vol. 52, no. 0, pp. 244–255, 2019, doi: 10.1016/j.ifset.2018.12.008

[25] G. Bolton, D. LaCasse, and R. Kuriyel, "Combined models of membrane

fouling: Development and application to microfiltration and ultrafiltration of biological fluids," *J. Memb. Sci.*, vol. 277, no. 1–2, pp. 75–84, 2006, doi: 10.1016/j.memsci.2004.12.053

[26] A. K. Tiwari and M. Jain, "A novel process for rutin recovery from model solutions using nanofiltration: Experimental study, mathematical modeling, and scale-up design," *J. Food Process Eng.*, vol. 47, no. 3, pp. e14592, 2024, doi: 10.1111/jfpe.14592

[27] C. Conidi, A. Cassano, and E. Drioli, "Food and bioproducts processing: Recovery of phenolic compounds from orange press liquor by nanofiltration," *Food Bioprod. Process.*, vol. 90, no. 4, pp. 867–874, 2012, doi: 10.1016/j.fbp.2012.07.005

[28] A. Chatterjee, A. Ahluwalia, S. Senthilmurugan, and S. K. Gupta, "Modeling of a radial flow hollow fiber module and estimating model parameters using numerical techniques," *J. Memb. Sci.*, vol. 236, no. 1–2, pp. 1–16, 2004, doi: 10.1016/j.memsci.2004.01.006

[29] D. Attarde, M. Jain, and S. K. Gupta, "Modeling of a forward osmosis and a pressure-retarded osmosis spiral wound module using the Spiegler-Kedem model and experimental validation," *Sep. Purif. Technol.*, vol. 164, no. 0, pp. 182–197, 2016, doi: 10.1016/j.seppur.2016.03.039

[30] K. H. Ruzvidzo, R. Kaur, and M. Jain, "Novel polyelectrolyte-glycol ether ternary phase-separating draw solutions for desalination using forward osmosis," *Desalination*, vol. 586, no. 0, pp. 117897, 2024, doi: 10.1016/j.desal.2024.117897

Chapter – 7
Conclusion, Future Scope, and Social Impact

CHAPTER – 7

CONCLUSION, FUTURE SCOPE, AND SOCIAL IMPACT

7.1 Conclusions

In summary, membrane-based operations for separating natural phenolic compounds have emerged as a highly efficient, sustainable, and scalable approach across industries such as food, pharmaceuticals, and nutraceuticals. Techniques such as UF, NF, and RO have demonstrated significant potential in selectively isolating and concentrating phenolic compounds from complex natural matrices while preserving their bioactivity and structural integrity. The versatility of membrane technologies, coupled with their low energy consumption and minimal use of organic solvents, aligns well with the growing demand for green and eco-friendly separation processes. As research continues to optimize membrane materials, configurations, and operational parameters, these methods are poised to play an increasingly pivotal role in the extraction and purification of bioactive phenolic compounds, offering a promising alternative to conventional separation techniques. This research has shown NF's efficiency in separating two phenolic compounds: betanin and rutin. The significant findings of this research work contribute towards overcoming the barriers to the widespread adoption of membrane filtration as a sustainable solution to concentrate natural phenolic compounds and are listed below:

- The pure water flux results evaluated the hydraulic permeability of the HFT-NF 150 membrane as 5.52×10^{-11} $m^3/m^2Pa.s$
- Rutin and betanin model solutions were successfully concentrated from their model solutions using the HFT-NF 150 membrane with a maximum rejection of 98.5% and 99%, respectively.
- The transport parameters for model rutin solutions were successfully optimized using the calculated L_p with values $B_m = 2.15\times10^{-7}$ m/s; $\sigma = 0.98$; $a = 1.755\times10^{-2}$; and $b = 0.089$.

- The transport parameters for model betanin solutions were optimized using two different methods. Method 1 successfully optimized the parameters using the calculated L_p, yielding $B_m = 4.86\times10^{-7}$ m/s; $\sigma = 0.969$; $a = 1.536\times10^{-2}$; and $b = 1.061\times10^{-1}$. Method 2 optimized all parameters, including hydraulic permeability, as $L_p = 5.046\times10^{-11}$ m^3/m^{2}sPa; $B_m = 4.35\times10^{-7}$ m/s; $\sigma = 0.967$; $a = 1.285\times10^{-2}$; and $b = 1.355\times10^{-1}$.
- The effect analysis of different operating conditions showed that high pressure and high feed flow rate were the optimum conditions for betanin and rutin solutions to achieve high permeate flux and rejection.
- The low water flux decrement was observed after experiments on rutin model solutions, indicating negligible fouling with a fouling index of 1.99
- For betanin model solutions, the maximum permeate flux of 3.14×10^{-5} m^3/m^{2}s was obtained at 600 mL/min and 6 bar, but at a low feed concentration of 0.1 g/L.
- For rutin model solutions, the maximum permeate flux of 3.04×10^{-5} m^3/m^{2}s was obtained at 600 mL/min and 6 bar, but at a low feed concentration of 0.020 g/L.
- For both model solutions, the variance-based sensitivity showed that hydraulic permeability and pressure were the most influential parameters for permeate flux and rejection percentages for betanin and rutin solutions.
- The simulation results for the scale-up studies showed that the filtration time decreased from 5.10 to 0.84 hours for concentrating betanin from 100 to 50,000 mg/L as the pressure increased from 2 to 6 bar at a fixed flow rate of 600 mL/min.
- For rutin model solutions, the filtration time decreased from 5.01 to 0.84 hours to concentrate rutin from 100 to 50,000 mg/L as the pressure is increased from 2 to 6 bar at a fixed feed flow rate of 600 mL/min.
- Low time requirement for concentrating compounds shows the feasibility of the NF process for commercial applications.

- ❖ A hybrid system was successfully employed to concentrate betanin from beetroot juice with a maximum rejection of 94%.
- ❖ For the experiments on beetroot juice, the permeate flux declined with time from 52% to 65% by lowering the feed flow rate from 600 mL/min to 200 mL/min at a constant pressure, suggesting higher fouling at low feed flow rates.
- ❖ For beetroot juice experiments, the fouling analysis showed that the complete blocking model was the best fit compared to other fouling models, with maximum R^2 values in the range of 0.88 to 0.92.

7.2 Future Scope

This research has laid down several vital avenues in the domain of membrane operations for separating and concentrating natural phenolic compounds.

- ❖ **Development of hybrid processes:** Building on the foundations established in this research, future investigations can move beyond incremental improvements toward transformative innovations in membrane-based separation of natural phenolic compounds. Future research should focus on developing hybrid processes that combine membrane technologies with conventional separation methods (such as integrating UF with adsorption or coupling NF with enzymatic treatments) or various membrane processes (such as integrating UF with NF). These have the potential to significantly improve separation efficiency while minimizing energy requirements and reducing solvent consumption.
- ❖ **Process optimization:** Equally promising is the convergence of digital intelligence with membrane engineering. The integration of computational fluid dynamics (CFD) with machine learning (ML) algorithms and artificial intelligence (AI) tools offers a pathway toward self-optimizing membrane systems capable of dynamically adjusting operating conditions in real time to maximize phenolic recovery, preserve molecular integrity, and minimize fouling. Such data-driven frameworks could underpin the development of “smart” membrane operations for complex botanical feeds.

- **Advanced membrane development:** The rational design of advanced functional membranes represents another frontier. Future work may focus on stimuli-responsive membranes that modulate permeability in response to pH, temperature, or ionic strength, affinity membranes endowed with molecular recognition ligands for target phenolics, and nanocomposite membranes engineered at the molecular level for superior selectivity, permeability, and antifouling performance. These materials could redefine the precision and efficiency of bioactive compound separations.
- **Scale-up and economic analysis:** Finally, translating laboratory breakthroughs into real-world impact will require a paradigm shift in scale-up philosophy and techno-economic integration. Future research should prioritize pilot-scale validation, digital twins for process scale-up, comprehensive life cycle and carbon footprint analyses, and robust techno-economic modeling to guide industrial deployment. Such efforts will be pivotal in demonstrating the long-term sustainability, economic competitiveness, and commercial readiness of membrane-based platforms for the nutraceutical, pharmaceutical, and food industries.

7.3 Social Impact

The social implications of this research extend across multiple dimensions of sustainable development and public welfare. This research opens the door to the separation of natural phenolic compounds, increasing access to purified natural phenolic compounds for medicinal applications, resulting in the development of more effective natural antioxidant supplements and, subsequently, better quality natural ingredients for functional foods and nutraceuticals. Also, the research shows enhanced membrane filtration efficiency for concentrating phenolic compounds, with reduced use of organic solvents, lower energy consumption compared to traditional separation methods, and minimized waste generation, contributing to environmental sustainability.

Appendices

APPENDICES

Appendix A1 Data for B_m, σ, a, and b estimation

P ×10^5 (Pa)	**Q_f (L/h)**	**C_f (mg/L)**	**Q_p exp (L/h)**	**Q_p the (L/h)**	**Error in Q_p (%)**	**C_p exp (mg/L)**	**C_P the (mg/L)**	**Error in C_p (%)**
2.0	12.0	20.0	0.28	0.31	-11.91	0.60	0.62	-2.74
2.0	18.0	20.0	0.30	0.31	-4.40	0.60	0.62	-2.73
2.0	24.0	20.0	0.31	0.31	-1.12	0.60	0.62	-2.73
2.0	30.0	20.0	0.32	0.31	2.07	0.50	0.62	-23.27
2.0	36.0	20.0	0.36	0.31	12.68	0.40	0.62	-54.08
2.0	12.0	40.0	0.26	0.31	-20.39	1.50	1.23	17.79
2.0	18.0	40.0	0.28	0.31	-11.87	1.40	1.23	11.93
2.0	24.0	40.0	0.28	0.31	-11.87	1.10	1.23	-12.09
2.0	30.0	40.0	0.30	0.31	-4.36	1.00	1.23	-23.29
2.0	36.0	40.0	0.34	0.31	8.10	0.90	1.23	-36.99
2.0	12.0	60.0	0.25	0.31	-25.19	2.50	1.85	26.00
2.0	18.0	60.0	0.26	0.31	-20.34	2.40	1.85	22.92
2.0	24.0	60.0	0.27	0.31	-16.01	1.60	1.85	-15.62
2.0	30.0	60.0	0.28	0.31	-11.83	1.50	1.85	-23.32
2.0	36.0	60.0	0.32	0.31	2.14	1.40	1.85	-32.12
2.0	12.0	80.0	0.25	0.31	-25.14	4.20	2.47	41.26
2.0	18.0	80.0	0.26	0.31	-20.29	3.80	2.47	35.08
2.0	24.0	80.0	0.26	0.31	-20.29	3.60	2.47	31.47
2.0	30.0	80.0	0.27	0.31	-15.96	3.30	2.47	25.25
2.0	36.0	80.0	0.31	0.31	-1.00	3.30	2.47	25.25

2.0	12.0	100.0	0.23	0.31	-36.06	4.80	3.08	35.74
2.0	18.0	100.0	0.25	0.31	-25.09	4.80	3.08	35.74
2.0	24.0	100.0	0.27	0.31	-15.92	4.50	3.08	31.46
2.0	30.0	100.0	0.29	0.31	-8.67	4.20	3.08	26.56
2.0	36.0	100.0	0.29	0.31	-7.86	4.20	3.08	26.57
3.0	12.0	20.0	0.41	0.47	-14.86	0.60	0.51	15.49
3.0	18.0	20.0	0.41	0.47	-14.86	0.50	0.51	-1.40
3.0	24.0	20.0	0.43	0.47	-9.10	0.50	0.51	-1.40
3.0	30.0	20.0	0.44	0.47	-6.43	0.40	0.51	-26.74
3.0	36.0	20.0	0.47	0.47	0.08	0.40	0.51	-26.74
3.0	12.0	40.0	0.39	0.47	-20.12	1.30	1.01	21.98
3.0	18.0	40.0	0.41	0.47	-14.83	1.30	1.01	21.99
3.0	24.0	40.0	0.43	0.47	-9.08	1.20	1.01	15.49
3.0	30.0	40.0	0.43	0.47	-9.08	1.00	1.01	-1.40
3.0	36.0	40.0	0.46	0.47	-2.24	0.90	1.01	-12.67
3.0	12.0	60.0	0.37	0.47	-27.10	2.10	1.52	27.55
3.0	18.0	60.0	0.39	0.47	-20.09	2.00	1.52	23.93
3.0	24.0	60.0	0.43	0.47	-9.05	1.60	1.52	4.92
3.0	30.0	60.0	0.45	0.47	-4.67	1.50	1.52	-1.41
3.0	36.0	60.0	0.45	0.47	-4.67	1.40	1.52	-8.65
3.0	12.0	80.0	0.37	0.47	-27.07	3.40	2.03	40.33
3.0	18.0	80.0	0.37	0.47	-27.07	3.00	2.03	32.38
3.0	24.0	80.0	0.35	0.47	-33.58	2.50	2.03	18.86
3.0	30.0	80.0	0.37	0.47	-27.07	2.00	2.03	-1.42
3.0	36.0	80.0	0.41	0.47	-14.77	2.00	2.03	-1.42

3.0	12.0	100.0	0.37	0.47	-27.04	4.00	2.54	36.59
3.0	18.0	100.0	0.38	0.47	-23.43	3.60	2.54	29.55
3.0	24.0	100.0	0.39	0.47	-20.02	3.60	2.54	29.56
3.0	30.0	100.0	0.39	0.47	-20.02	3.20	2.54	20.75
3.0	36.0	100.0	0.41	0.47	-14.74	2.80	2.54	9.44
4.0	12.0	20.0	0.55	0.63	-14.03	0.50	0.46	8.26
4.0	18.0	20.0	0.57	0.63	-9.72	0.50	0.46	8.27
4.0	24.0	20.0	0.59	0.63	-6.37	0.50	0.46	8.28
4.0	30.0	20.0	0.61	0.63	-2.61	0.40	0.46	-14.64
4.0	36.0	20.0	0.62	0.63	-0.82	0.40	0.46	-14.64
4.0	12.0	40.0	0.55	0.63	-14.01	1.00	0.92	8.26
4.0	18.0	40.0	0.56	0.63	-11.81	1.00	0.92	8.27
4.0	24.0	40.0	0.57	0.63	-9.70	0.90	0.92	-1.92
4.0	30.0	40.0	0.59	0.63	-6.35	0.90	0.92	-1.91
4.0	36.0	40.0	0.62	0.63	-1.39	0.80	0.92	-14.64
4.0	12.0	60.0	0.53	0.63	-17.85	1.60	1.38	13.99
4.0	18.0	60.0	0.55	0.63	-13.99	1.50	1.38	8.26
4.0	24.0	60.0	0.57	0.63	-9.68	1.40	1.38	1.72
4.0	30.0	60.0	0.59	0.63	-6.33	1.40	1.38	1.73
4.0	36.0	60.0	0.62	0.63	-1.37	1.40	1.38	1.73
4.0	12.0	80.0	0.52	0.63	-20.27	2.20	1.84	16.59
4.0	18.0	80.0	0.53	0.63	-17.83	2.10	1.83	12.63
4.0	24.0	80.0	0.55	0.63	-13.97	2.10	1.83	12.63
4.0	30.0	80.0	0.55	0.63	-13.97	1.80	1.83	-1.92
4.0	36.0	80.0	0.57	0.63	-9.66	1.80	1.83	-1.92

4.0	12.0	100.0	0.53	0.63	-17.80	2.80	2.29	18.07
4.0	18.0	100.0	0.55	0.63	-13.94	2.60	2.29	11.78
4.0	24.0	100.0	0.55	0.63	-13.94	2.80	2.29	18.09
4.0	30.0	100.0	0.57	0.63	-9.64	2.40	2.29	4.44
4.0	36.0	100.0	0.57	0.63	-9.64	2.30	2.29	0.29
5.0	12.0	20.0	0.63	0.78	-24.59	0.40	0.43	-8.53
5.0	18.0	20.0	0.67	0.78	-17.21	0.40	0.43	-8.52
5.0	24.0	20.0	0.69	0.78	-13.54	0.40	0.43	-8.51
5.0	30.0	20.0	0.71	0.78	-10.09	0.40	0.43	-8.50
5.0	36.0	20.0	0.71	0.78	-10.09	0.30	0.43	-44.65
5.0	12.0	40.0	0.61	0.78	-28.24	1.10	0.87	21.07
5.0	18.0	40.0	0.63	0.78	-24.57	1.00	0.87	13.18
5.0	24.0	40.0	0.63	0.78	-24.57	1.00	0.87	13.19
5.0	30.0	40.0	0.65	0.78	-20.43	0.90	0.87	3.55
5.0	36.0	40.0	0.65	0.78	-20.43	0.90	0.87	3.56
5.0	12.0	60.0	0.61	0.78	-28.22	1.50	1.30	13.17
5.0	18.0	60.0	0.63	0.78	-24.55	1.40	1.30	6.98
5.0	24.0	60.0	0.63	0.78	-24.55	1.30	1.30	-0.17
5.0	30.0	60.0	0.64	0.78	-22.45	1.20	1.30	-8.50
5.0	36.0	60.0	0.64	0.78	-22.45	1.40	1.30	7.00
5.0	12.0	80.0	0.61	0.78	-28.20	2.20	1.74	21.06
5.0	18.0	80.0	0.61	0.78	-28.20	2.00	1.74	13.18
5.0	24.0	80.0	0.63	0.78	-24.53	1.80	1.74	3.54
5.0	30.0	80.0	0.64	0.78	-22.43	1.80	1.74	3.55
5.0	36.0	80.0	0.64	0.78	-22.43	1.70	1.74	-2.12

5.0	12.0	100.0	0.59	0.78	-32.88	3.00	2.17	27.64
5.0	18.0	100.0	0.62	0.78	-26.69	2.50	2.17	13.18
5.0	24.0	100.0	0.61	0.78	-28.18	2.00	2.17	-8.52
5.0	30.0	100.0	0.61	0.78	-28.18	2.40	2.17	9.57
5.0	36.0	100.0	0.63	0.78	-24.51	2.30	2.17	5.65
6.0	12.0	20.0	0.84	0.94	-11.76	0.40	0.42	-5.21
6.0	18.0	20.0	0.84	0.94	-11.76	0.40	0.42	-5.19
6.0	24.0	20.0	0.84	0.94	-11.76	0.40	0.42	-5.18
6.0	30.0	20.0	0.86	0.94	-9.42	0.30	0.42	-40.23
6.0	36.0	20.0	0.86	0.94	-9.42	0.30	0.42	-40.22
6.0	12.0	40.0	0.82	0.94	-14.69	1.00	0.84	15.83
6.0	18.0	40.0	0.82	0.94	-14.69	1.10	0.84	23.50
6.0	24.0	40.0	0.84	0.94	-11.75	0.80	0.84	-5.18
6.0	30.0	40.0	0.86	0.94	-9.40	0.70	0.84	-20.20
6.0	36.0	40.0	0.86	0.94	-9.40	1.00	0.84	15.87
6.0	12.0	60.0	0.76	0.94	-23.93	1.80	1.26	29.86
6.0	18.0	60.0	0.80	0.94	-17.78	1.60	1.26	21.10
6.0	24.0	60.0	0.80	0.94	-17.25	1.20	1.26	-5.18
6.0	30.0	60.0	0.82	0.94	-14.68	1.20	1.26	-5.17
6.0	36.0	60.0	0.83	0.94	-13.18	1.20	1.26	-5.17
6.0	12.0	80.0	0.74	0.94	-26.93	2.00	1.68	15.83
6.0	18.0	80.0	0.75	0.94	-25.10	2.00	1.68	15.84
6.0	24.0	80.0	0.76	0.94	-23.91	1.60	1.68	-5.18
6.0	30.0	80.0	0.80	0.94	-17.76	1.60	1.68	-5.17
6.0	36.0	80.0	0.74	0.94	-26.93	1.60	1.68	-5.17

6.0	12.0	100.0	0.72	0.94	-30.72	2.20	2.10	4.35
6.0	18.0	100.0	0.72	0.94	-30.72	2.10	2.10	-0.19
6.0	24.0	100.0	0.69	0.94	-35.19	2.10	2.10	-0.18
6.0	30.0	100.0	0.70	0.94	-34.84	2.50	2.10	15.86
6.0	36.0	100.0	0.70	0.94	-34.84	2.10	2.10	-0.16

Fixed average parameter: $L_p = 5.52\times10^{-11}$ m^3/m^{2}sPa.

Predicted average parameters: $B_m = 2.15\times10^{-7}$ m/s, $\sigma = 0.98$, a = 1.755×10^{-2}, b = 0.0809;

Appendix A2 Data for parameter estimation of B_m, σ, a, and b (Method 1)

P (MPa)	**Q_f ($\times10^{-6}$ m^3/s)**	**C_f (kg/m^3)**	**J_v exp ($\times10^{-5}$ m/s)**	**J_v the ($\times10^{-5}$ m/s)**	**Error in J_v (%)**	**R% exp**	**R% the**	**Error in R (%)**
0.2	3.3	0.1	1.10	1.11	-0.99	0.94	0.94	-0.06
0.2	5.0	0.1	1.17	1.11	5.17	0.94	0.94	-0.06
0.2	6.6	0.1	1.20	1.11	7.89	0.95	0.94	0.99
0.2	8.3	0.1	1.24	1.11	10.54	0.95	0.94	0.99
0.2	10.0	0.1	1.37	1.11	19.49	0.96	0.94	2.02
0.2	3.3	0.2	1.03	1.11	-7.84	0.94	0.94	-0.06
0.2	5.0	0.2	1.10	1.11	-0.95	0.95	0.94	0.47
0.2	6.6	0.2	1.10	1.11	-0.95	0.95	0.94	0.99
0.2	8.3	0.2	1.17	1.11	5.21	0.96	0.94	1.51
0.2	10.0	0.2	1.31	1.11	15.61	0.96	0.94	1.51
0.2	3.3	0.3	0.99	1.11	-11.68	0.93	0.94	-0.77
0.2	5.0	0.3	1.03	1.11	-7.80	0.94	0.94	-0.06
0.2	6.6	0.3	1.06	1.11	-4.30	0.95	0.94	0.99

0.2	8.3	0.3	1.10	1.11	-0.91	0.95	0.94	0.99
0.2	10.0	0.3	1.24	1.11	10.61	0.95	0.94	1.34
0.2	3.3	0.4	0.99	1.11	-11.63	0.92	0.94	-2.23
0.2	5.0	0.4	1.03	1.11	-7.75	0.94	0.94	-0.06
0.2	6.6	0.4	1.03	1.11	-7.75	0.94	0.94	-0.59
0.2	8.3	0.4	1.06	1.11	-4.26	0.94	0.94	-0.59
0.2	10.0	0.4	1.20	1.11	8.00	0.94	0.94	-0.06
0.2	3.3	0.5	0.92	1.11	-20.24	0.92	0.94	-2.68
0.2	5.0	0.5	0.99	1.11	-11.59	0.94	0.94	-0.05
0.2	6.6	0.5	1.06	1.11	-4.22	0.93	0.94	-0.91
0.2	8.3	0.5	1.12	1.11	1.68	0.93	0.94	-1.13
0.2	10.0	0.5	1.13	1.11	2.35	0.94	0.94	-0.05
0.3	3.3	0.1	1.55	1.66	-6.93	0.95	0.95	-0.35
0.3	5.0	0.1	1.55	1.66	-6.93	0.96	0.95	0.70
0.3	6.6	0.1	1.63	1.66	-1.91	0.96	0.95	0.70
0.3	8.3	0.1	1.67	1.66	0.42	0.95	0.95	-0.35
0.3	10.0	0.1	1.77	1.66	6.15	0.96	0.95	0.70
0.3	3.3	0.2	1.49	1.66	-11.47	0.94	0.95	-1.42
0.3	5.0	0.2	1.55	1.66	-6.90	0.94	0.95	-1.96
0.3	6.6	0.2	1.63	1.66	-1.89	0.95	0.95	-0.35
0.3	8.3	0.2	1.63	1.66	-1.89	0.96	0.95	0.70
0.3	10.0	0.2	1.73	1.66	4.11	0.97	0.95	1.21
0.3	3.3	0.3	1.41	1.66	-17.46	0.93	0.95	-2.14
0.3	5.0	0.3	1.49	1.66	-11.43	0.94	0.95	-1.41
0.3	6.6	0.3	1.63	1.66	-1.86	0.95	0.95	-0.35

0.3	8.3	0.3	1.69	1.66	1.97	0.96	0.95	0.70
0.3	10.0	0.3	1.69	1.66	1.97	0.96	0.95	0.70
0.3	3.3	0.4	1.41	1.66	-17.43	0.93	0.95	-2.50
0.3	5.0	0.4	1.41	1.66	-17.43	0.94	0.95	-1.96
0.3	6.6	0.4	1.35	1.66	-22.97	0.94	0.95	-1.41
0.3	8.3	0.4	1.41	1.66	-17.43	0.94	0.95	-1.41
0.3	10.0	0.4	1.55	1.66	-6.84	0.95	0.95	-0.88
0.3	3.3	0.5	1.41	1.66	-17.39	0.93	0.95	-2.28
0.3	5.0	0.5	1.45	1.66	-14.30	0.94	0.95	-1.41
0.3	6.6	0.5	1.49	1.66	-11.37	0.93	0.95	-2.50
0.3	8.3	0.5	1.49	1.66	-11.37	0.94	0.95	-1.41
0.3	10.0	0.5	1.55	1.66	-6.81	0.94	0.95	-1.41
0.4	3.3	0.1	2.05	2.21	-8.04	0.95	0.96	-0.99
0.4	5.0	0.1	2.13	2.21	-4.16	0.95	0.96	-0.99
0.4	6.6	0.1	2.19	2.21	-1.13	0.96	0.96	0.06
0.4	8.3	0.1	2.27	2.21	2.28	0.96	0.96	0.06
0.4	10.0	0.1	2.30	2.21	3.90	0.97	0.96	1.09
0.4	3.3	0.2	2.05	2.21	-8.02	0.95	0.96	-1.53
0.4	5.0	0.2	2.09	2.21	-6.04	0.94	0.96	-2.07
0.4	6.6	0.2	2.13	2.21	-4.14	0.95	0.96	-0.99
0.4	8.3	0.2	2.19	2.21	-1.11	0.94	0.96	-2.07
0.4	10.0	0.2	2.29	2.21	3.38	0.96	0.96	0.06
0.4	10.0	0.3	1.99	2.21	-11.46	0.94	0.96	-2.07
0.4	5.0	0.3	2.05	2.21	-8.00	0.95	0.96	-1.35
0.4	6.6	0.3	2.13	2.21	-4.12	0.95	0.96	-0.99

0.4	8.3	0.3	2.19	2.21	-1.09	0.96	0.96	0.06
0.4	10	0.3	2.29	2.21	3.40	0.97	0.96	1.09
0.4	3.3	0.4	1.95	2.21	-13.62	0.94	0.96	-2.61
0.4	5.0	0.4	1.99	2.21	-11.43	0.94	0.96	-2.61
0.4	6.6	0.4	2.05	2.21	-7.97	0.94	0.96	-2.07
0.4	8.3	0.4	2.05	2.21	-7.97	0.95	0.96	-1.53
0.4	10.0	0.4	2.13	2.21	-4.09	0.96	0.96	0.06
0.4	3.3	0.5	1.99	2.21	-11.41	0.94	0.96	-2.06
0.4	5.0	0.5	2.05	2.21	-7.95	0.94	0.96	-2.06
0.4	6.6	0.5	2.05	2.21	-7.95	0.94	0.96	-2.06
0.4	8.3	0.5	2.13	2.21	-4.07	0.94	0.96	-1.63
0.4	10.0	0.5	2.13	2.21	-4.07	0.95	0.96	-0.99
0.5	3.3	0.1	2.33	2.77	-18.82	0.96	0.96	-0.30
0.5	5.0	0.1	2.47	2.77	-12.08	0.96	0.96	-0.30
0.5	6.6	0.1	2.55	2.77	-8.72	0.97	0.96	0.74
0.5	8.3	0.1	2.62	2.77	-5.55	0.97	0.96	0.74
0.5	10.0	0.1	2.62	2.77	-5.55	0.97	0.96	0.74
0.5	3.3	0.2	2.27	2.77	-22.14	0.95	0.96	-1.35
0.5	5.0	0.2	2.33	2.77	-18.80	0.96	0.96	-0.30
0.5	6.6	0.2	2.33	2.77	-18.80	0.97	0.96	0.22
0.5	8.3	0.2	2.41	2.77	-15.03	0.97	0.96	0.22
0.5	10.0	0.2	2.41	2.77	-15.03	0.97	0.96	0.74
0.5	3.3	0.3	2.27	2.77	-22.12	0.96	0.96	-0.30
0.5	5.0	0.3	2.33	2.77	-18.78	0.95	0.96	-1.35
0.5	6.6	0.3	2.33	2.77	-18.78	0.95	0.96	-1.35

0.5	8.3	0.3	2.37	2.77	-16.86	0.96	0.96	-0.30
0.5	10.0	0.3	2.37	2.77	-16.86	0.97	0.96	0.74
0.5	3.3	0.4	2.27	2.77	-22.10	0.94	0.96	-2.16
0.5	5.0	0.4	2.27	2.77	-22.10	0.95	0.96	-1.89
0.5	6.6	0.4	2.33	2.77	-18.76	0.94	0.96	-2.43
0.5	8.3	0.4	2.37	2.77	-16.85	0.95	0.96	-1.35
0.5	10.0	0.4	2.37	2.77	-16.85	0.96	0.96	-0.30
0.5	3.3	0.5	2.19	2.77	-26.33	0.94	0.96	-1.99
0.5	5.0	0.5	2.29	2.77	-20.72	0.95	0.96	-1.35
0.5	6.6	0.5	2.27	2.77	-22.08	0.96	0.96	-0.29
0.5	8.3	0.5	2.27	2.77	-22.08	0.94	0.96	-2.43
0.5	10.0	0.5	2.33	2.77	-18.74	0.96	0.96	-0.29
0.6	3.3	0.1	3.08	3.32	-7.83	0.97	0.96	0.52
0.6	5.0	0.1	3.08	3.32	-7.83	0.97	0.96	0.52
0.6	6.6	0.1	3.08	3.32	-7.83	0.97	0.96	0.52
0.6	8.3	0.1	3.14	3.32	-5.64	0.98	0.96	1.54
0.6	10.0	0.1	3.14	3.32	-5.64	0.99	0.96	2.53
0.6	3.3	0.2	3.00	3.32	-10.55	0.96	0.96	-1.04
0.6	5.0	0.2	3.00	3.32	-10.55	0.97	0.96	0.52
0.6	6.6	0.2	3.08	3.32	-7.81	0.97	0.96	0.01
0.6	8.3	0.2	3.14	3.32	-5.63	0.97	0.96	0.52
0.6	10.0	0.2	3.14	3.32	-5.63	0.97	0.96	0.52
0.6	3.3	0.3	2.79	3.32	-19.12	0.96	0.96	-0.51
0.6	5.0	0.3	2.93	3.32	-13.42	0.96	0.96	-0.86
0.6	6.6	0.3	2.94	3.32	-12.93	0.97	0.96	0.18

0.6	8.3	0.3	3.00	3.32	-10.54	0.96	0.96	-0.51
0.6	10.0	0.3	3.04	3.32	-9.15	0.97	0.96	0.52
0.6	3.3	0.4	2.72	3.32	-21.88	0.95	0.96	-1.30
0.6	5.0	0.4	2.76	3.32	-20.20	0.95	0.96	-1.57
0.6	6.6	0.4	2.79	3.32	-19.10	0.95	0.96	-1.57
0.6	8.3	0.4	2.93	3.32	-13.40	0.96	0.96	-0.51
0.6	10.0	0.4	2.72	3.32	-21.88	0.96	0.96	-0.51
0.6	3.3	0.5	2.65	3.32	-25.38	0.94	0.96	-2.21
0.6	5.0	0.5	2.65	3.32	-25.38	0.94	0.96	-2.21
0.6	6.6	0.5	2.56	3.32	-29.49	0.96	0.96	-0.51
0.6	8.3	0.5	2.57	3.32	-29.17	0.96	0.96	-0.51
0.6	10.0	0.5	2.57	3.32	-29.17	0.96	0.96	-0.51

Fixed parameter: $L_p = 5.52\times10^{-8}$ kg/m^{2}sPa.

Predicted parameters: $B_m = 4.86\times10^{-7}$ m/s; $\sigma = 0.969$; a = 1.54×10^{-2} ; b = 1.067×10^{-1}

Appendix A3 Data for parameter estimation of L_p, B_m, σ, a, and b (Method 2)

P (MPa)	**Q_f ($\times10^{-6}$ m^3/s)**	**C_f (kg/m^3)**	**J_v exp ($\times10^{-5}$ m/s)**	**J_v the ($\times10^{-5}$ m/s)**	**Error in J_v (%)**	**R% exp**	**R% the**	**Error in R (%)**
0.2	3.3	0.1	1.10	1.01	7.68	0.94	0.94	-0.01
0.2	5.0	0.1	1.17	1.01	13.32	0.94	0.94	-0.01
0.2	6.6	0.1	1.20	1.01	15.80	0.95	0.94	1.04
0.2	8.3	0.1	1.24	1.01	18.22	0.95	0.94	1.04
0.2	10.0	0.1	1.37	1.01	26.40	0.96	0.94	2.07
0.2	3.3	0.2	1.03	1.01	1.42	0.94	0.94	-0.01
0.2	5.0	0.2	1.10	1.01	7.72	0.95	0.94	0.52

0.2	6.6	0.2	1.10	1.01	7.72	0.95	0.94	1.04
0.2	8.3	0.2	1.17	1.01	13.35	0.96	0.94	1.56
0.2	10.0	0.2	1.31	1.01	22.86	0.96	0.94	1.56
0.2	3.3	0.3	0.99	1.01	-2.09	0.93	0.94	-0.72
0.2	5.0	0.3	1.03	1.01	1.46	0.94	0.94	-0.01
0.2	6.6	0.3	1.06	1.01	4.65	0.95	0.94	1.04
0.2	8.3	0.3	1.10	1.01	7.75	0.95	0.94	1.04
0.2	10.0	0.3	1.24	1.01	18.29	0.95	0.94	1.39
0.2	3.3	0.4	0.99	1.01	-2.05	0.92	0.94	-2.18
0.2	5.0	0.4	1.03	1.01	1.50	0.94	0.94	-0.01
0.2	6.6	0.4	1.03	1.01	1.50	0.94	0.94	-0.54
0.2	8.3	0.4	1.06	1.01	4.69	0.94	0.94	-0.54
0.2	10.0	0.4	1.20	1.01	15.90	0.94	0.94	-0.01
0.2	3.3	0.5	0.92	1.01	-9.92	0.92	0.94	-2.63
0.2	5.0	0.5	0.99	1.01	-2.00	0.94	0.94	-0.01
0.2	6.6	0.5	1.06	1.01	4.73	0.93	0.94	-0.87
0.2	8.3	0.5	1.12	1.01	10.13	0.93	0.94	-1.08
0.2	10.0	0.5	1.13	1.01	10.73	0.94	0.94	-0.01
0.3	3.3	0.1	1.55	1.52	2.25	0.95	0.95	-0.26
0.3	5.0	0.1	1.55	1.52	2.25	0.96	0.95	0.78
0.3	6.6	0.1	1.63	1.52	6.84	0.96	0.95	0.78
0.3	8.3	0.1	1.67	1.52	8.97	0.95	0.95	-0.26
0.3	10.0	0.1	1.77	1.52	14.21	0.96	0.95	0.78
0.3	3.3	0.2	1.49	1.52	-1.89	0.94	0.95	-1.33
0.3	5.0	0.2	1.55	1.52	2.28	0.94	0.95	-1.87

0.3	6.6	0.2	1.63	1.52	6.86	0.95	0.95	-0.26
0.3	8.3	0.2	1.63	1.52	6.86	0.96	0.95	0.79
0.3	10.0	0.2	1.73	1.52	12.34	0.97	0.95	1.30
0.3	3.3	0.3	1.41	1.52	-7.37	0.93	0.95	-2.05
0.3	5.0	0.3	1.49	1.52	-1.87	0.94	0.95	-1.33
0.3	6.6	0.3	1.63	1.52	6.89	0.95	0.95	-0.26
0.3	8.3	0.3	1.69	1.52	10.39	0.96	0.95	0.79
0.3	10.0	0.3	1.69	1.52	10.39	0.96	0.95	0.79
0.3	3.3	0.4	1.41	1.52	-7.34	0.93	0.95	-2.41
0.3	5.0	0.4	1.41	1.52	-7.34	0.94	0.95	-1.87
0.3	6.6	0.4	1.35	1.52	-12.41	0.94	0.95	-1.32
0.3	8.3	0.4	1.41	1.52	-7.34	0.94	0.95	-1.32
0.3	10.0	0.4	1.55	1.52	2.34	0.95	0.95	-0.79
0.3	3.3	0.5	1.41	1.52	-7.31	0.93	0.95	-2.19
0.3	5.0	0.5	1.45	1.52	-4.49	0.94	0.95	-1.32
0.3	6.6	0.5	1.49	1.52	-1.81	0.93	0.95	-2.41
0.3	8.3	0.5	1.49	1.52	-1.81	0.94	0.95	-1.32
0.3	10.0	0.5	1.55	1.52	2.36	0.94	0.95	-1.32
0.4	3.3	0.1	2.05	2.02	1.24	0.95	0.96	-0.88
0.4	5.0	0.1	2.13	2.02	4.78	0.95	0.96	-0.88
0.4	6.6	0.1	2.19	2.02	7.55	0.96	0.96	0.17
0.4	8.3	0.1	2.27	2.02	10.67	0.96	0.96	0.17
0.4	10.0	0.1	2.30	2.02	12.15	0.97	0.96	1.20
0.4	3.3	0.2	2.05	2.02	1.26	0.95	0.96	-1.41
0.4	5.0	0.2	2.09	2.02	3.06	0.94	0.96	-1.95

0.4	6.6	0.2	2.13	2.02	4.80	0.95	0.96	-0.88
0.4	8.3	0.2	2.19	2.02	7.57	0.94	0.96	-1.95
0.4	10.0	0.2	2.29	2.02	11.68	0.96	0.96	0.18
0.4	10.0	0.3	1.99	2.02	-1.89	0.94	0.96	-1.95
0.4	5.0	0.3	2.05	2.02	1.28	0.95	0.96	-1.23
0.4	6.6	0.3	2.13	2.02	4.82	0.95	0.96	-0.88
0.4	8.3	0.3	2.19	2.02	7.59	0.96	0.96	0.18
0.4	10	0.3	2.29	2.02	11.70	0.97	0.96	1.20
0.4	3.3	0.4	1.95	2.02	-3.86	0.94	0.96	-2.49
0.4	5.0	0.4	1.99	2.02	-1.87	0.94	0.96	-2.49
0.4	6.6	0.4	2.05	2.02	1.30	0.94	0.96	-1.95
0.4	8.3	0.4	2.05	2.02	1.30	0.95	0.96	-1.41
0.4	10.0	0.4	2.13	2.02	4.84	0.96	0.96	0.18
0.4	3.3	0.5	1.99	2.02	-1.84	0.94	0.96	-1.95
0.4	5.0	0.5	2.05	2.02	1.32	0.94	0.96	-1.95
0.4	6.6	0.5	2.05	2.02	1.32	0.94	0.96	-1.95
0.4	8.3	0.5	2.13	2.02	4.86	0.94	0.96	-1.52
0.4	10.0	0.5	2.13	2.02	4.86	0.95	0.96	-0.87
0.5	3.3	0.1	2.33	2.53	-8.62	0.96	0.96	-0.16
0.5	5.0	0.1	2.47	2.53	-2.46	0.96	0.96	-0.16
0.5	6.6	0.1	2.55	2.53	0.61	0.97	0.96	0.87
0.5	8.3	0.1	2.62	2.53	3.51	0.97	0.96	0.87
0.5	10.0	0.1	2.62	2.53	3.51	0.97	0.96	0.87
0.5	3.3	0.2	2.27	2.53	-11.65	0.95	0.96	-1.22
0.5	5.0	0.2	2.33	2.53	-8.60	0.96	0.96	-0.16

0.5	6.6	0.2	2.33	2.53	-8.60	0.97	0.96	0.36
0.5	8.3	0.2	2.41	2.53	-5.15	0.97	0.96	0.36
0.5	10.0	0.2	2.41	2.53	-5.15	0.97	0.96	0.87
0.5	3.3	0.3	2.27	2.53	-11.63	0.96	0.96	-0.16
0.5	5.0	0.3	2.33	2.53	-8.58	0.95	0.96	-1.21
0.5	6.6	0.3	2.33	2.53	-8.58	0.95	0.96	-1.21
0.5	8.3	0.3	2.37	2.53	-6.83	0.96	0.96	-0.16
0.5	10.0	0.3	2.37	2.53	-6.83	0.97	0.96	0.87
0.5	3.3	0.4	2.27	2.53	-11.61	0.94	0.96	-2.02
0.5	5.0	0.4	2.27	2.53	-11.61	0.95	0.96	-1.75
0.5	6.6	0.4	2.33	2.53	-8.56	0.94	0.96	-2.29
0.5	8.3	0.4	2.37	2.53	-6.81	0.95	0.96	-1.21
0.5	10.0	0.4	2.37	2.53	-6.81	0.96	0.96	-0.16
0.5	3.3	0.5	2.19	2.53	-15.49	0.94	0.96	-1.86
0.5	5.0	0.5	2.29	2.53	-10.35	0.95	0.96	-1.21
0.5	6.6	0.5	2.27	2.53	-11.59	0.96	0.96	-0.16
0.5	8.3	0.5	2.27	2.53	-11.59	0.94	0.96	-2.29
0.5	10.0	0.5	2.33	2.53	-8.54	0.96	0.96	-0.16
0.6	3.3	0.1	3.08	3.04	1.43	0.97	0.96	0.67
0.6	5.0	0.1	3.08	3.04	1.43	0.97	0.96	0.67
0.6	6.6	0.1	3.08	3.04	1.43	0.97	0.96	0.67
0.6	8.3	0.1	3.14	3.04	3.43	0.98	0.96	1.69
0.6	10.0	0.1	3.14	3.04	3.43	0.99	0.96	2.68
0.6	3.3	0.2	3.00	3.04	-1.06	0.96	0.96	-0.89
0.6	5.0	0.2	3.00	3.04	-1.06	0.97	0.96	0.67

0.6	6.6	0.2	3.08	3.04	1.45	0.97	0.96	0.16
0.6	8.3	0.2	3.14	3.04	3.44	0.97	0.96	0.67
0.6	10.0	0.2	3.14	3.04	3.44	0.97	0.96	0.67
0.6	3.3	0.3	2.79	3.04	-8.89	0.96	0.96	-0.36
0.6	5.0	0.3	2.93	3.04	-3.68	0.96	0.96	-0.71
0.6	6.6	0.3	2.94	3.04	-3.23	0.97	0.96	0.33
0.6	8.3	0.3	3.00	3.04	-1.04	0.96	0.96	-0.36
0.6	10.0	0.3	3.04	3.04	0.22	0.97	0.96	0.67
0.6	3.3	0.4	2.72	3.04	-11.42	0.95	0.96	-1.15
0.6	5.0	0.4	2.76	3.04	-9.88	0.95	0.96	-1.42
0.6	6.6	0.4	2.79	3.04	-8.87	0.95	0.96	-1.42
0.6	8.3	0.4	2.93	3.04	-3.67	0.96	0.96	-0.36
0.6	10.0	0.4	2.72	3.04	-11.42	0.96	0.96	-0.36
0.6	3.3	0.5	2.65	3.03	-14.61	0.94	0.96	-2.06
0.6	5.0	0.5	2.65	3.03	-14.61	0.94	0.96	-2.06
0.6	6.6	0.5	2.56	3.03	-18.37	0.96	0.96	-0.36
0.6	8.3	0.5	2.57	3.03	-18.08	0.96	0.96	-0.36
0.6	10.0	0.5	2.57	3.03	-18.08	0.96	0.96	-0.36

Predicted parameters: L_p = 5.046×10^{-8} kg/m^{2}sPa. B_m = 4.35×10^{-7} m/s; σ = 0.967; a = 1.285×10^{-2} ; b = 1.355×10^{-1}

Appendix A4 The fouling rate constant (k') and R^2 of different fouling models

Press. (bar)	Flowrate (mL /min)	Cake layer		Complete blocking		Intermediate blocking		Standard blocking	
		k'	R^2	k'	R^2	k'	R^2	k'	R^2
6	600	0.083	0.764	0.027	0.890	0.033	0.830	0.015	0.861

6	500	0.095	0.744	0.030	0.885	0.038	0.818	0.017	0.853
6	400	0.108	0.728	0.032	0.881	0.042	0.807	0.018	0.846
6	300	0.120	0.712	0.035	0.877	0.046	0.798	0.020	0.839
6	200	0.134	0.696	0.038	0.872	0.051	0.786	0.022	0.831
5	600	0.064	0.795	0.022	0.898	0.027	0.850	0.012	0.875
5	500	0.075	0.779	0.025	0.894	0.031	0.840	0.014	0.869
5	400	0.087	0.758	0.028	0.889	0.035	0.827	0.016	0.859
5	300	0.098	0.741	0.030	0.884	0.039	0.816	0.017	0.852
5	200	0.111	0.724	0.033	0.880	0.043	0.805	0.019	0.844
4	600	0.049	0.822	0.018	0.904	0.021	0.866	0.010	0.886
4	500	0.058	0.805	0.020	0.900	0.024	0.856	0.011	0.879
4	400	0.070	0.785	0.024	0.895	0.029	0.844	0.013	0.871
4	300	0.083	0.765	0.027	0.890	0.033	0.831	0.015	0.862
4	200	0.096	0.743	0.030	0.885	0.038	0.817	0.017	0.852
3	600	0.034	0.849	0.013	0.910	0.015	0.881	0.007	0.896
3	500	0.041	0.834	0.016	0.905	0.018	0.872	0.008	0.889
3	400	0.051	0.815	0.019	0.902	0.022	0.861	0.010	0.883
3	300	0.064	0.792	0.022	0.897	0.027	0.847	0.012	0.873
3	200	0.077	0.766	0.025	0.890	0.032	0.831	0.014	0.861
2	600	0.023	0.869	0.010	0.912	0.010	0.892	0.005	0.902
2	500	0.028	0.860	0.011	0.911	0.012	0.887	0.006	0.899
2	400	0.035	0.849	0.014	0.910	0.016	0.882	0.007	0.896
2	300	0.046	0.831	0.017	0.906	0.020	0.871	0.010	0.890
2	200	0.056	0.812	0.020	0.903	0.024	0.861	0.011	0.883
6	600	0.083	0.764	0.027	0.890	0.033	0.830	0.015	0.861

Appendix A5 Model fitting graphs for fouling analysis

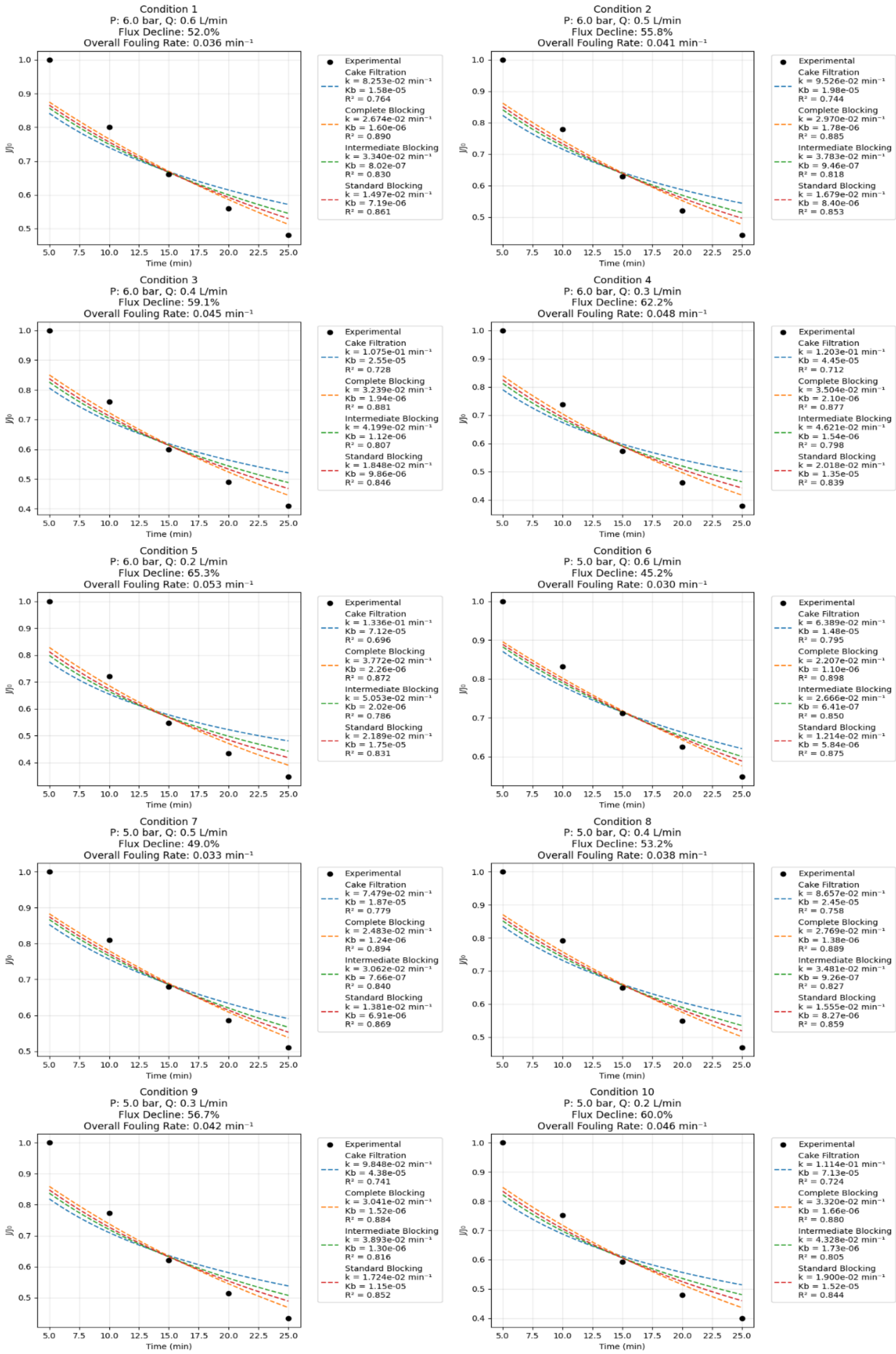

Condition 11
P: 4.0 bar, Q: 0.6 L/min
Flux Decline: 38.3%
Overall Fouling Rate: 0.024 min^{-1}

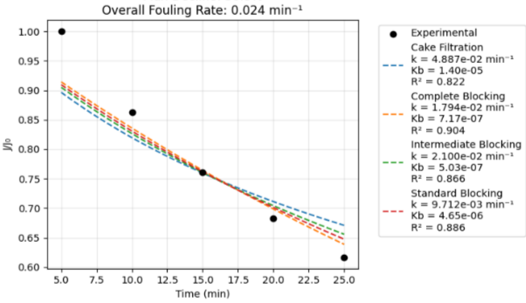

Condition 12
P: 4.0 bar, Q: 0.5 L/min
Flux Decline: 42.5%
Overall Fouling Rate: 0.028 min^{-1}

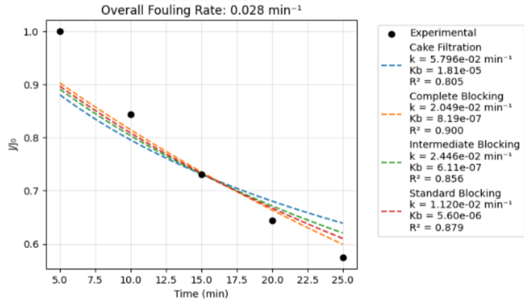

Condition 13
P: 4.0 bar, Q: 0.4 L/min
Flux Decline: 47.3%
Overall Fouling Rate: 0.032 min^{-1}

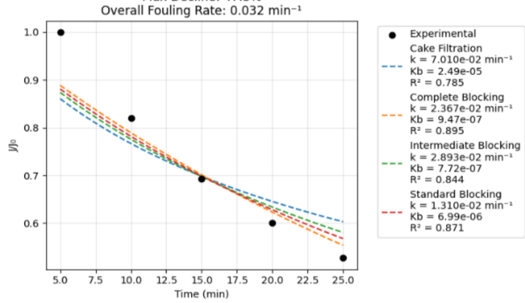

Condition 14
P: 4.0 bar, Q: 0.3 L/min
Flux Decline: 51.7%
Overall Fouling Rate: 0.036 min^{-1}

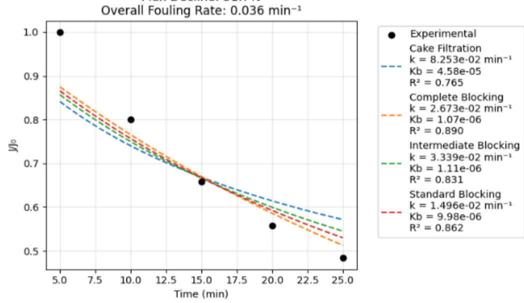

Condition 15
P: 4.0 bar, Q: 0.2 L/min
Flux Decline: 56.0%
Overall Fouling Rate: 0.041 min^{-1}

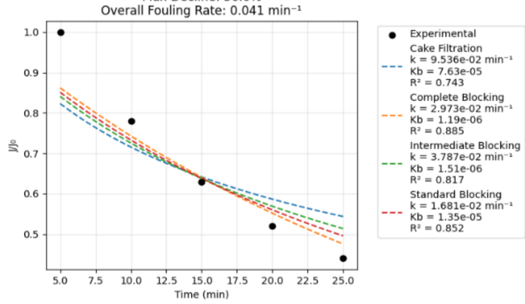

Condition 16
P: 3.0 bar, Q: 0.6 L/min
Flux Decline: 30.4%
Overall Fouling Rate: 0.018 min^{-1}

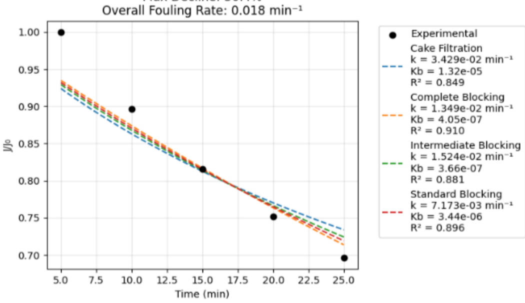

Condition 17
P: 3.0 bar, Q: 0.5 L/min
Flux Decline: 34.2%
Overall Fouling Rate: 0.021 min^{-1}

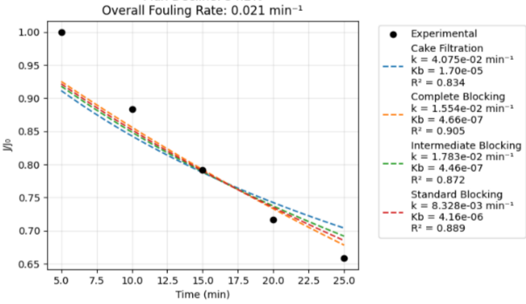

Condition 18
P: 3.0 bar, Q: 0.4 L/min
Flux Decline: 39.8%
Overall Fouling Rate: 0.025 min^{-1}

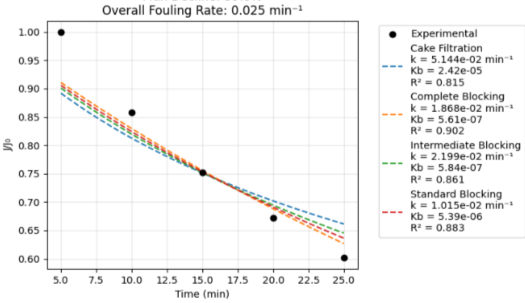

Condition 19
P: 3.0 bar, Q: 0.3 L/min
Flux Decline: 45.6%
Overall Fouling Rate: 0.030 min^{-1}

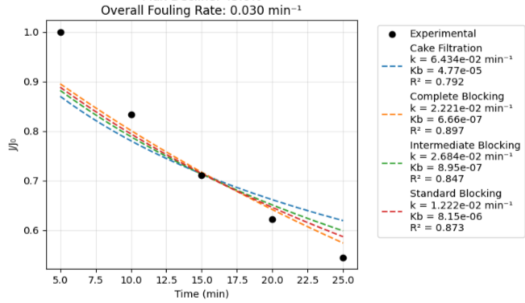

Condition 20
P: 3.0 bar, Q: 0.2 L/min
Flux Decline: 50.7%
Overall Fouling Rate: 0.035 min^{-1}

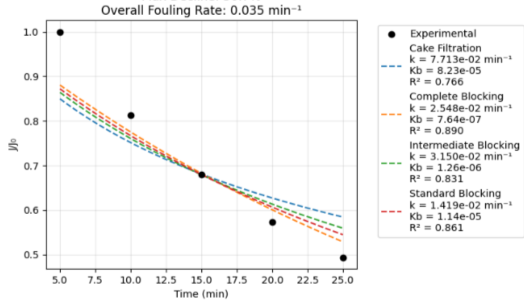

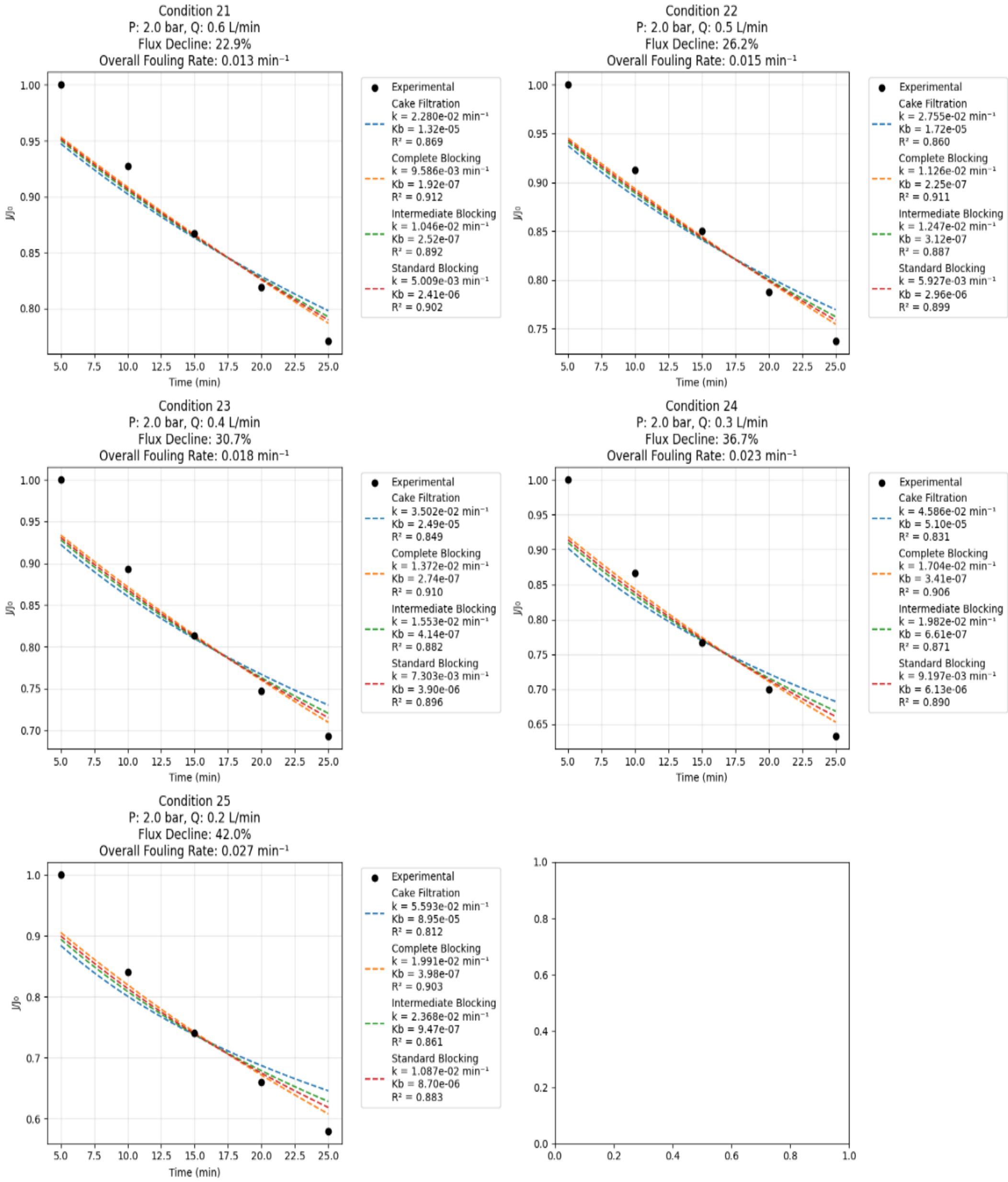

Condition 21
P: 2.0 bar, Q: 0.6 L/min
Flux Decline: 22.9%
Overall Fouling Rate: 0.013 min^{-1}
Experimental
Cake Filtration
k = 2.280e-02 min^{-1}
Kb = 1.32e-05
R^2 = 0.869
Complete Blocking
k = 9.586e-03 min^{-1}
Kb = 1.92e-07
R^2 = 0.912
Intermediate Blocking
k = 1.046e-02 min^{-1}
Kb = 2.52e-07
R^2 = 0.892
Standard Blocking
k = 5.009e-03 min^{-1}
Kb = 2.41e-06
R^2 = 0.902
Time (min)
J/J_0
Condition 22
P: 2.0 bar, Q: 0.5 L/min
Flux Decline: 26.2%
Overall Fouling Rate: 0.015 min^{-1}
Experimental
Cake Filtration
k = 2.755e-02 min^{-1}
Kb = 1.72e-05
R^2 = 0.860
Complete Blocking
k = 1.126e-02 min^{-1}
Kb = 2.25e-07
R^2 = 0.911
Intermediate Blocking
k = 1.247e-02 min^{-1}
Kb = 3.12e-07
R^2 = 0.887
Standard Blocking
k = 5.927e-03 min^{-1}
Kb = 2.96e-06
R^2 = 0.899
Time (min)
J/J_0
Condition 23
P: 2.0 bar, Q: 0.4 L/min
Flux Decline: 30.7%
Overall Fouling Rate: 0.018 min^{-1}
Experimental
Cake Filtration
k = 3.502e-02 min^{-1}
Kb = 2.49e-05
R^2 = 0.849
Complete Blocking
k = 1.372e-02 min^{-1}
Kb = 2.74e-07
R^2 = 0.910
Intermediate Blocking
k = 1.553e-02 min^{-1}
Kb = 4.14e-07
R^2 = 0.882
Standard Blocking
k = 7.303e-03 min^{-1}
Kb = 3.90e-06
R^2 = 0.896
Time (min)
J/J_0
Condition 24
P: 2.0 bar, Q: 0.3 L/min
Flux Decline: 36.7%
Overall Fouling Rate: 0.023 min^{-1}
Experimental
Cake Filtration
k = 4.586e-02 min^{-1}
Kb = 5.10e-05
R^2 = 0.831
Complete Blocking
k = 1.704e-02 min^{-1}
Kb = 3.41e-07
R^2 = 0.906
Intermediate Blocking
k = 1.982e-02 min^{-1}
Kb = 6.61e-07
R^2 = 0.871
Standard Blocking
k = 9.197e-03 min^{-1}
Kb = 6.13e-06
R^2 = 0.890
Time (min)
J/J_0
Condition 25
P: 2.0 bar, Q: 0.2 L/min
Flux Decline: 42.0%
Overall Fouling Rate: 0.027 min^{-1}
Experimental
Cake Filtration
k = 5.593e-02 min^{-1}
Kb = 8.95e-05
R^2 = 0.812
Complete Blocking
k = 1.991e-02 min^{-1}
Kb = 3.98e-07
R^2 = 0.903
Intermediate Blocking
k = 2.368e-02 min^{-1}
Kb = 9.47e-07
R^2 = 0.861
Standard Blocking
k = 1.087e-02 min^{-1}
Kb = 8.70e-06
R^2 = 0.883
Time (min)
J/J_0

Research Publications

RESEARCH PUBLICATIONS

Publication from the thesis

1. **Ashwani Kumar Tiwari** and Manish Jain, "A novel process for rutin recovery from model solutions using nanofiltration: Experimental study, mathematical modeling, and scale-up design", *Journal of Food Process Engineering*, vol. 47(3), art. no. e14592, 2024, doi: 10.1111/jfpe.14592

2. **Ashwani Kumar Tiwari** and Manish Jain, "Concentration of betanin from model beetroot extracts using nanofiltration: Parameter estimation and sensitivity analysis*", Journal of Chemical Technology and Biotechnology,* vol. 99, pp. 1976-1983, 2024, doi: 10.1002/jctb.7698

3. **Ashwani Kumar Tiwari,** Kudzai Hamish Ruzvidzo, Prafull Kumar Meena, and Manish Jain, "Extraction of Betanin From Beetroot Juice Using a Hybrid System: System Performance and Fouling Analysis of the Membrane", *Journal of Food Process Engineering*, vol. 48(11), art. no. e70272, 2025, doi: 10.1111/jfpe.70272

4. **Ashwani Kumar Tiwari,** Kudzai Hamish Ruzvidzo, Ritu Sharma, and Manish Jain, "Membrane technology - A promising tool for recovering bioactive compounds from natural sources, *ChemBioEng Rev.* (Submitted)

Additional Publications

1) Ketan Mahawer, **Ashwani Kumar Tiwari,** Abeer Mutto, and Manish Jain, "Modeling and experimental investigation of factors responsible for maximizing the betanin concentration by spiral-wound FO module using Na2SO4-based draw solution", *Food and Bioproducts Processing,* vol. 152, pp. 54-63, 2025, doi: 10.1016/j.fbp.2025.05.001

2) Kudzai Hamish Ruzvidzo, **Ashwani Kumar Tiwari,** Raminder Kaur, and Manish Jain, "A critical review of the progress, challenges, and future outlook of forward osmosis desalination in the 21st century", *Water Environment Research,* vol. 97(10), pp e70191, 2025, doi: 10.1002/wer.70191

3) Kudzai Hamish Ruzvidzo, **Ashwani Kumar Tiwari,** Raminder Kaur, and Manish Jain, "Artificial neural network-based modeling of forward osmosis-phase separation desalination processes with novel ternary organic draw solutions", *J. Indian Chem. Soc.* (Submitted).

Received: 23 October 2023 | Revised: 5 February 2024 | Accepted: 2 March 2024

DOI: 10.1111/jfpe.14592

ORIGINAL ARTICLE

Journal of Food Process Engineering WILEY

A novel process for rutin recovery from model solutions using nanofiltration: Experimental study, mathematical modeling, and scale-up design

Ashwani Kumar Tiwari | Manish Jain

Department of Applied Chemistry, Delhi Technological University, New Delhi, India

Correspondence
Manish Jain, Department of Applied Chemistry, Delhi Technological University, New Delhi 110042, India.
Email: manishjain@dtu.ac.in

Funding information
IRD, Delhi Technological University, Grant/Award Number: DTU/IRD/619/2019/2109

Abstract

Pressure-driven membrane processes represent a credible method for the separation and concentration of natural polyphenols. The separation characteristics and their productivity depend on several factors such as molecular weight cut-off, operating conditions, and test cell parameters. In this study, a compact polyamide HFT-NF150 nanofiltration membrane has been tested to separate different model solutions of rutin, and the effects of operating conditions like trans-membrane pressure, feed concentration, and feed flow rates were analyzed. All the findings of the experiment revealed that the maximum permeate flux of 3.04×10^{-5} m^3/m^2 s and 98.5% rejection were obtained at a high feed flow rate of 36 L/h and a high pressure of 6×10^5 Pa. Also, the Spiegler–Kedem model is used to report the mass transport phenomenon across the membrane. The unconstrained minimization technique based on the simplex search method was applied for the estimation of the unknown parameters. The theoretical and experimental values for permeate characteristics were then compared for each experimental data point for the model validation. Later, a mathematical model was used to check the scale-up viability of the process to the commercial limit.

Practical applications

In the past few years, naturally occurring bioactive compounds have revolutionized the whole scientific community for their exploration. Rutin is one such phenolic compound that is present in significant amounts in buckwheat and has a wide range of applications in the food and pharmaceutical industries. In this work, an energy-efficient and cleaner method of nanofiltration is applied to concentrate the rutin from the model plant extract. Experiments were performed on a polyamide nanofiltration membrane with a molecular weight cut-off of 150 Da at different operating conditions. Experimental results were fitted in a three-parameter Spiegler–Kedem model to determine the transport parameters of the membrane for rutin. The values of transport parameters were also successfully validated using the experimental results. Experimental results and model predictions were then used to analyze the effects of different operating parameters. A scale-up setup has been designed and simulated to check the feasibility of the process at the commercial level.

Research Article

Received: 24 February 2024 Revised: 31 May 2024 Published online in Wiley Online Library:

(wileyonlinelibrary.com) DOI 10.1002/jctb.7698

Concentration of betanin from model beetroot extracts by using nanofiltration: parameter estimation and sensitivity analysis

Ashwani Kumar Tiwari and Manish Jain*

Abstract

BACKGROUND: Nowadays, research focusing on natural compounds is getting more importance across the globe. Recently, natural bioactive compounds have gained the attention of researchers as a consequence of their exemplary physicochemical properties and exceptional utility in the food and pharma industries. However, separating and concentrating these bioactive compounds from their origin sources still poses a considerable challenge to their profitable commercial usage. The current study focuses on the application of a facile nanofiltration method for recovering betanin from model beetroot extract solutions using a polyamide nanofiltration membrane. Furthermore, the three-parameter Spiegler–Kedem model was used to determine the transport parameters of the membrane and theoretically predict the performance of the membrane. Additionally, variance-based sensitivity analysis methods were deployed to study the sensitivity of different operating and membrane transport parameters.

RESULT: The results indicate that the membrane exhibited the highest rejection of 99% and permeate flux of 3.14 10^{-5} m^3 m^{-2} s^{-1} at 0.6 MPa pressure and 600 mL min^{-1} flow rate. The data obtained through the Spiegler–Kedem model were coherent with the experimental observations. Simulations on sensitivity analysis revealed that specific hydraulic permeability and cross-membrane pressure majorly influence permeate flux and rejection.

CONCLUSION: This study showed that nanofiltration with 150 Da cut-off membranes effectively concentrated betanin with 99% rejection. Higher cross-membrane pressure and higher feed flow rates were preferable operating conditions for higher rejections. Variance-based sensitivity analysis showed that cross-membrane pressure and hydraulic permeability are the most influential parameters affecting permeate flux and rejection.

Supporting information may be found in the online version of this article.

Keywords: Betanin; nanofiltration; phenolic compound; NF process modeling; sensitivity analysis

INTRODUCTION

Phenolic compounds are one of the most abundant subsidiary metabolites in plants and are identified by single or more aromatic rings that contain single or multiple hydroxyl groups.[1-3] These compounds offer many human-health-related functional benefits. Phenolics exhibit physiological benefits such as anti-aging, anti-infective, anti-inflammatory and antiproliferative properties.[4-7] Betanin is one such phenolic compound. It is a water-soluble vacuolar chromo-alkaloid found in *Beta vulgaris* L, also known as beetroot and chukandar.[8] Betanin finds applications in various industries, including the food industry as a colorant and the pharmaceutical industry as an active ingredient in medicines. It is also used for coloring meat substitutes, gelatine, desserts, sausages and dairy products.

The recovery of phenolic bioactive compounds such as betanin from their natural sources is tedious owing to the high enzyme activity in most foods and plants. Therefore, the choice of extraction method must be made with the greatest caution to prevent the chemical change of the target molecules.[9] The standard method for separating and concentrating phenolic compounds is liquid–liquid extraction followed by evaporation or crystallization. Liquid–liquid extraction requires organic solvents such as chloroform, *n*-hexane, ethanol, propanol, ethyl acetate, and acetone.[10,11] These solvent-based processes are very costly, and the phenolic extracts may contain residual solvents, making them unfit or undesirable for food applications.[1]

Nanofiltration (NF) seems to be a promising technology for concentrating phenolic compounds owing to certain benefits, such as no involvement of phase transition, low energy consumption, no use of organic solvents and low waste disposal. Moreover, other biological molecules such as sugars and proteins can be easily separated from phenolic solutions, and concentration and purification steps can be combined in one step, reducing operational costs and time. Membrane-based processes can run continuously

* *Correspondence to: M Jain, Department of Applied Chemistry, Delhi Technological University, New Delhi 110042, India. E-mail: manishjain@dtu.ac.in*

Department of Applied Chemistry, Delhi Technological University, New Delhi, India

Journal of Food Process Engineering

WILEY

Journal of Food Process Engineering

ORIGINAL ARTICLE

Extraction of Betanin From Beetroot Juice Using a Hybrid System: System Performance and Fouling Analysis of the Membrane

Ashwani Kumar Tiwari[1] | Kudzai Hamish Ruzvidzo[1] | Prafful Kumar Meena[2] | Manish Jain[1]

[1]Department of Applied Chemistry, Delhi Technological University, New Delhi, India | [2]Department of Biotechnology, Delhi Technological University, New Delhi, India

Correspondence: Manish Jain (manishjain@dtu.ac.in)

Received: 30 August 2025 | **Revised:** 30 August 2025 | **Accepted:** 10 November 2025

Funding: This work was supported by the Delhi Technological University.

Keywords: betanin | fouling analysis | hybrid system | nanofiltration | ultrafiltration

ABSTRACT

The world's ever-increasing population has expanded the need to study sustainable technologies for green synthesis. Scientists and researchers have focused on exploring natural bioactives in the food and pharmaceutical industries in the last few years. Betanin is a naturally occurring bioactive compound with exceptional antioxidant properties found in beetroots in significant amounts. However, due to its environmental sensitivity, the extraction and concentration of this compound from beetroot juice is difficult. This study investigates a cleaner, more energy-efficient hybrid system combining ultrafiltration (UF) and nanofiltration (NF) to concentrate betanin while preserving its stability and bioactivity. UF was employed as a pre-treatment step to remove high-molecular-weight impurities, while the NF step enabled selective concentration of betanin. The hybrid process significantly improved betanin retention, with an observed percentage rejection in the 87%–94% range. Additionally, a maximum flux decline of 65% was observed at high pressure and low flow rates, indicating fouling. The fouling mechanism analysis showed that the complete blocking model is the best-fit model for experimental values. These findings contribute to the development of eco-friendly and cost-effective membrane-based techniques for the recovery of natural compounds.

1 | Introduction

Natural foods and bioactives have been part of the human diet for ages (Alasalvar et al. 2020). However, over the last few decades, the demand for natural food colors and bioactives has grown significantly as people have shown an increasing interest in healthier options over artificial additives (Trishitman et al. 2023). Research shows that natural ingredients from plants make food more appealing and offer health benefits, such as fighting aging, infections, inflammation, and abnormal cell growth (Delgado Vargas et al. 2010; Vinson et al. 2001; Žitňanová et al. 2006). Phenolics are a highly prevalent secondary metabolite in plants, contributing to their health and sensory qualities. These compounds, identified by their unique aromatic rings with hydroxyl groups, boast over 8000 known varieties in many vegetables and fruits (Shi et al. 2005; Pandey and Rizvi 2009; Tiwari and Jain 2024a). Phenolic compounds come in diverse forms, including flavonoids, tannins (both condensed and straightforward), phenolic acids, stilbenes, lignans, coumarins, and lignins. Each of these has its functions in plants, providing defense and contributing to the plant's flavor, color, and even oxidative stability.

Regarding human health, these compounds are genuinely remarkable. These compounds exhibit numerous health benefits in humans, primarily due to their antioxidant properties. They

Food and Bioproducts Processing 152 (2025) 54–63

Contents lists available at ScienceDirect

Food and Bioproducts Processing

journal homepage: www.elsevier.com/locate/fbp

Modeling and experimental investigation of factors responsible for maximizing the betanin concentration by spiral-wound FO module using Na_2SO_4-based draw solution

Ketan Mahawer [a], Ashwani Kumar Tiwari [b], Abeer Mutto [a], Manish Jain [b,*]

[a] Department of Chemical Engineering, Indian Institute of Technology Delhi, New Delhi 110016, India
[b] Department of Applied Chemistry, Delhi Technological University, Delhi 110042, India

ARTICLE INFO

Keywords:
Forward osmosis
Process modeling
Betanin
Parameter estimation
Specific energy consumption

ABSTRACT

The conventional process for concentrating betanin from beetroot juice is expensive due to the requirement of solvents and high energy consumption. However, concentrating betanin using a forward osmosis (FO) process offers a cost-effective alternative without phase change. This modeling and experimental study investigated the most significant factors responsible for enriching the feed side betanin concentration by the FO process using a Na_2SO_4-based draw solution. The module-scale FO transport model parameters were estimated and validated by performing the lab-scale experiments. Furthermore, the FO model is simulated to explore the influence of the process operating variables, draw solution temperature, and the active membrane area to maximize the betanin concentration in the outlet process stream. The results show that the inlet draw flow rate significantly enhances the betanin concentration in the outlet feed stream. Furthermore, simulations investigate the FO membrane parameter (solvent permeability) and its influence on enriching the feed side betanin concentration inside the feed stream. The simulated results show that maintaining the same operating conditions, an increase in water permeability (1.22×10^{-12} to 5.5×10^{-11}m/Pa.s) concentrates 66.6 % betanin inside the feed stream more compared to the inlet draw flow rate at 25 L/h. In contrast, variations in solute permeability have a negligible impact on the increase in betanin concentration. Finally, the study concludes that the water permeability and inlet draw flow rate were the most significant factors responsible for enriching the feed side betanin or any other organic compound using FO membrane.

1. Introduction

The non-toxicity and health benefits associated with natural pigments and bioactive additives, compared to synthetic colors, have led to a massive resurgence in their use in recent times. Natural color pigments are also rich in polyphenols, which are known to reduce the risks of cardiovascular ailments, cancer, and several other health conditions (Vinson et al., 2001). Subsequently, consumer demand for minimally processed and high-quality nutritional food has also established an extensive market for these pigments. Exhaustive literature can be found on the extraction of such pigments from various natural and plant-based sources, including fruit juices, vegetables, teas, and coffees (Alara et al., 2021). However, even though these compounds can be found in several plant materials, their yield and purity largely depend on the extraction and concentration method.

Among these, the betanin compound, found in significant quantities in beetroot juice, is widely utilized as the primary source of red color. It has numerous applications in food industries, such as additives to gelatins, baked food desserts, confectionaries, dairy products, jellybeans, and fruit beer-like beverages. While various artificial colors and bioactive compounds similar to the original beetroot color are also available in markets, betanin stands out as a cheaper alternative. In addition, these synthetic colors, though widely used in edible juices due to the increasing industrial demand, are also extremely detrimental to juice quality and human health. In contrast, betanin extracted from beetroot has higher sugar strength, gives high nutritional value to the juice, and can be produced at a low cost, thereby having the potential to supplant synthetic food colorants. However, the quality and stability of betanins when extracted from natural juices/organic solutions are strongly influenced by factors such as pH value, oxygen, and sugar content of the

* Corresponding author.
E-mail address: manishjain@dtu.ac.in (M. Jain).

https://doi.org/10.1016/j.fbp.2025.05.001
Received 13 February 2025; Received in revised form 27 April 2025; Accepted 5 May 2025
Available online 6 May 2025

Water Environment Research

REVIEW

A Critical Review on the Progress, Challenges, and Future Outlook of Forward Osmosis Desalination in the 21st Century

Kudzai Hamish Ruzvidzo[1] | Ashwani Kumar Tiwari[1] | Raminder Kaur[1] | Deshraj Meena[2] | Manish Jain[1]

[1]Department of Applied Chemistry, Delhi Technological University, New Delhi, India | [2]Department of Applied Physics, Delhi Technological University, New Delhi, India

Correspondence: Manish Jain (manishjain@dtu.ac.in)

Received: 26 January 2025 | **Revised:** 30 August 2025 | **Accepted:** 16 September 2025

Keywords: commercialization | desalination | draw solution | energy consumption | forward osmosis | hybrid systems | machine learning | membrane fouling | renewable energy

ABSTRACT

The escalating global water crisis, driven by population growth, climate change, and increasing industrial demands, has positioned water scarcity as one of the most pressing challenges of the 21st century. With freshwater resources becoming increasingly limited and unevenly distributed, desalination technologies have emerged as critical solutions to meet growing water demands. Among various desalination approaches, forward osmosis (FO) has garnered significant attention as a promising low fouling technology that offers distinct advantages over conventional methods. This critical review provides a comprehensive analysis of FO's evolution, challenges, mechanisms, and prospects. It offers an in-depth examination of some significant literature reviews since 2019 to identify current research gaps in FO desalination and advance the field. The review evaluates draw agents and membrane properties, investigates FO's energy efficiency compared with other techniques, and environmental impacts. A three-phase roadmap is proposed involving collaborative integration of key stakeholders, scaling up for remote applications, and development of autonomous artificial intelligence networks for adaptive treatment responses.

1 | Introduction

1.1 | Global Water Scarcity

Freshwater scarcity is a global issue exacerbated by population growth and climate change (Jury and Vaux 2005; Vushe 2021). Water scarcity occurs when freshwater demand exceeds supply (Mekonnen and Hoekstra 2016). India, now the world's most populous nation, is projected to face a water crisis by 2030. This is due to various factors, including population growth, industrialization, urbanization, poor water management, pollution, and climate change (Lancet 2023; Mahato et al. 2022). In 2025, over 1.8 billion people will face severe water shortages, particularly in Southeast Asia and Africa (Kim 2020). The latest global levels of water stress as given by the UN-Water SDG 6 Data Portal are shown in Figure S1. Despite India's projected improvement by 2040, its vast coastline provides an opportunity for innovative solutions like desalination (Manju and Sagar 2017). Access to clean water is vital to prevent waterborne diseases, as demonstrated by the 2023 cholera outbreak in Zimbabwe (Pal et al. 2018; Olatunji et al. 2024).

1.2 | Pressure-Driven Membrane Separation Processes

Addressing global freshwater scarcity requires a comprehensive strategy that preserves water, improves governance, and develops novel technologies to tap into nontraditional water sources (Nabhan et al. 2023). Membrane separation processes

Certificate of Conferences

IPS ACADEMY
Institute of Engineering & Science, Indore
(A UGC Autonomous Institute Affiliated to RGPV Bhopal)

CERTIFICATE OF PARTICIPATION

This certificate is award to

Ashwani Kumar Tiwari

Who has successfully delivered an oral presentation for the paper entitled

Application of Membrane - Based Operations in Separation of Natural Phenolic Compounds

at the International Conference on Emerging Techno-Economic Development for Sustainable Environment during January, 12-13, 2024

Organized by IPS Academy, Institute of Engineering & Science, Indore
Department of Chemical Engineering

Principal | Convenor | Co-Convenor

CERTIFICATE

OF PARTICIPATION

Ashwani Kumar Tiwari

Has successfully **presented** poster in the **Conference on Desalination, Brine Management and Water Recycling, DeSaltM 23** organized by the Environmental Science and Engineering Department, **Indian Institute of Technology Bombay**, Mumbai

21st to 22nd July, 2023

Prof. Subhankar Karmakar
(Head , ESED, IIT Bombay)

Prof. Swatantra Pratap Singh
Convener

CERTIFICATE

ICMW 2023

INTERNATIONAL WORKSHOP AND CONFERENCE ON MEMBRANE ASSISTED WATER PURIFICATION PROCESSES
MAHATMA GANDHI UNIVERSITY, KOTTAYAM, KERALA, INDIA
9-12 March 2023

Organized jointly by

School Of Energy Materials (SEM) Mahatma Gandhi University, Kottayam, Kerala, India
National Research Centre, Cairo , Egypt & Lund University, Sweden

Ashwani Kumar Tiwari

PhD scholar,Department of Applied Chemistry, Delhi technological University, Delhi
has "Presented a paper" (short Invited talk)
at the
International Workshop and Conference on Membrane Assisted Water Purification Processes (ICMW – 2023)
held at Mahatma Gandhi University, Kottayam, Kerala, India.
from 9th -12th, March 2023

Prof. Dr. Sabu Thomas
Chairman ICMW-2023

This is to certify that ....Ashwani Kumar Tiwari....from Delhi Technological University, Delhi.... has participated and presented the work (Oral Presentation) in International Conference on "**Chemical & Allied Science and their Applications**", organized by **Department of Applied Chemistry**, **Delhi Technological University** on Friday, 20th January, 2023.

Convener	Co-Convener	Prof. Anil Kumar
Prof. Ram Singh	Dr. Richa Srivastava	Head of Department

MANAV RACHNA vidyanatariksha | MANAV RACHNA UNIVERSITY

Declared as State Private University Vide Haryana Act 26 of 2014

Sponsored by NHPC

2ND INTERNATIONAL CONFERENCE

ON GREEN AND SUSTAINABLE CHEMISTRY CONFERENCE - 2022

November 17th - 19th, 2022

Organised by

Department of Chemistry

Manav Rachna University, Faridabad, Haryana - 121004 (INDIA)

Sponsored by SERB INSA

Certificate of Participation

This is to certify that Prof./Dr./Mr./Ms./Mrs. Ashwani Kumar Tiwari of Delhi Technological University has attended 2nd International Conferences on Green & Sustainable Chemistry Conference GSCC 2022 organized by Department of Chemistry, Manav Rachna University, Faridabad, during November 17-19, 2022.

He / She has participated as Session Chair/Invited Speaker/Organizer/Paper Presenter (Oral/Poster)/Delegate in the GSCC-2022.

Dr. Arpit Sand	Dr. A. Jayamani	Prof. Sudhish Kumar Shukla	Prof. I. K. Bhat
Convener & Head	Co-Convener	Organizing Secretary	Chairman

MANAV RACHNA vidyanatariksha | MANAV RACHNA UNIVERSITY

Declared as State Private University Vide Haryana Act 26 of 2014

Sponsored by NHPC

2ND INTERNATIONAL CONFERENCE

ON GREEN AND SUSTAINABLE CHEMISTRY CONFERENCE - 2022

November 17th - 19th, 2022

Organised by

Department of Chemistry

Manav Rachna University, Faridabad, Haryana - 121004 (INDIA)

Sponsored by SERB INSA

Certificate of Appreciation

This is to certify that ASHWANI KUMAR TIWARI has been awarded with Best Oral Presentation Award for the paper Titled "Concentration of natural phenolic compound using membrane" in 2nd International Conferences On Green & Sustainable Chemistry Conference GSCC-2022 held at Department of Chemistry Manav Rachna University Faridabad during November 17-19, 2022

Dr. Arpit Sand	Dr. A. Jayamani	Prof. Sudhish Kumar Shukla	Prof. I. K. Bhat
Convener & Head	Co-Convener	Organizing Secretary	Chairman

Department of Applied Chemistry

DELHI TECHNOLOGICAL UNIVERSITY

Shahbad Daulatpur, Bawana Road, Delhi-110042

CERTIFICATE OF PARTICIPATION

Awarded to

Ashwani Kumar Tiwari, Department of Applied Chemistry

for participating in one day Industry Academia seminar on **"Petrochemicals in Today's World"**, organized by Department of Applied Chemistry in association with Just Polymer Solutions and PLUSS Advanced Technologies, held on 21 April, 2023.

Prof Roli Purwar
Coordinator, Dept. of Applied Chemistry

Prof Anil Kumar
Head, Dept. of Applied Chemistry

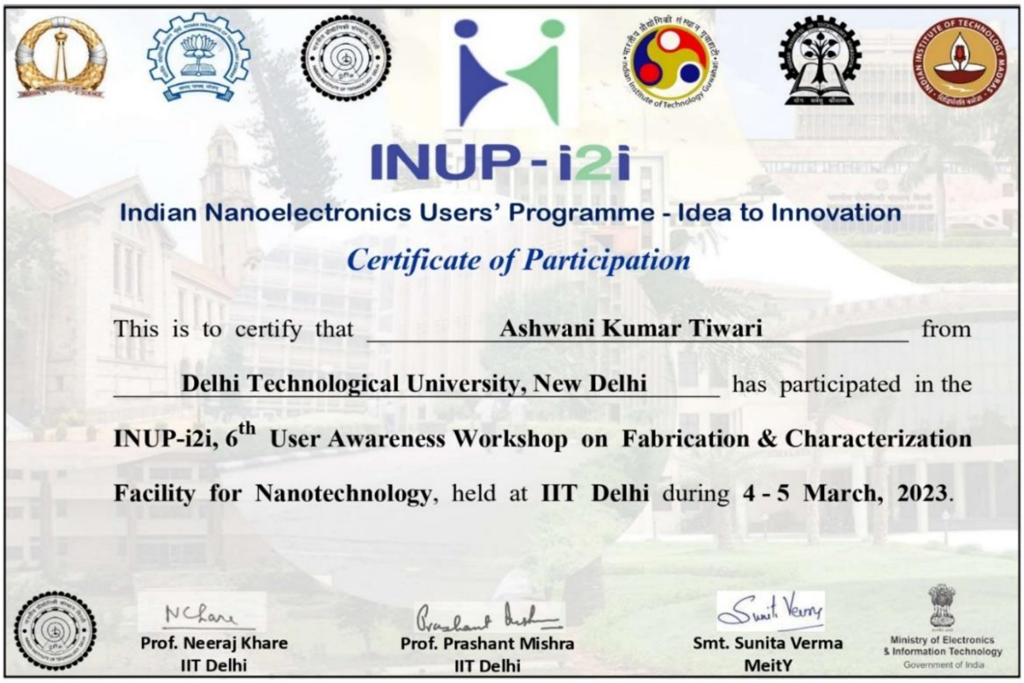

INUP-i2i

Indian Nanoelectronics Users' Programme - Idea to Innovation

Certificate of Participation

This is to certify that **Ashwani Kumar Tiwari** from **Delhi Technological University, New Delhi** has participated in the **INUP-i2i, 6th User Awareness Workshop on Fabrication & Characterization Facility for Nanotechnology**, held at **IIT Delhi** during **4 - 5 March, 2023**.

Prof. Neeraj Khare
IIT Delhi

Prof. Prashant Mishra
IIT Delhi

Smt. Sunita Verma
MeitY

Ministry of Electronics & Information Technology
Government of India

IEEE

EDS

G20 भारत 2023 INDIA

75 Azadi Ka Amrit Mahotsav

DEPARTMENT OF APPLIED PHYSICS
DELHI TECHNOLOGICAL UNIVERSITY
BAWANA ROAD, DELHI-110042

ONE DAY NATIONAL SEMINAR
ON

RECENT ADVANCEMENTS IN SEMICONDUCTOR DEVICES AND MATERIALS
(RASDM-2023)

Certificate

This is to certify that Prof./Dr./Mr./Ms.....Ashwani Kumar Tiwari.......has attended/organized/chaired session in One Day National Seminar on "RECENT ADVANCEMENTS IN SEMICONDUCTOR DEVICES AND MATERIALS (RASDM-2023)" organized by Department of Applied Physics, Delhi Technological University (DTU) on January 30, 2023.

Prof. A.S. Rao	Prof. Suresh C. Sharma	Dr. Amrish K. Panwar	Dr. Deshraj Meena	Dr. Renuka Bokolia
(Chairman, RASDM-2023)	(Co- Chairman, RASDM-2023)	(Convener, RASDM-2023)	(Co-Convener, RASDM-2023)	(Treasurer, RASDM-2023)

INTELLECTUAL PROPERTY INDIA
PATENTS | DESIGNS | TRADE MARKS
GEOGRAPHICAL INDICATIONS

NIPAM
NATIONAL IP AWARENESS MISSION

सत्यमेव जयते

Government of India
Ministry of Commerce and Industry
Department for Promotion of Industry and Internal Trade
Office of the Controller General of Patents, Designs and Trade Marks

CERTIFICATE

This is to certify that, **MR. ASHWANI KUMAR TIWARI** of **DELHI TECHNOLOGICAL UNIVERSITY** has successfully participated in IP Awareness/Training program under

NATIONAL INTELLECTUAL PROPERTY AWARENESS MISSION

on November 30,2022

Azadi Ka Amrit Mahotsav

Organized by
Intellectual Property Office, India

Date:February 09,2023

(Prof. (Dr) Unnat P. Pandit)
CONTROLLER GENERAL OF PATENTS, DESIGNS & TRADE MARKS

DELTECH UNIVERSITY — DELHI TECHNOLOGICAL UNIVERSITY

INSTITUTION'S INNOVATION COUNCIL
(Ministry of HRD Initiative)

Certificate of Participation

This is to certify that ………ASHWANI KUMAR TIWARI………from ………DELHI TECHNOLOGICAL UNIVERSITY……… has participated in One-Day virtual Workshop on "**Accelerators/Incubation - Opportunities for Students & Faculties - Early Stage Entrepreneurs**", recommended by the Institute Innovation Council (IIC) of DTU as per mandate of Innovation Cell, Ministry of Education (MoE) GOI, organized by **Department of Applied Chemistry**, **Delhi Technological University** on Saturday, 19th June, 2021.

Dr. Ram Singh
Coordinator

Plagiarism

DELHI TECHNOLOGICAL UNIVERSITY
(Formerly Delhi College of Engineering)
Shahbad Daulatpur, Main Bawana Road, Delhi-110042, India

PLAGIARISM VERIFICATION

Title of the Thesis: **"Applications of membrane-based operations in separation of natural phenolic compounds"**

Total Pages **193,** Name of the Scholar: **Ashwani Kumar Tiwari**

Supervisor (s)

(1) Dr. Manish Jain

Department of **Applied Chemistry**

This is to report that the above thesis was scanned for similarity detection. Process and outcome are given below:

Software used: **Turnitin,** Similarity Index: **10 %,** Total Word Count: **45,403**

Date**: 26-01-2026**

Candidate's Signature **Supervisor(s) Signature**

Thesis.pdf

Delhi Technological University

Document Details

Submission ID
trn:oid:::27535:126931832

Submission Date
Jan 26, 2026, 11:02 PM GMT+5:30

Download Date
Jan 26, 2026, 11:14 PM GMT+5:30

File Name
Thesis.pdf

File Size
7.8 MB

193 Pages

45,403 Words

231,368 Characters

turnitin Page 1 of 204 - Cover Page Submission ID trn:oid:::27535:126931832

10% Overall Similarity

The combined total of all matches, including overlapping sources, for each database.

Filtered from the Report

- Bibliography
- Quoted Text
- Cited Text
- Small Matches (less than 10 words)

Match Groups

160 Not Cited or Quoted 10%
Matches with neither in-text citation nor quotation marks

0 Missing Quotations 0%
Matches that are still very similar to source material

0 Missing Citation 0%
Matches that have quotation marks, but no in-text citation

0 Cited and Quoted 0%
Matches with in-text citation present, but no quotation marks

Top Sources

6% Internet sources
7% Publications
5% Submitted works (Student Papers)

Integrity Flags

0 Integrity Flags for Review

No suspicious text manipulations found.

Our system's algorithms look deeply at a document for any inconsistencies that would set it apart from a normal submission. If we notice something strange, we flag it for you to review.

A Flag is not necessarily an indicator of a problem. However, we'd recommend you focus your attention there for further review.

Curriculum Vitae

Ashwani Kumar Tiwari

CAREER OBJECTIVE

Aiming for an innovative, challenging, responsible, and rewarding career.

EXPERIENCE

Working as Examiner of Patents & Designs since June, 2025 (Government of India)

CONTACT

8896447427

EMAIL

ashwanitiwari087@gmail.com

HOBBIES

Listening Music

Travelling and Trekking

EDUCATION

M.Tech – Polymer Technology, 8.01 SGPA
2018-2020
Delhi Technological University

B.Tech – Plastic Engineering, 76.22 %
2014-2018
Central Institute of Petrochemicals Engineering and Technology

Intermediate – Science Stream, 89 %
2012-2013
Red Rose Senior Secondary School

High School – Science Stream, 10 CGPA
2010-2011
Red Rose Senior Secondary School

SKILLS

Time Management

Problem-Solving Approach

Adaptable and Hardworking